

SYNTHESIS & MICROCONTACT
MOLDING OF
FUNCTIONALIZABLE HYDROGELS

by

Serap Yapar

B.S. in Chemistry, Boğaziçi University, 2008

Submitted to the Institute for Graduate Studies in
Science and Engineering in partial fulfillment of
the requirements for the degree of
Master of Science

Graduate Program in Chemistry

Boğaziçi University

2010

to my family

ACKNOWLEDGEMENTS

First of all, I am grateful to my thesis supervisor Assist. Prof. Rana SANYAL and Assist. Prof. Amitav SANYAL for their guidance, suggestions and for all the support. I also extend my thanks to them for giving me the opportunity to work in their lab where I have learned and enjoyed so much.

I wish to express my thanks to Prof. İlknur DOĞAN and Assoc. Prof. Ramazan Altundaş for their careful and constructive review of the final manuscript.

I would also like to thank Assist. Prof. Şenol Mutlu for letting me work in his lab during microcontact molding experiments.

I would like to extend my thanks to Burcu SELEN ÇAĞLAYAN and Ayla TÜRKEKUL for their patience and help in running NMR experiments supporting my laboratory work.

I would also like to thank to Bilge GEDİK ULUOCAK for her helps during taking my SEM images

I would also want to thank the entire chemistry department for supplying me this much of a fun and home like place.

Finally my deepest thanks go to my whole family and all my friends for their endless love

And ultimately, I would want to thank to all of the former and present SANYAL lab members for their friendships.

This research has been supported by Bogazici University (BAP 5521), TÜBİTAK (108T898).

ABSTRACT

SYNTHESIS & MICROCONTACT MOLDING OF FUNCTIONALIZABLE HYDROGELS

Hydrogels are crosslinked polymers that have large number of hydrophilic groups and capacity to hold water in their three dimensional network structure. These materials have a wide range of application in biomedical and materials science due to their controllable chemical and physical properties.

Dendron-polymer-dendron conjugate systems are novel polymeric materials to fabricate hydrogels. Multivalent dendron-polymer-dendron copolymers can be used to synthesize hydrogels that can be further functionalized with molecules and biomolecules of interest. In this project, synthesis of functionalizable hydrogels, characterizations, and post functionalization of hydrogels from dendron-polymer-dendron conjugates are reported. The resulting hydrogels are biodegradable and multivalent due to utilization of polyester dendrons, possess high swelling capacity due to presence of high molecular weight poly ethylene glycol. Since the hydrogel precursors have alkene and alkyne groups on their surfaces, crosslinking via photopolymerization and post functionalization by click chemistry is possible. Additionally, by micromolding methods, different surface patterns of functionalizable hydrogels can be realized. Successful covalent modification of these hydrogels via control of degree of functionalization was demonstrated by immobilization of fluorescent dyes and enzymes.

ÖZET

FONKSİYONEL HİDROJELLERİN SENTEZ VE MİKROKONTAK KALIPLANMASI

Hidrojeller çok sayıda hidrofilik gruba sahip ve bu yüzden yüksek seviye su tutma özelliği olan çarpaz bağlanmış polimerlerdir. Bu maddeler kontrol edilebilir kimyasal ve fiziksel özellikleri sayesinde, biomedikal uygulamalar ve malzeme bilimini de içeren geniş bir uygulama alanına sahiplerdir.

Dendron-polimer-dendron konjuge sistemleri, hidrojel yapımında kullanılan yeni plimer yapılarıdır. Çok dallı dendron-polimer-dendron kopolimerleri, istenilen moleküller ve biomoleküllerle ileri işlevselleştirilebilen hidrojellerin yapımında kullanılabilirler. Bu projede, dendron-polimer-dendron kopolimerlerinden sentezlenen aktif hidrojellerin karakterizasyonu ve ileri işlevselleştirilmesi anlatılmaktadır. Oluşan hidrojeller, kullanılan poliester dendron sayesinde çok dallı ve bioçözünürlüğü olan ve yapısındaki yüksek moleküler ağırlıktaki PEG sayesinde yüksek derecede su çekme özelliğine sahiptirler. Hidrojel ön maddesi üzerindeki alken ve alkin gruplarına sahip olduğundan foto polimerleşme ile çarpaz bağlanıp “klik” kimyası ile ileri işlevselleştirilebilirler. Bununla beraber, mikro kalıplama yöntemleri yüzey üzerine farklı şekillerde kalıplanmış hidrojeller elde edilebilir. Hidrojellerin başarılı kovalent modifikasyonlarla kontrollü işlevselleştirilmeleri, floresan boya ve enzim bağlanmasıyla gösterildi.

TABLE OF CONTENTS

ACKNOWLEDGEMENTS	iii
ABSTRACT	v
ÖZET v	
LIST OF FIGURES	ixx
LIST OF TABLES	xiv
LIST OF ABBREVIATIONS	xv
1. INTRODUCTION	1
1.1. Hydrogels	1
1.2. Methods to Synthesize Hydrogels	3
1.3. Dendrimer	5
1.4. Dendritic Hydrogels	7
1.5. Reactive Hydrogels	10
1.6. Patterning of Hydrogels	12
2. AIM OF THE STUDY	14
3. RESULTS AND DISCUSSION	15
3.1. Synthesis of Functional Hydrogels	15
3.2. Characterization of Copolymers and Functional Hydrogels	18
3.3 Swelling Properties of Hydrogels	20
3.4 Morphological Studies	23
3.5. Functionalization of Hydrogels	24
3.6. Microcontact Molding of Hydrogels	28
3.4.1. PDMS Molding	28
3.4.2. Spin Coating and Patterning via UV Mask	30
4. EXPERIMENTAL	32
4.1. General Methods and Materials	32
4.2. Preparation of Dendron-Polymer-Dendron Triblock Copolymer Systems	32
4.2.1. Synthesis of Compound 2	32
4.2.2. Synthesis of Compound 3	33
4.2.3. Synthesis of Compound 4	34
4.2.4. Synthesis of Compound 5	34

4.2.5. Synthesis of Compound 6	35
4.2.6. Synthesis of Compound 7	37
4.2.7. Synthesis of Compound 8	37
4.2.8. Synthesis of Compound 9	37
4.2.9. Synthesis of Compound 10	38
4.2.10. Synthesis of Compound 11	38
4.2.11. Synthesis of Compound 12	38
4.2.12. Synthesis of Compound 13	39
4.2.13. Synthesis of Compound 14	39
4.3. General Synthesis of Hydrogels via Photocrosslinking Chemistry	40
4.4. Functionalization of Hydrogels	40
4.4.1. Functionalization with BODIPY azide	40
4.4.2. Functionalization with Biotin azide	41
4.5. Microcontact Molding of Hydrogels	41
4.5.1. PDMS Molding	41
4.5.2. Spin Coating and Patterning via UV mask	42
4.6. Measurements	42
4.6.1. Scanning Electron Microscopy (SEM) Analysis	42
4.6.2. Physical Property Analysis	42
5. CONCLUSIONS	43
APPENDIX A: SPECTROSCOPY DATA	44
6. REFERENCES	71

LIST OF FIGURES

Figure 1.1. Schematic representation of a swelling hydrogel	1
Figure 1.2. Hydrogels as a tool for cell encapsulation and cell adhesion	2
Figure 1.3. Hydrogel used to control angiogenic growth factor delivery	3
Figure 1.4. Gelation of sodium alginate by addition of Ca ⁺² ions.	3
Figure 1.5. Chemical modification of gelatin with methacrylamide side groups	4
Figure 1.6. Hydrogel examples via chemical crosslinking methods	4
Figure 1.7. Dendrimer structure.	5
Figure 1.8. G2 benzyl ester dendron synthesized by coupling reaction	5
Figure 1.9. Dendrimer synthesized by Huisgen “click” reaction	6
Figure 1.10. Schematic representation of a hydrogel constructed by linear and dendritic fragments	8
Figure 1.11. Scheme of the photocrosslinked hydrogel formation	9
Figure 1.12. Schematic representation of photopolymerization of PEG4600 diacrylate and <i>N</i> -hydroxysuccinimide-PEG-acrylate, conjugation an antibody to the surface of these hydrogels	10
Figure 1.13. Hydrogel formation via Crosslinking of Dendron-Polymer Conjugates	11
Figure 1.14. Schematic representation chemical patterning in hydrogels.	12

Figure 1.15. Confocal micrographs of fluorescent hydrogels in geometric shapes and shape of a grid	13
Figure 1.16. Fluorescent photomicrograph of cells plated on patterned hydrogels .	13
Figure 2.1. General representation of the synthesis of functional hydrogels . .	14
Figure 3.1. Synthesis of G3 polyester dendron.	16
Figure 3.2. Synthesis and functionalization of G3 block copolymers	17
Figure 3.3. Schematic representation of hydrogel formation	18
Figure 3.4. ¹ H NMR spectrum of compound 2 and compound 3	18
Figure 3.5. ¹ H NMR spectrum of compound 6 and compound 8	19
Figure 3.6. FTIR spectroscopies of PEG6K bisazide, PEG-dendron copolymer, functionalized copolymer, functional hydrogel	20
Figure 3.7. Water Uptake Comparison of 6KG2 _(2:1) ;6KG2 _(1:1) ;6KG2 _(1:2) Hydrogels	21
Figure 3.8. Water Uptake Comparison of 6KG3 _(2:1) ; 6KG3 _(1:1) ; 6KG3 _(1:2) ; 6KG3 _(1:3) Hydrogels	21
Figure 3.9. Water Uptake Comparison of 2KG3 _(1:1) ; 4KG3 _(1:1) ; 6KG3 _(1:1) Hydrogels Figure 3.6. Azides that are used for hydrogel functionalization	22
Figure 3.10. SEM images of dry hydrogel G36K _(2:1)	23
Figure 3.11. SEM images of dry hydrogel G36K _(1:1)	23
Figure 3.12. SEM images of dry hydrogel of G36K _(1:2)	24

Figure 3.13. SEM images of dry hydrogel of G36K _(1:3)	24
Figure 3.14. Azides that are used for hydrogel functionalization.	25
Figure 3.15. Fluorescence microscope images of functionalized hydrogels with biotin azide, control without catalyst	25
Figure 3.16. Relative fluorescence intensities of functionalized hydrogels with bodipy and their controls that contain descending amount of functional groups	26
Figure 3.17. Fluorescence microscope images of functionalized hydrogels with biotin azide, control without catalyst	27
Figure 3.18. Relative fluorescence intensities of functionalized hydrogels with streptavidin and their controls that contain descending amount of functional groups.	27
Figure 3.19. Schematic representation of PDMS molding on hydrogels.	28
Figure 3.20. SEM images of patterned. hydrogel G36K _(1:1) by PDMS molding.	29
Figure 3.21. The microscope image of hydrogel precursor from compound 7 that patterned with PDMS mold, functionalized with bodipy azide and biotin azide	29
Figure 3.22. Representative scheme of spin coating and UV-mask system, fluorescence microscope images of patterned hydrogels from compound 7 by this system	30
Figure 3.23. SEM images of patterned. hydrogel G36K _(1:1) by “spin coating and UV mask system”	31
Figure 4.1. Schematic synthesis of compound 2	33
Figure 4.2. Schematic synthesis of compounds 3, 4, 5	34

Figure 4.3. Schematic synthesis of compound 6	35
Figure 4.4. Schematic synthesis of compounds 7, 8, 9, 10	36
Figure 4.5. Chemical structure of BODIPY azide	41
Figure 4.6. Chemical structure of Biotin azide.	41
Figure A.1. ¹ H NMR spectrum of [G2]4OH[PEG6K] 2	45
Figure A.2. ATR FTIR spectrum of [G2]4OH[PEG6K] 2	46
Figure A.3. ¹ H NMR spectrum of [1:1] [G2]4OR[PEG6K] 3	47
Figure A.4. ATR FTIR spectrum of [1:1] [G2]4OR[PEG6K] 3	48
Figure A.5. ¹ H NMR spectrum of [1:2] [G2]4OR[PEG6K] 4	49
Figure A.6. ATR FTIR spectrum of [1:2] [G2]4OR[PEG6K] 4	50
Figure A.7. ¹ H NMR spectrum of [2:1] [G2]4OR[PEG6K] 5	51
Figure A.8. ATR FTIR spectrum of [2:1] [G2]4OR[PEG6K] 5	52
Figure A.9. ¹ H NMR spectrum of [G3]8OH[PEG6K] 6	53
Figure A.10. ATR FTIR spectrum of [G3]8OH[PEG6K] 6	54
Figure A.11. ¹ H NMR spectrum of [2:1] [G3]8OR[PEG6K] 7	55
Figure A.12. ATR FTIR spectrum of [2:1] [G3]8OR[PEG6K] 7	56
Figure A.13. ¹ H NMR spectrum of [1:1] [G3]8OR[PEG6K] 8	57

Figure A.14. ATR FTIR spectrum of [1:1] [G3]8OR[PEG6K] 8	58
Figure A.15. ¹ H NMR spectrum of [1:2] [G3]8OR[PEG6K] 9	59
Figure A.16. ATR FTIR spectrum of [1:2] [G3]8OR[PEG6K] 9	60
Figure A.17. ¹ H NMR spectrum of [1:3] [G3]8OR[PEG6K] 10	61
Figure A.18. ATR FTIR spectrum of [1:3] [G3]8OR[PEG6K] 10	62
Figure A.19. ¹ H NMR spectrum of [G3]8OH[PEG2K] 11	63
Figure A.20. ATR FTIR spectrum of [G3]8OH[PEG2K] 11	63
Figure A.21. ¹ H NMR spectrum of [1:1] [G3]8OR[PEG2K] 12	65
Figure A.22. ATR FTIR spectrum of [1:1] [G3]8OR[PEG2K] 12	66
Figure A.23. ¹ H NMR spectrum of [G3]8OH[PEG4K] 13	67
Figure A.24. ATR FTIR spectrum of [G3]8OH[PEG4K] 13	68
Figure A.25. ¹ H NMR spectrum of [1:1] [G3]8OR[PEG4K] 14	69
Figure A.26. ATR FTIR spectrum of [1:1] [G3]8OR[PEG2K] 14	70

LIST OF TABLES

Table 3.1. Properties of hydrogels with variations in dendron-polymer structure, alkene to alkyne ratio and polymer length	22
--	----

LIST OF ABBREVIATIONS

Bis-MPA	2,2-bis(hydroxymethyl)propionic acid
CDCl ₃	Deuterated chloroform
CH ₂ Cl ₂	Dichloromethane
D ₂ O	Deuterated water
DCC	Dicyclohexylcarbodiimide
DMAP	N,N Dimethylaminopyridine
EtOAc	Ethyl Acetate
FT-IR	Fourier Transform Infrared
MeOH	Methanol
NMR	Nuclear Magnetic Resonance
PEG	Poly(ethylene glycol)
py	Pyridine
TEA	Triethylamine
TEG	Triethyleneglycol
THF	Tetrahydrofuran
FITC	Fluorescein isothiocyanate

1. INTRODUCTION

1.1 Hydrogels

Hydrogels are polymers crosslinked via ionic interactions, chemical bonds, hydrogen bonds, hydrophilic interactions or physical bonds. These materials have large number of hydrophilic groups and capacity to hold fluid in their three dimensional network structure. Hydrogels absorb water and swell readily without dissolving (Figure 1.1) and shrink on drying.

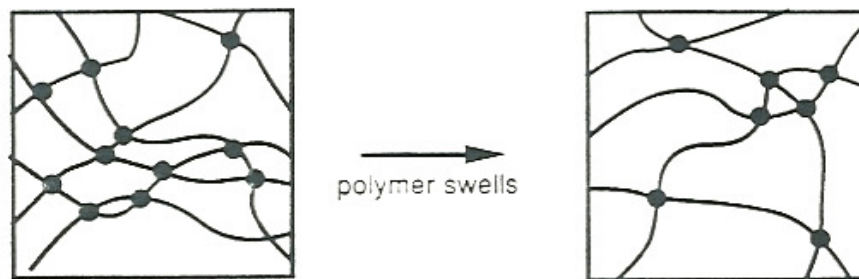


Figure 1.1. Schematic representation of a swelling hydrogel

Hydrogels have a wide range of application area as biomedical applications including drug delivery, cell encapsulation and tissue repair, coating materials and devices. As a deep look for cell encapsulation application of hydrogels, scientists take advantage of the critical interactions between cells and extracellular matrix (ECM) to create bioactive materials capable of controlling cell function and tissue evolution (Figure 1.2). To determine the requirements of the microenvironment, they utilize hydrogels easily modified with respect to mechanical integrity, adhesive peptides, ECM molecules, degradability, and incorporation of drugs, to direct cellular differentiation through a variety of mechanisms [1-18].

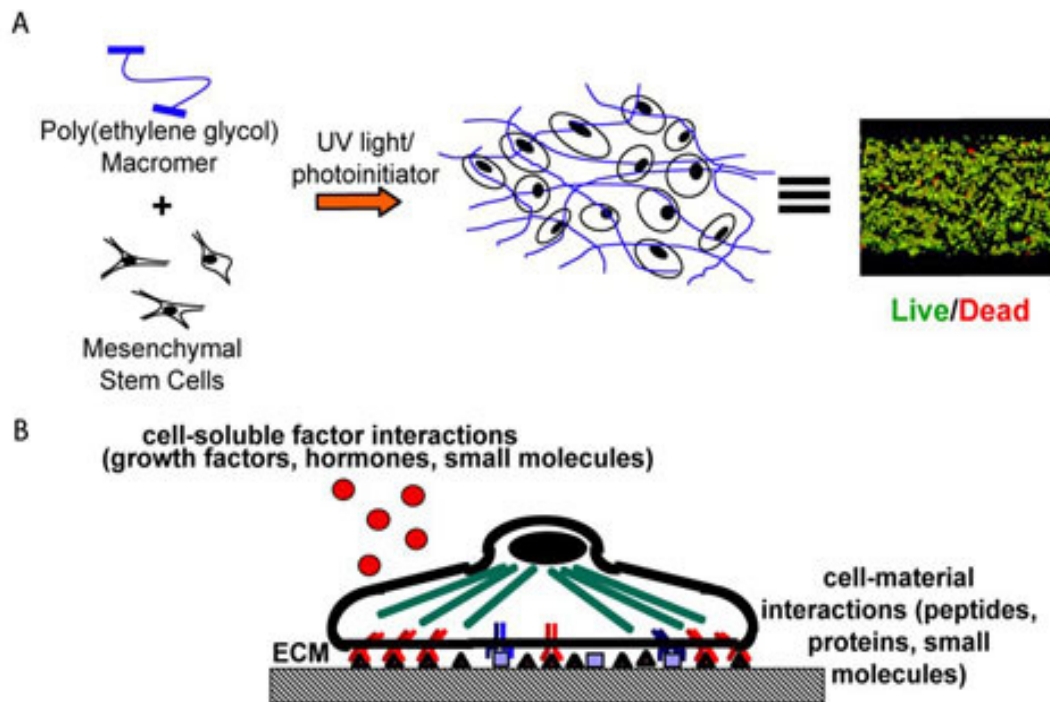


Figure 1.2. Hydrogels as a tool for cell encapsulation (A) and cell adhesion (B)

Solution of poly(ethylene glycol) macromolecules with vinyl functionalities is combined with stem cells and photopolymerized yielding viable encapsulated cells (Figure 1.2.a). Utilizing hydrogel microenvironments to direct encapsulated adult stem cell function in tissue engineering is an important area of interest. A thorough understanding of how material properties effect cell differentiation and tissue evolution is essential to tailor ‘instructive materials’ to direct cell function. Besides, hydrogel characteristics are altered to provide environment for cell-material interactions and soluble factor delivery to control cell differentiation and function (Figure 1.2.b) [19].

Hydrogels can be exploited to encapsulate and deliver cells and biomolecules therapeutically. Delivery characteristics can be controlled through alterations in hydrogel biophysical and biochemical structure and used as a powerful tool in tissue regeneration, wound healing, or control inflammation. Their biophysical and biochemical characteristics can be also altered to control angiogenic growth factor delivery.

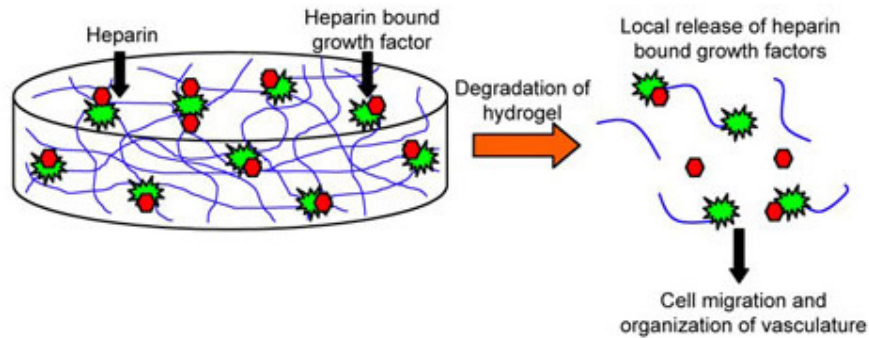


Figure 1.3. Hydrogel used to control angiogenic growth factor delivery

Hydrogels that designed to encapsulate cells and control the availability of therapeutic molecules such as growth factors, gene vectors, or small interfering RNA, will be useful for these therapeutic strategies. As an example, heparin functionalities which represent a blood thinner that prevents the formation of blood clots can be incorporated into hydrogels to control the release of angiogenic growth factors for treatment of chronic wounds (Figure 1.3.) [20].

1.2. Methods to Synthesize Hydrogels

Hydrogels can be represented according to their methods of synthesis as physically or chemically crosslinked. Physical hydrogels are formed by various reversible links [21]. These can be ionic interactions as in ionically crosslinked hydrogels and polyelectrolyte complexes and ionically crosslinked hydrogels are generally considered as biocompatible and well-tolerated. Ionic polymers can be crosslinked by the addition of di- or tri-valent counterions (Figure 1.4) [22].

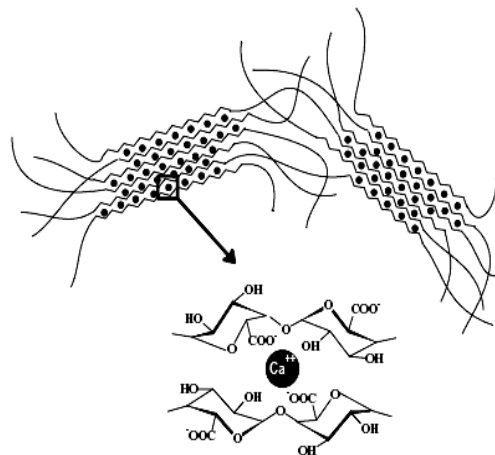


Figure 1.4. Gelation of sodium alginate by addition of Ca^{+2} ions

Covalent crosslinking leads to formation of hydrogels with a permanent network structure, since irreversible chemical links are formed. This type of linkage allows absorption of water and/or bioactive compounds without dissolution and permits drug release by diffusion. Their non-permanent network is formed by reversible links.

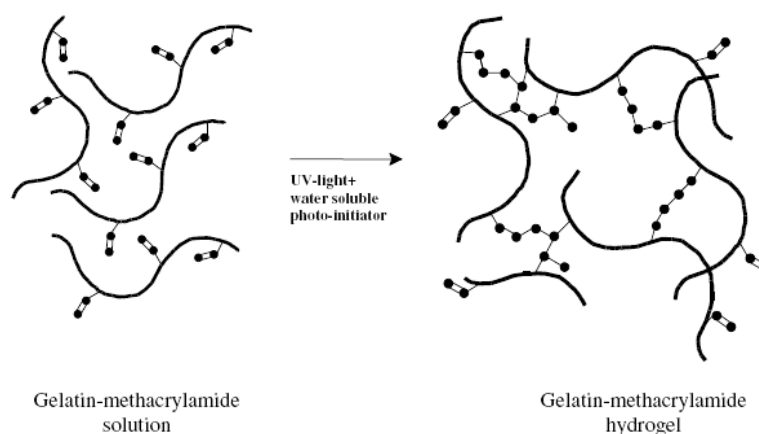


Figure 1.5. Chemical modification of gelatin with methacrylamide side groups

The methacrylamide side groups are introduced by reaction with methacrylic anhydride with the amino groups of lysine residues (Figure 1.5) [22]. The degree of modification, which can be varied by controlling the reaction conditions, determines to a large extent the mechanical properties of the resulting hydrogel. Photopolymerization, Michael addition reaction and click chemistry examples are some of the chemical crosslinking examples (Figure 1.6).

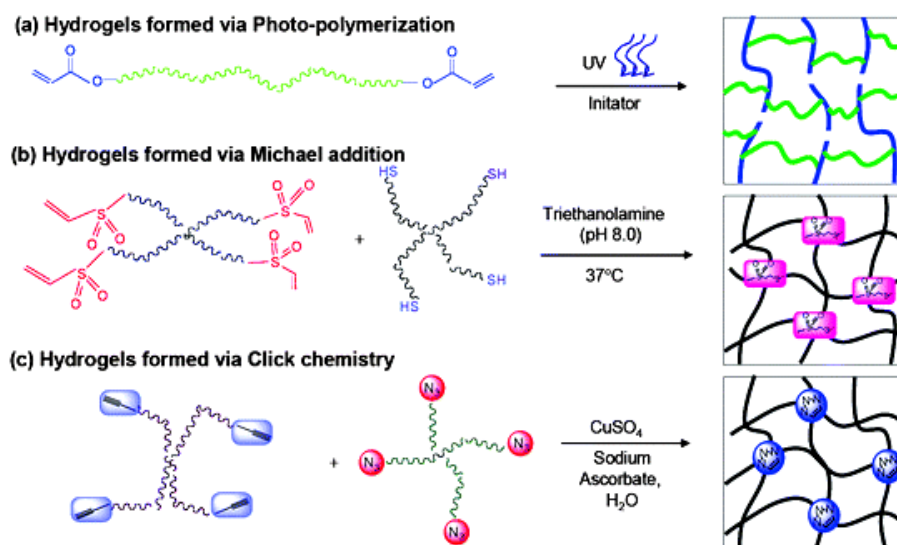


Figure 1.6. Hydrogel examples via chemical crosslinking methods [23]

1.3. Dendrimers

A synthetic, three-dimensional macromolecule formed using a nanoscale fabrication process. “Dendrimer” word comes from the Greek “dendra”, meaning “tree”. A dendrimer is built up from monomers, with new branches added in steps until a tree-like structure is created.

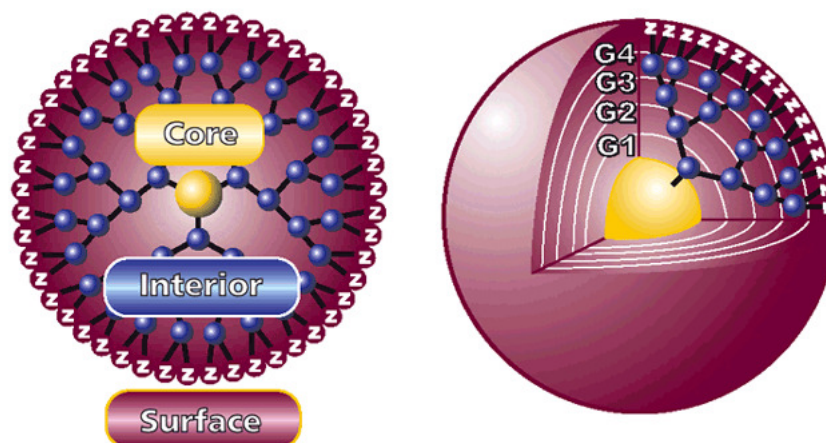


Figure 1.7. Dendrimer structure [24]

For a deeper look to dendrimer structure, the repeated units of the dendrimer between the core and surface that multiplies the number of surfaces each generation are the “branches”. The branches play a key roll in defining the chemical environment and void spaces of the interior of the dendrimer. The center of the dendrimer where the branches are attached is “core”. The core determines the initial degree of branching and contributes to the internal properties of the dendrimer and “dendron” is the dendrimer that radiates from fewer than all of its branch points at the core, often half a dendrimer. Finally, the number of synthesis cycles that the dendrimer has gone through is the “generation”; G1, G2, etc [24-25].

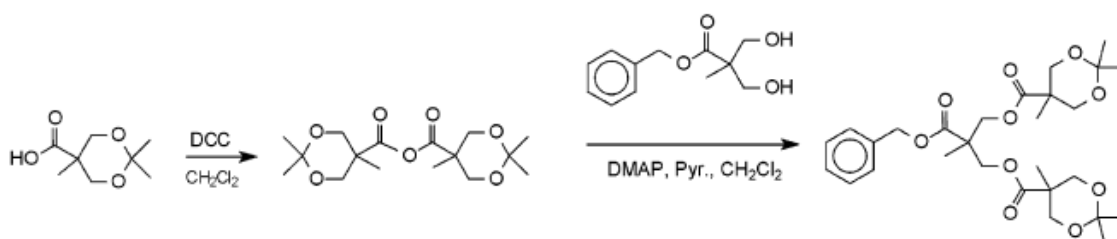


Figure 1.8. G2 benzyl ester dendron synthesized by coupling reaction

Dendrimers are very promising candidates as components of drug delivery systems. In contrast to conventional polymers, these molecules with their well-defined architecture possess a very low polydispersity or even a unique molecular weight, together with a highly regular branching pattern, and a strictly controlled multiplicity of reactive chain ends [26-30]. Therefore, it is possible to introduce or modify a specific number of functional groups on the periphery of a dendrimer, which can be used to alter its properties, such as its solubility or hydrodynamic volume, or can provide a specified number of readily accessed attachment points for drug loading. The design and synthesis of a polyester dendrimer scaffold based on 2,2-bis(hydroxymethyl)propionic acid reported in Figure 1.8. This scaffold is a promising candidate for drug delivery applications, as it shows very good biocompatibility and can be easily prepared [31].

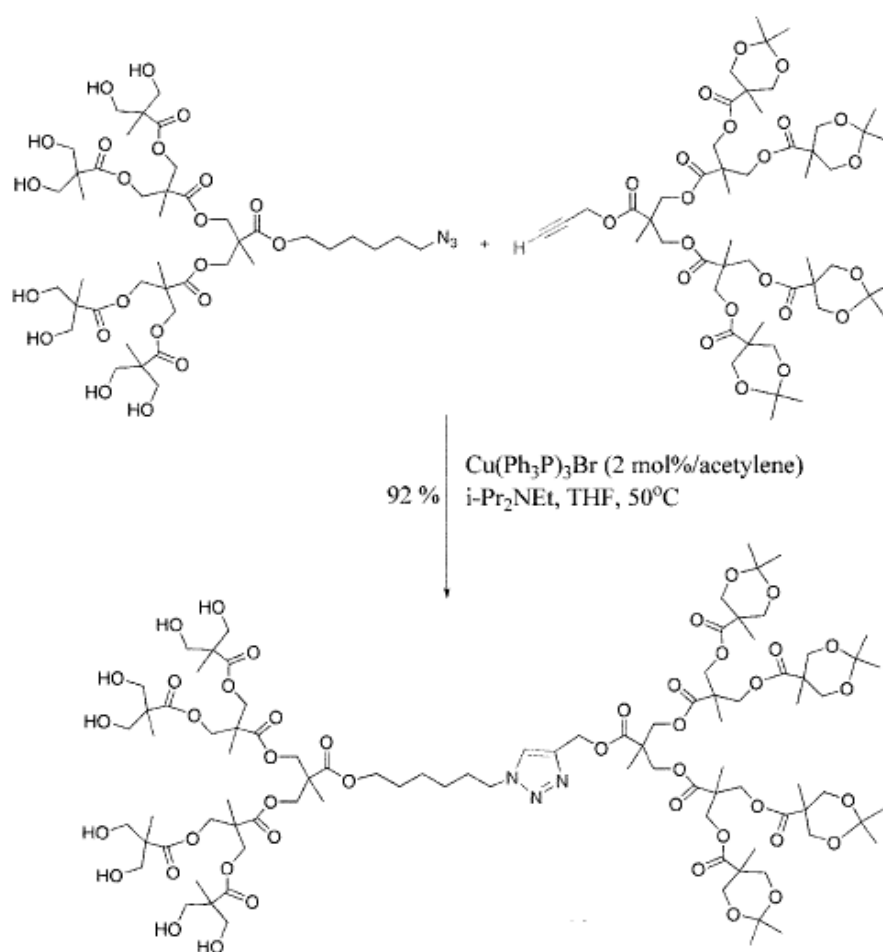


Figure 1.9. Dendrimer synthesized by Huisgen cycloaddition reaction

The same synthetic approach is selected that is based on 2,2-bis(hydroxymethyl)propionic acid (bis-MPA) as a biocompatible building block and the resulting anhydride provides easy access to both the dendritic blocks containing either a single acetylene or azide group at the focal point. Coupling of the differentiated dendritic blocks containing a variety of chain end functional groups proceeded smoothly under the copper(I)- catalysis conditions using Click methodology (Figure 1.9) [31-37].

1.4. Dendritic Hydrogels

Dendritic macromolecules would be the ideal candidates or cross-linking agents [38, 39]. They have highly symmetrical, perfectly branched structures and multiple reactive sites placed in the interior and at the periphery of the macromolecules. The number of the junctions and their chemical composition can be easily controlled by the generation of the dendrimer. The fractal character of the dendritic interior provides unique possibilities for size-selective encapsulation, manipulation and release of different substrates [40].

The synthesis of amphiphilic hydrogels with highly shape persistent cross-link junctions using PEG as linear blocks and surface-functionalized poly(benzyl ether) dendrimers is shown by Gitsov and Zhu (Figure 1.10). The synthetic strategy is based on the reaction of PEG with isocyanate or epoxy end groups as the hydrophilic component and hydrophobic dendritic poly(benzyl ethers) with amino groups at the periphery.

Dendrimers are highly branched polymers possessing three main structural zones consisting of a central core, internal branching layers, and peripheral groups [38]. Importantly, since these polymers possess narrow molecular weight distributions, unlike most polymers, one can correlate a specific biological response and physical property to an exact structure.

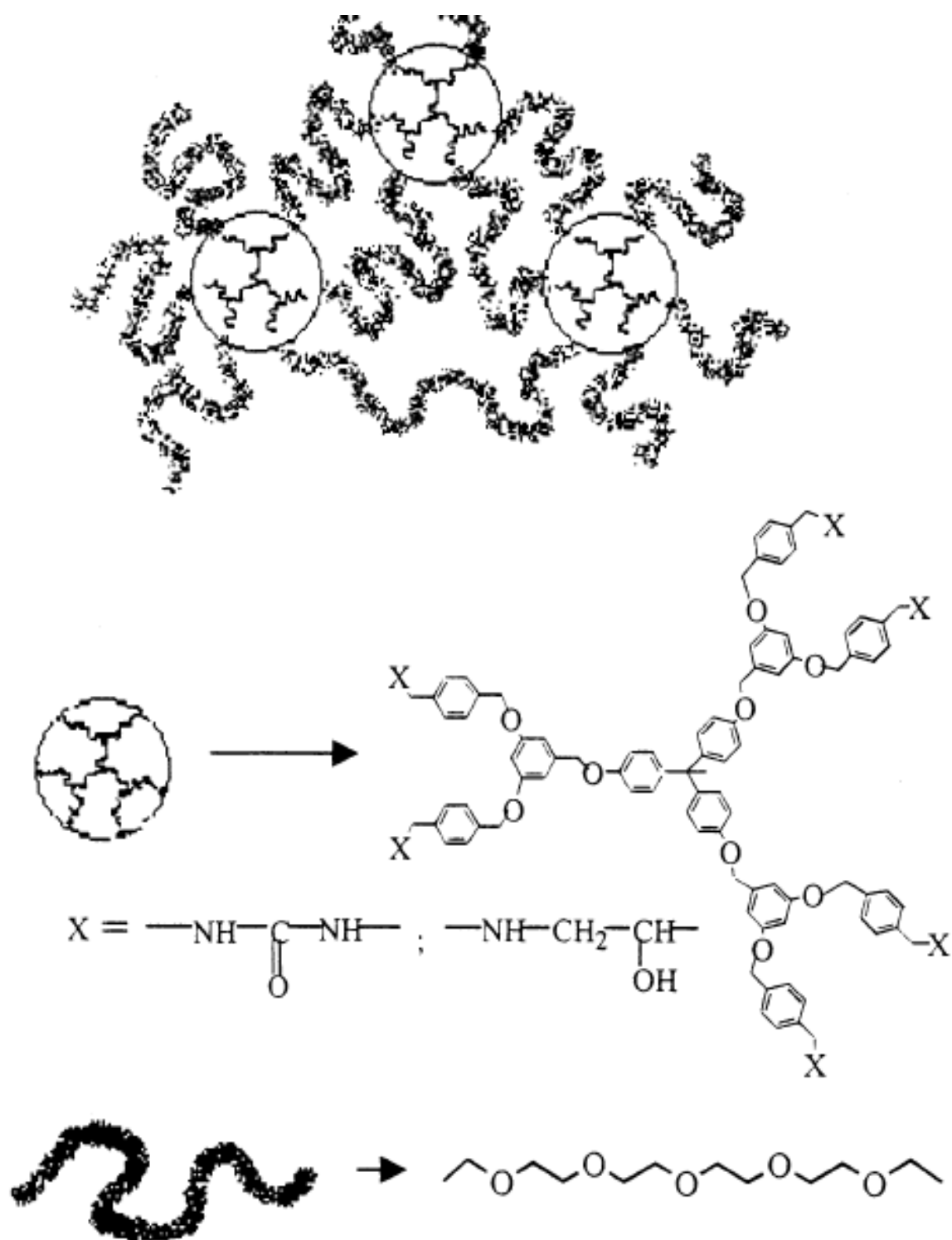


Figure 1.10. Schematic representation of a hydrogel constructed by linear and dendritic fragments

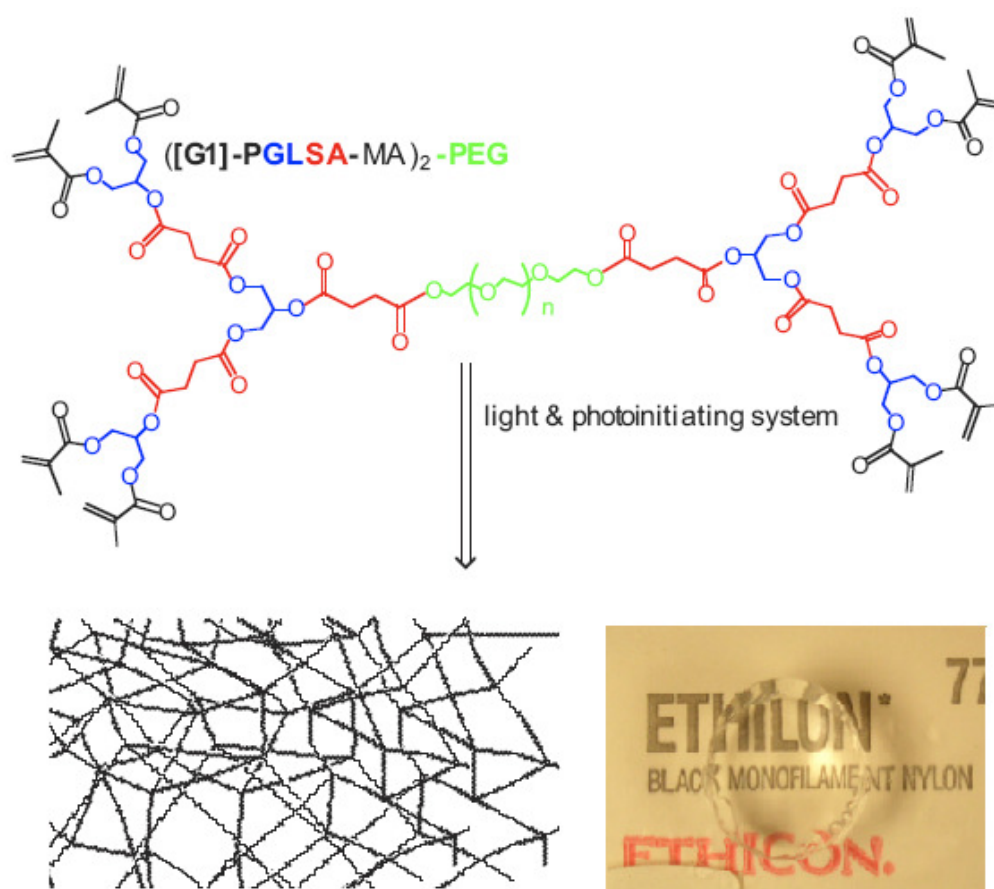


Figure 1.11. Scheme of the photocrosslinked hydrogel formation

The end groups of the dendritic macromolecule are modified to contain an acrylate or other free-radical polymerization group. Upon exposure to visible light the acrylated-modified dendritic macromolecule crosslinks to form a hydrogel. Photolysis of the solution using a 514 nm light initiates the free radical polymerization of the methacrylate moieties on the dendritic polymer (Figure 1.11). This initiating system has been previously used and shown to be non-toxic [41-44]. This photocrosslinking approach which delivers a liquid polymer to a site followed by solidification of the polymer via light to form a three-dimensional hydrogel network is an exciting modality being explored by many groups because of the advantages of photopolymerization including the ability to convert rapidly a liquid monomer or macromer to a gel at physiological temperatures with temporal and control during polymerization to form complex three-dimensional architectures with controlled mechanics [45].

1.5. Reactive Hydrogels

The ability to functionalize hydrogels is a useful tool for applications such as protein delivery in tissue engineering, guided cell growth and controlled drug delivery. Immobilization is generally accomplished either by physisorption or by covalent attachment of molecules of interest [46, 47].

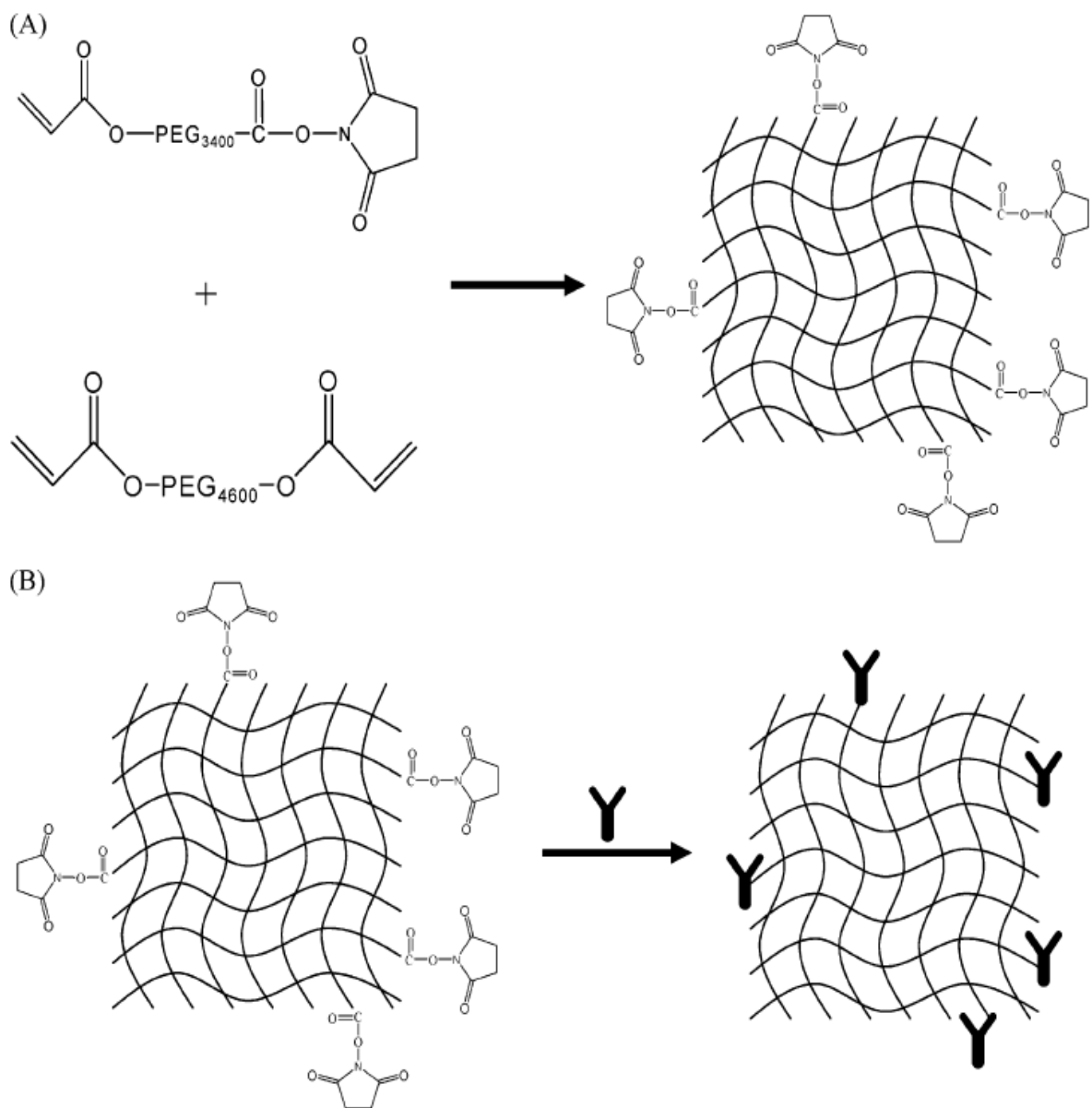


Figure 1.12. (A) Schematic representation of photopolymerization of PEG4600 diacrylate and *N*-hydroxysuccinimide-PEG-acrylate, (B) conjugation an antibody to the surface of these hydrogels

As Charles Y. Cheung and Kristi S. Anseth reported, poly(ethylene glycol diacrylate) was polymerized with *N*-hydroxysuccinimide-PEG-acrylate by UV-initiated photopolymerization. Thereafter, mouse anti-human IgG was conjugated to these hydrogels (Figure 1.12). Developing systems with higher degrees of grafting proteins or any other biomolecules on hydrogel surfaces allows long-term graft survival [48].

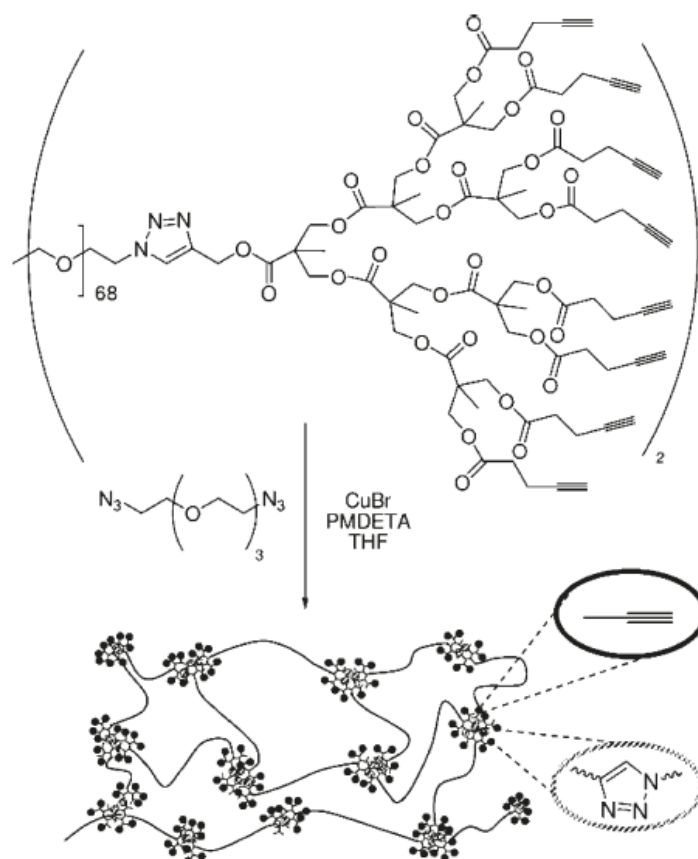


Figure 1.13. Hydrogel Formation via Cross-Linking of Dendron-Polymer Conjugates

Another functionalizable hydrogel model is shown by Huseyin Altun via Huisgen-type copper-catalyzed click reaction between polyester dendrons and linear PEG polymers to access dendron-polymerdendron conjugates necessary for the hydrogel formation [56, 57]. Functionalization of the dendron periphery with alkyne groups affords hydrogel precursors and some of these alkyne groups are cross-linked using a bisazide. Residual alkynes of the resulting hydrogel allow covalent functionalization of the hydrogel via “click” reaction. [46]

1.6. Patterning of Hydrogels

Tissue engineering requires a matrix to guide cell growth and differentiation within a three-dimensional system and cells are needed to be guided in chemically patterned volumes inside a hydrogel [49, 50]. For control of cell growth in a spatially directed manner and better mimic the complex cell-adhesive architecture of the central nervous system, there should be more sophisticated 3D-modified volumes such as chemical channels, subsurface tunnels, and networks.

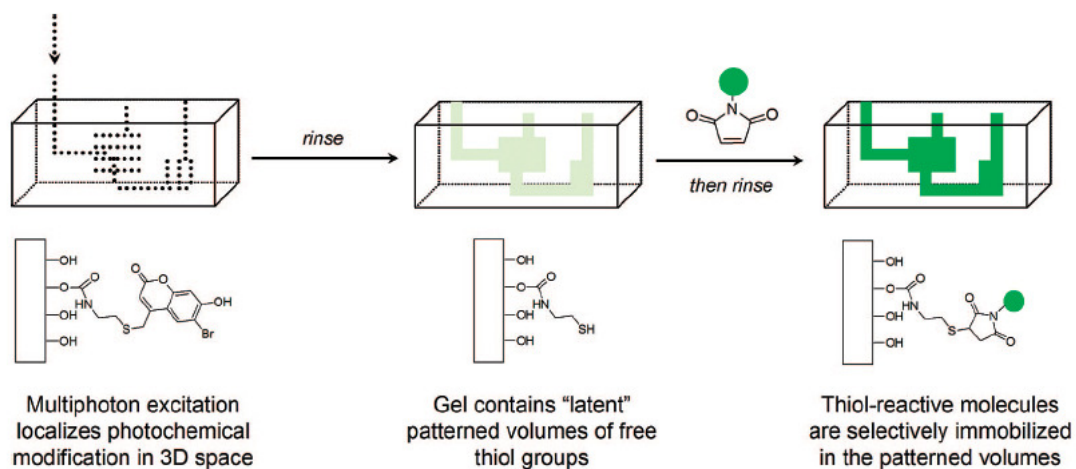


Figure 1.14. Schematic representation chemical patterning in hydrogels

Therefore, 3D chemically defined patterns used for photoinitiated polymerization. The resulting gel contains free thiol groups which can go further functionalization meaning thiol reactive groups can be immobilized in the patterned volumes (Figure 1.14) [51]. The resulting patterned hydrogels have applications in tissue engineering, where they can be used to control cell behavior, alter gene expression [52], regulate the structure of the resulting tissue [53], and affect the mechanical properties of the developing tissue [54, 55].

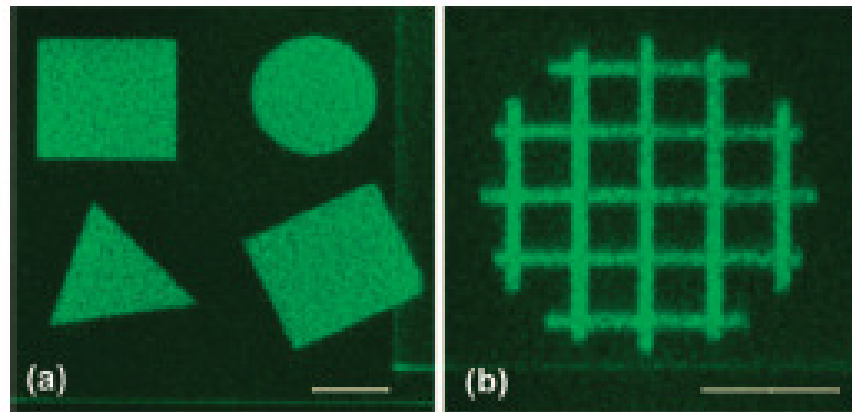


Figure 1.15. Confocal micrographs of fluorescent hydrogels in geometric shapes (*a*) and shape of a grid (*b*) [51]

Fluorescent pictures of hydrogels were created by photochemical immobilization of fluorescently labeled maleimide molecule on hydrogel sample having scale bars of $50\ \mu\text{m}$ (Figure 1.15).

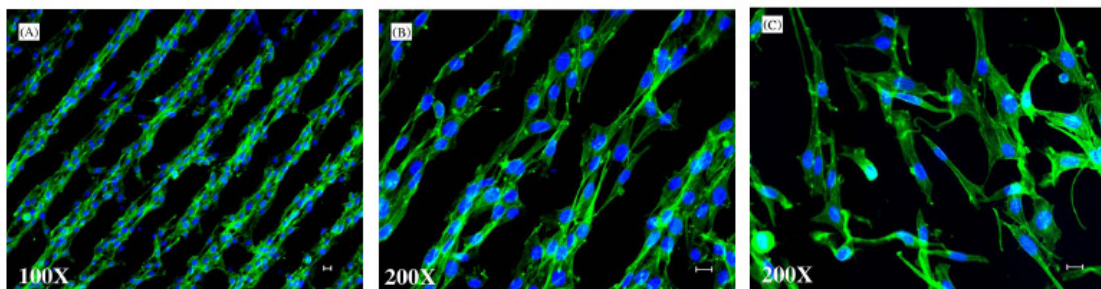


Figure 1.16. Fluorescent photomicrograph of cells plated on patterned hydrogels (Size bar $20\ \mu\text{m}$)

The surfaces of HA (hyaluronic acid) and HA–collagen hydrogels were patterned by casting on Teflon dishes that contained patterns. Immediately after crosslinking, the pattern on the hydrogel was complementary to the pattern of the Teflon dish. Fluorescence microscopy showed that the cells were aligned with the pattern when plated on the patterned surface after hydration (Figure 1.16) [55].

2. AIM OF THE STUDY

Multivalency in dendrons is a promising property to have reactive crosslinked materials. In our study dendrons are combined with polyethylene glycol molecules to have Dendron-polymer-dendron conjugates by Huisgen click reaction. The surface of these conjugates functionalized with methacrylate and alkyne groups. In the presence of different ratios of methacrylates, UV curing is used to form crosslinked materials which still have unreacted alkyne groups on the surface. These unreacted alkyne groups are used for further functionalization of the obtained hydrogels.

Characterization methods like IR spectroscopy and fluorescent microscopy, the presence of triple bonds in the hydrogels is proved. Thereafter, with microcontact printing methods, we show the shape and size control of the hydrogels. Overall, we achieve the synthesis of hydrogels that have high water absorbance, biocompatibility and biodegradability, have controlled shape and size as candidates for medical applications.

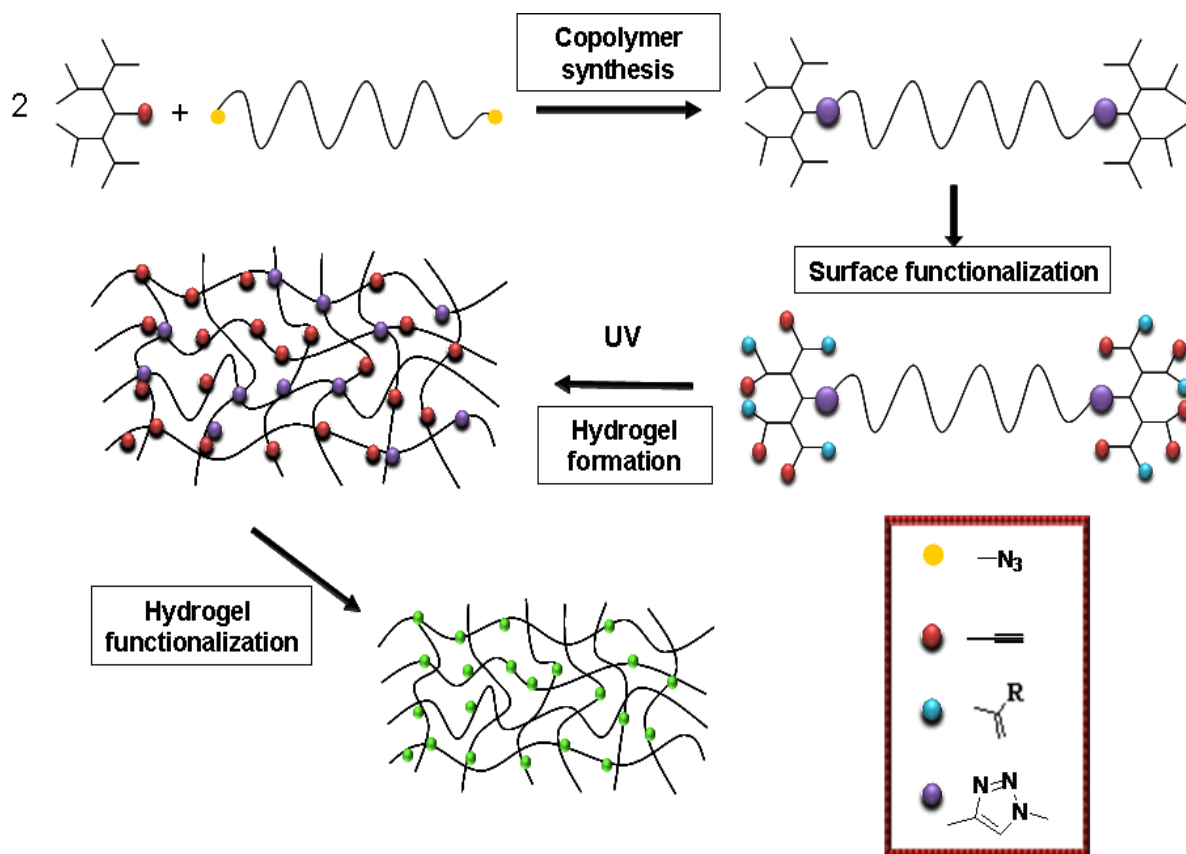


Figure 2.1. General representation of the synthesis of functional hydrogels

3. RESULTS AND DISCUSSION

3.1. Synthesis of Functional Hydrogels

Dendron-polymer-dendron copolymer hydrogel precursors are synthesized by combining biodegradable polyester dendrons and biocompatible and hydrophilic linear polyethylene glycol molecules via Huisgen cycloaddition reaction. The surface groups of the dendrons are functionalized with methacrylic anhydride and pentynoic anhydride to obtain alkyne and alkene functionalities at the periphery. Finally, hydrogels are synthesized via UV irradiation and further functionalized by again Huisgen cycloaddition reaction.

Synthesis of ABA type triblock copolymers that consist of G3 polyester dendrons and PEG molecules and their functionalization are shown in Figure 3.2. As A block of this copolymer, polyester dendrons were chosen. Synthesis of these second and third generation dendrons was performed according to literature. B block of the copolymer were linear PEG diazides, were synthesized according to literature. The copolymers were named according to their dendron generation, surface functionality and length of the PEG group i.e. [G3]8OH[PEG6K] represents the third generation dendrons are third generation having eight alcohol groups on the surface with the middle block PEG MW=6000.

The copolymers were synthesized via the “click” reaction of G2 and G3 polyester dendrons that bear alkyne functionality at their core and PEG diazide molecules with 2K, 4K and 6K molecular weight in the presence of CuBr and PMDETA and THF as solvent. Functionalization of the terminal alcohol groups was performed by acylation reaction with pentynoic anhydride and methacrylic anhydride in different ratios in the presence of pyridine and DMAP yielding molecules **3, 4, 5, 7, 8, 9, 10, 12, 14**. The methacrylate groups of the copolymers were utilized for the crosslinking by UV irradiation forming desired hydrogels.

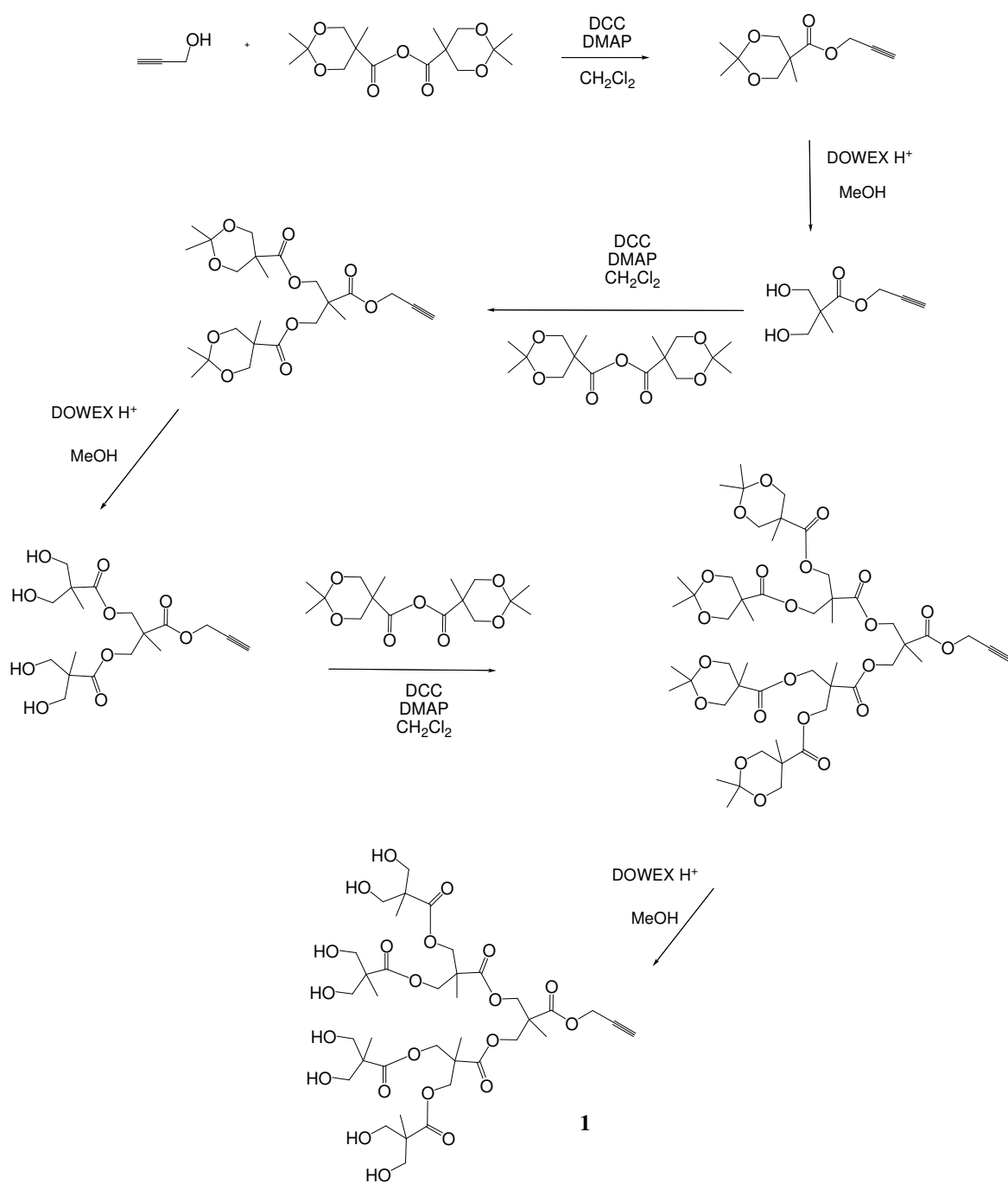


Figure 3.1. Synthesis of G3 polyester dendron

Alkene functionalized copolymers were dissolved copolymers in water and EtOH mixture and crosslinked in the presence of a photoinitiator under UV for 5 minutes to obtain hydrogels. To improve the solubility of the copolymers EtOH was used as a cosolvent. Depending on the ratio of alkene to alkyne groups at the periphery, hydrogels with different alkyne amounts were obtained.

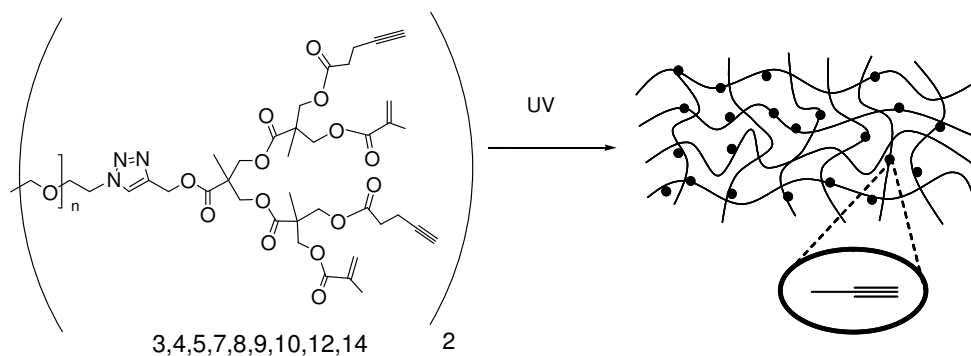


Figure 3.3. Schematic representation of hydrogel formation

3.2. Characterization of Copolymers and Functional Hydrogels

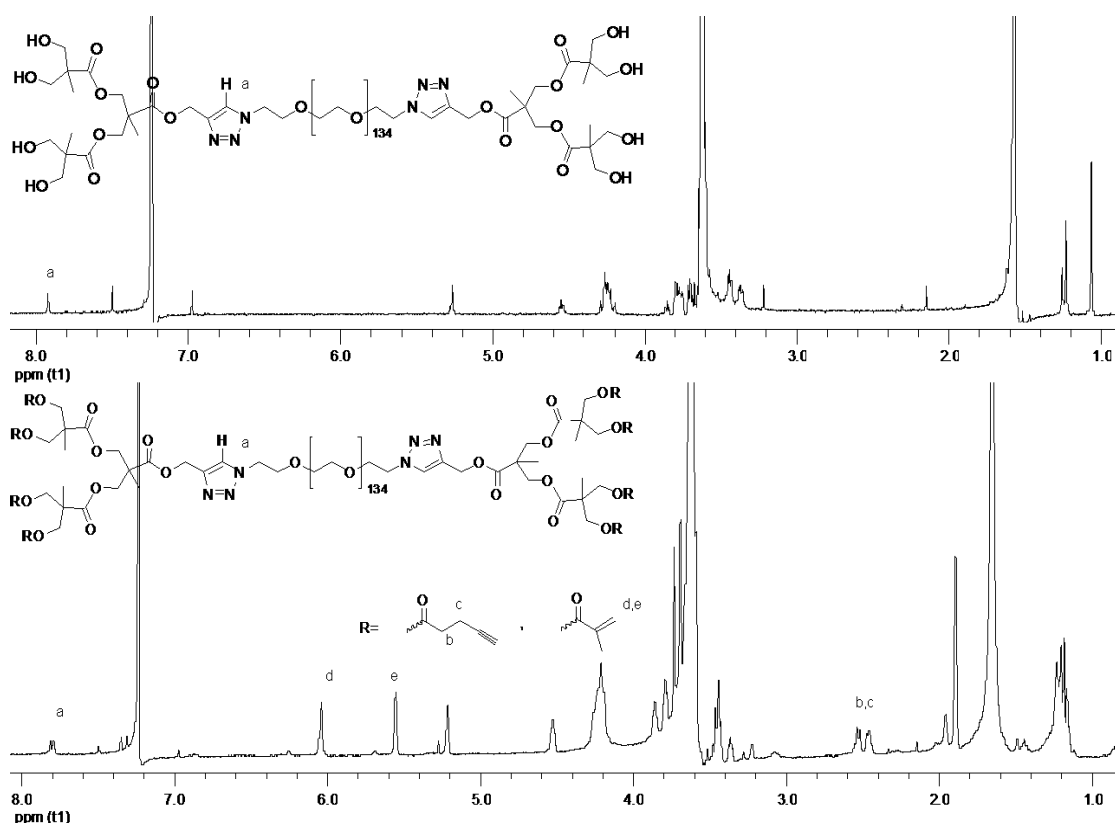


Figure 3.4. ^1H NMR spectrum of $[\text{G}2]4\text{OH}[\text{PEG}6\text{K}]$ **2** and $[1:1] [\text{G}2]4\text{OR}[\text{PEG}6\text{K}]$ **3**

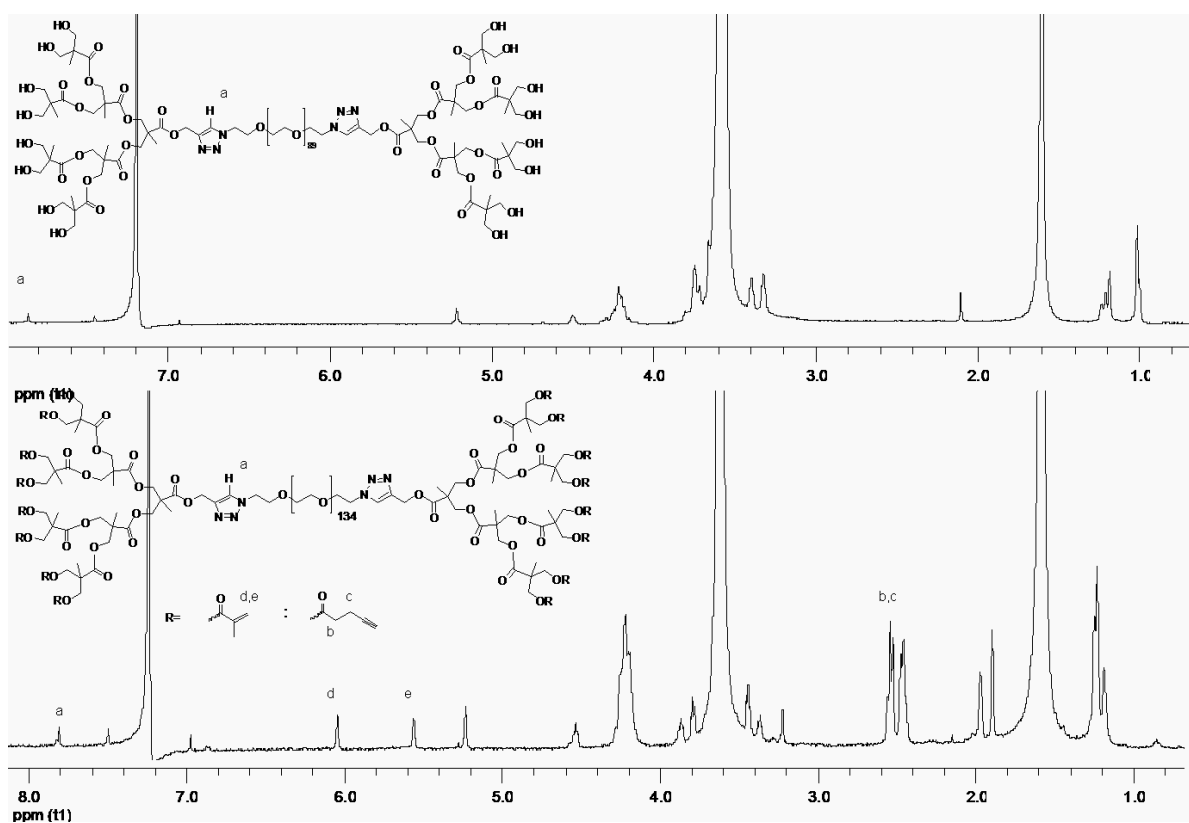


Figure 3.5. ^1H NMR spectrum of [G3]8OH[PEG6K] **6** and [1:1] [G3]8OR[PEG6K] **8**

In ^1H NMR spectrum copolymers G26K_(1:1) and G36K_(1:1) have additional peaks coming from alkene and alkyne functionalities. The hydrogen of the triazole ring that is formed after cycloaddition reaction was observed as a peak at around 7.8 ppm and signed as “a”. The two hydrogens of the alkene carbon in functionalized copolymers were observed at around 6.1 ppm and 5.6 ppm and signed as “d” and “e”. Finally the peak due to the four hydrogens next to the alkyne group was observed at around 2.5 ppm and signed as “b” and “c” (Figure 3.4, Figure 3.5).

IR spectra were also taken for characterization of the copolymers and hydrogels to show some specific peaks of these molecules.

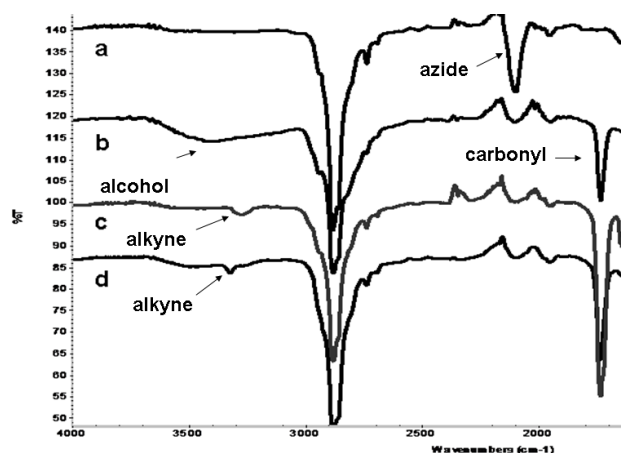


Figure 3.6. FTIR spectroscopies of (a) PEG6K bisazide, (b) PEG-dendron copolymer, (c) functionalized copolymer, (d) functional hydrogel

IR spectroscopy of PEG6K-bisazide has the specific stretching value at around 2100 cm^{-1} due to azide functionality (Figure 3.6 a). Subsequently, in IR spectroscopy of the G3 dendron PEG6K combination, disappearance of the peak due to azide group and formation of a new peak of carbonyl groups at around 1730 cm^{-1} and a broad peak at 3440 cm^{-1} due to alcohol groups of dendrons were observed (Figure 3.6 b). Thereafter, functionalization of the copolymer was performed and stretching due to alcohol groups of the dendrons in copolymer structure was exchanged with a new peak of alkyne functionality at 3280 cm^{-1} (Figure 3.6 c). In order to check the availability of these alkyne groups after crosslinking step, we need to see the same stretching and it was observed at again around 3280 cm^{-1} (Figure 3.6 d).

3.3. Swelling Properties of Hydrogels

Hydrogels are examined to understand their swelling properties. Formation of hydrogels from constructs 6KG2 and 6KG3 having PEG molecular weight of 6000 were discussed according to different ratios of double and triple bonds; 2:1, 1:1, 1:2 and 1:1, 1:2, 1:3, respectively and water uptake measurements were attempted as explained above. As anticipated, a decrease in triple bond ratio resulted in an increase in the water uptake of the hydrogel. Swelling behaviour of G26K constructed hydrogels are compared as a function of time and the equilibrium hydration levels are described in Figure 3.7. The same data also collected and a diagram representation was given for 6KG3 constructed hydrogels in Figure 3.8. The hydrogels containing higher number of alkene functionality than alkyne

showed higher degree of swelling for 6KG2(2:1), where for 6KG3 the same equivalent of alkene and triplalkyne containing hydrogel 6KG3(2:1) gave the highest swelling among all. Besides, as the PEG length increases water absorption degree increases so, the hydrogel that is of PEG6K absorbs more water than PEG4K and it absorbs more than PEG2K. (Figure 3.9)

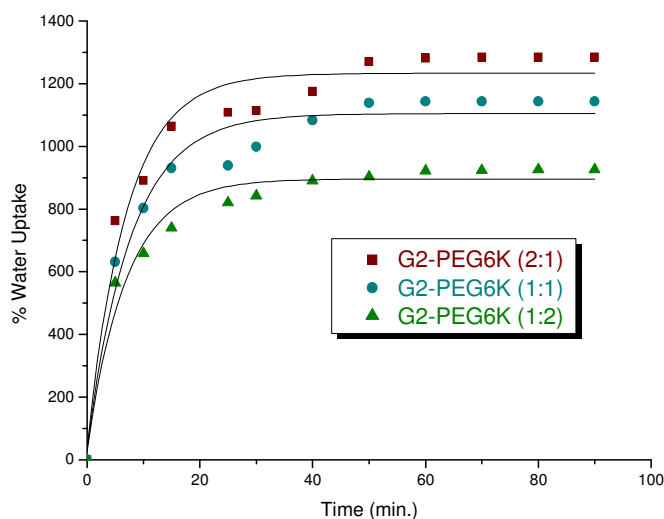


Figure 3.7. Water Uptake Comparison of $6KG2_{(2:1)}$; $6KG2_{(1:1)}$; $6KG2_{(1:2)}$ Hydrogels.

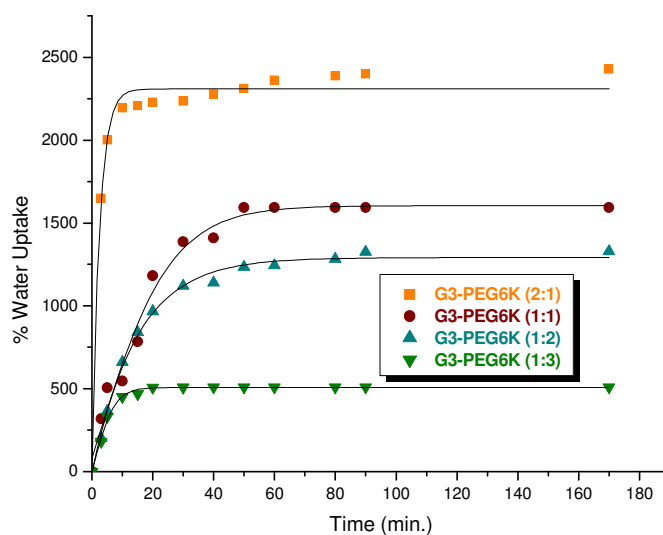


Figure 3.8. Water Uptake Comparison of $6KG3_{(2:1)}$; $6KG3_{(1:1)}$; $6KG3_{(1:2)}$; $6KG3_{(1:3)}$ Hydrogels

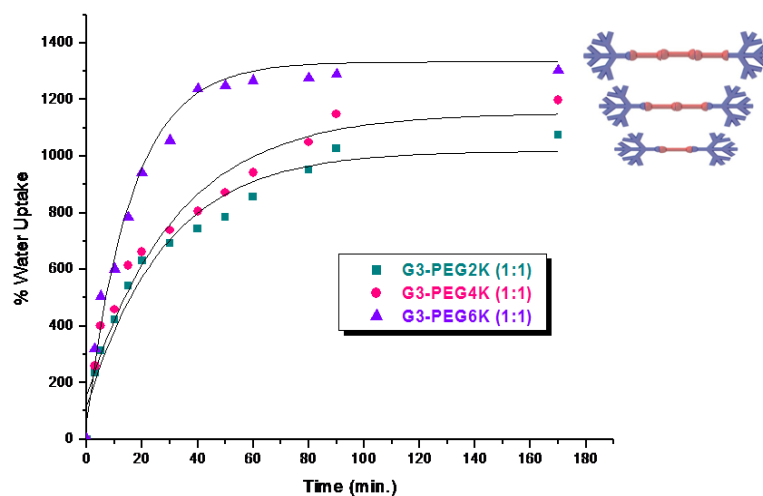


Figure 3.9. Water Uptake Comparison of **2KG3**_(1:1); **4KG3**_(1:1); **6KG3**_(1:1)Hydrogels.

The macromolecules **3**, **4**, **5**, **7**, **8**, **9**, **10**, **12**, **14** that are combinations of dendrons and PEG have different alkene to alkyne ratio and different PEG lengths. (Table 3.1)

Table 3.1. Properties of hydrogels with variations in dendron-polymer structure, alkene to alkyne ratio and polymer length.

Item	HYDROGEL	PEG	DENDRON	Double bond:Triple bond ratio	Water uptake %	Available functional groups
1	PEG6KG2 (2:1)	6000	G2	2 : 1	1286	2
2	PEG6KG2 (1:1)	6000	G2	1 : 1	1144	4
3	PEG6KG2 (1:2)	6000	G2	1 : 2	926	6
4	PEG6KG3 (2:1)	6000	G3	2 : 1	2428	6
5	PEG6KG3 (1:1)	6000	G3	1 : 1	1593	8
6	PEG6KG3 (1:2)	6000	G3	1 : 2	1329	10
7	PEG6KG3 (1:3)	6000	G3	1 : 3	510	12
8	PEG2KG3 (1:1)	2000	G3	1 : 1	1075	8
9	PEG4KG3 (1:1)	4000	G3	1 : 1	1197	8

The hydrogels labeled according to their dendron generation first, PEG length second and finally double bond to triple bond ratio. As alkene ratio on the copolymer periphery decreases, alkyne ratio increases, meaning that in the resulting hydrogel number of available functional group increases.

3.4. Morphological Studies

SEM micrographs of dry hydrogels are clearly observed 100 μm and 10 μm scales (Figure 3.10-11-12-13). As the crosslinker ratio increases, the smaller pores on the hydrogel surface can be easily observed referring that the G36K_(1:3) hydrogel is the one that has smallest pore size (Figure 3.13)

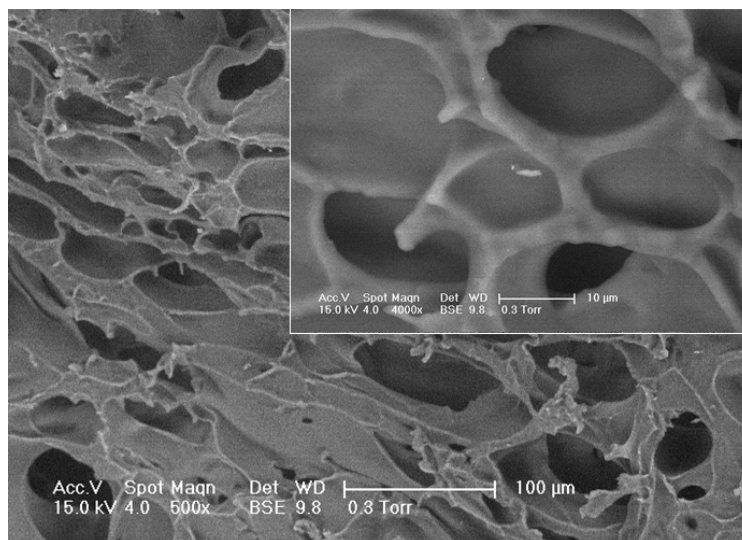


Figure 3.10. SEM images of dry hydrogel G36K_(2:1)

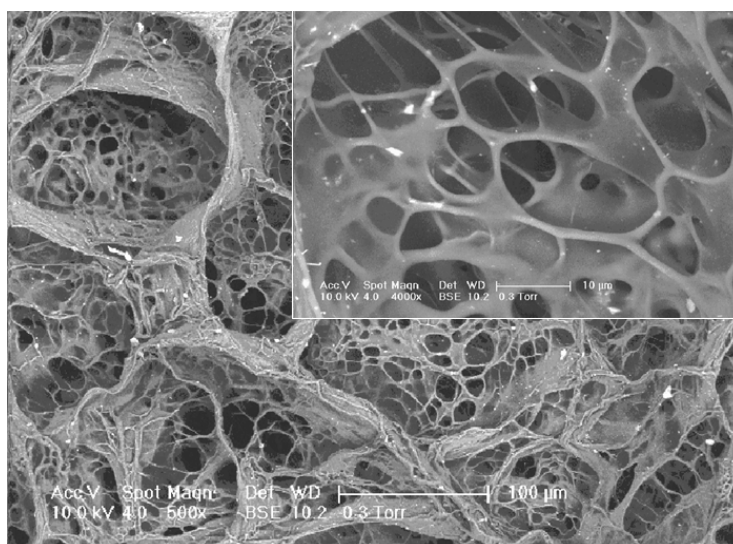


Figure 3.11. SEM images of dry hydrogel G36K_(1:1)

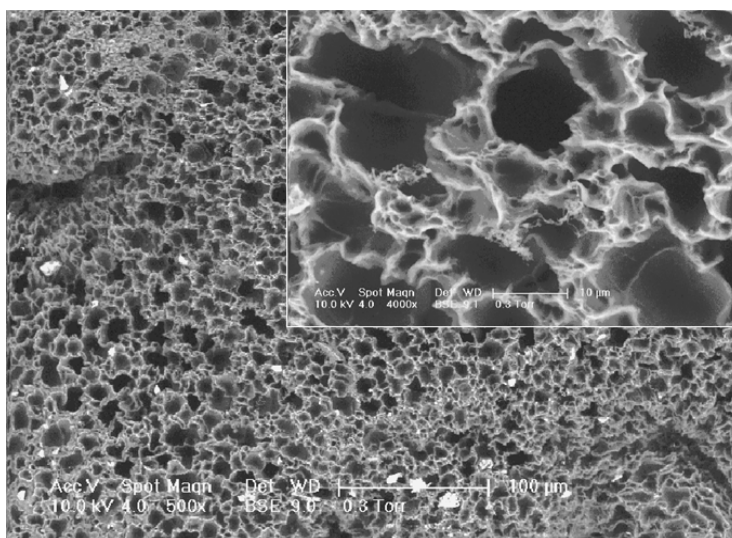


Figure 3.12. SEM images of dry hydrogel of G36K (1:2)

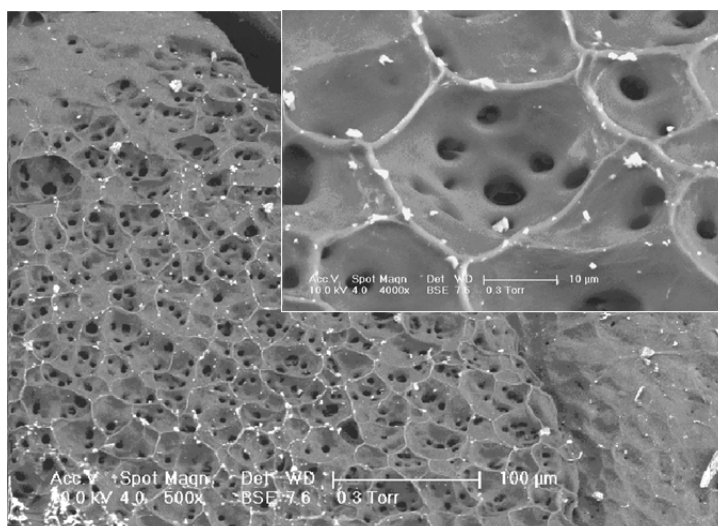


Figure 3.13. SEM images of dry hydrogel of G36K (1:3)

3.5. Functionalization of Hydrogels

To further demonstrate the presence and reactivity of alkyne groups, the hydrogels were reacted with azide containing molecules: bodipy azide and biotin azide in a [3+2] Huisgen cycloaddition.

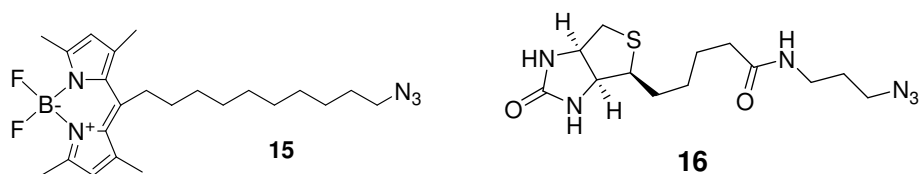


Figure 3.14. Azides that are used for hydrogel functionalization

Bodipy azide **15** has an emission at green shifted wavelengths and it is used for visualization under fluorescence microscope. The second azide: biotin azide was attached for immobilization as an example of protein attachment.

Two identical hydrogels were treated with desired azide, one with and the other without the CuSO_4 – sodium ascorbate and catalyst system to observe the physical absorption. The functionalized hydrogels became fluorescent and were observed under fluorescence microscope. Bodipy dye immobilized hydrogel were observed under fluorescence microscope in 1 ms fluorescent light (Figure 3.15).

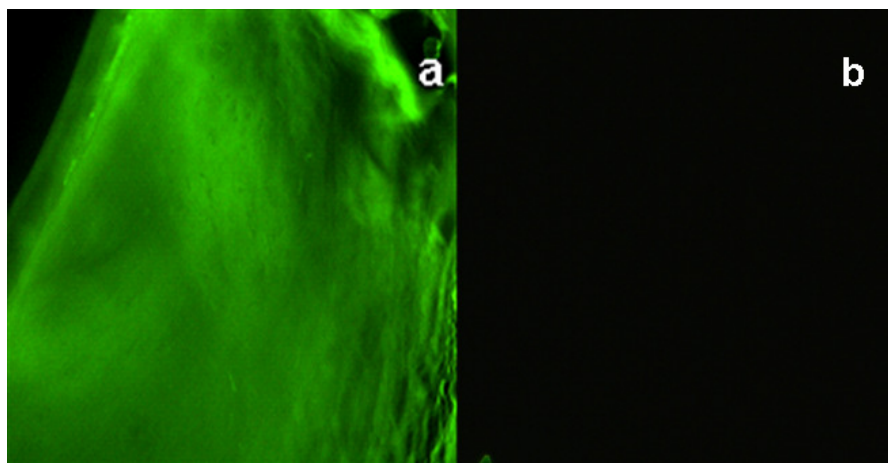


Figure 3.15. Fluorescence microscope images of functionalized hydrogels (*a*) with biotin azide (*b*) control without catalyst

Since we had many hydrogels that have different numbers of functional groups, fluorescent intensities altered according to change of available alkyne groups of hydrogels (Figure 3.16, Figure 3.18).

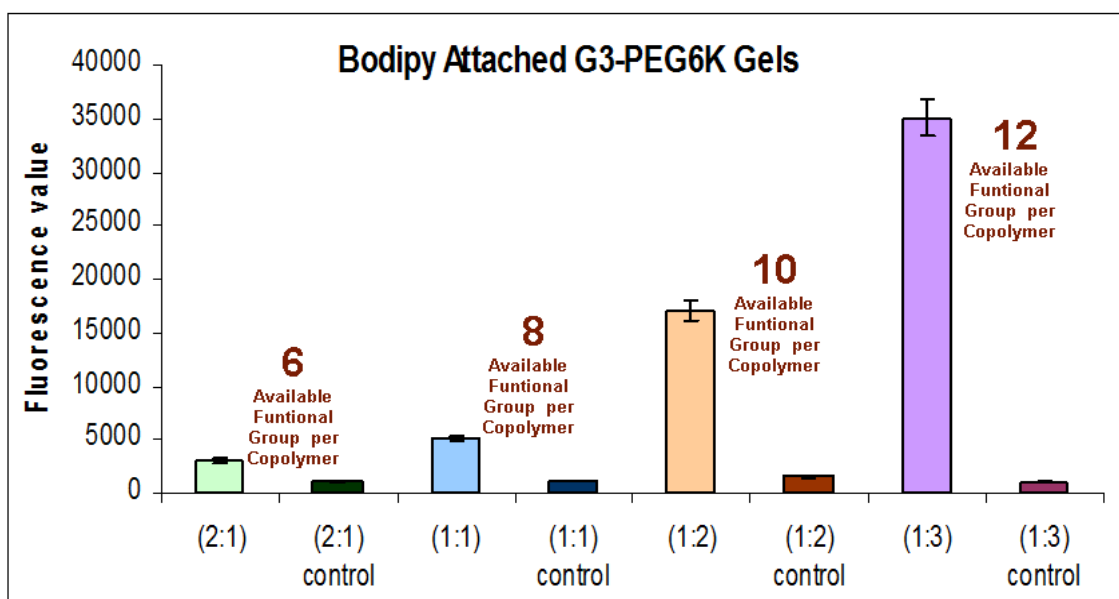


Figure 3.16. Relative fluorescence intensities of functionalized hydrogels with bodipy and their controls that contain descending amount of functional groups. (Under 1 ms fluorescence light)

Hydrogels from alkene – alkyne functionalized G3-PEG6K copolymers that have different number of alkyne groups were reacted with bodipy azide. Figure 3.9 is a summary of the results that shows the fluorescence intensity of the bodipy functionalized hydrogels increases as the number of the available alkyne groups in the hydrogels increases. The most fluorescent one is the hydrogel of G36K_(1:3) which has the largest number of available alkyne groups among the all hydrogels.

To demonstrate the enzyme immobilization, two identical hydrogels were reacted with biotin azide **16** one in the presence of CuSO₄ – sodium ascorbate catalyst and one in the absence of the catalyst. The both hydrogels were incubated with FITC labeled streptavidin under 50 ms fluorescent light. (Figure 3.17)

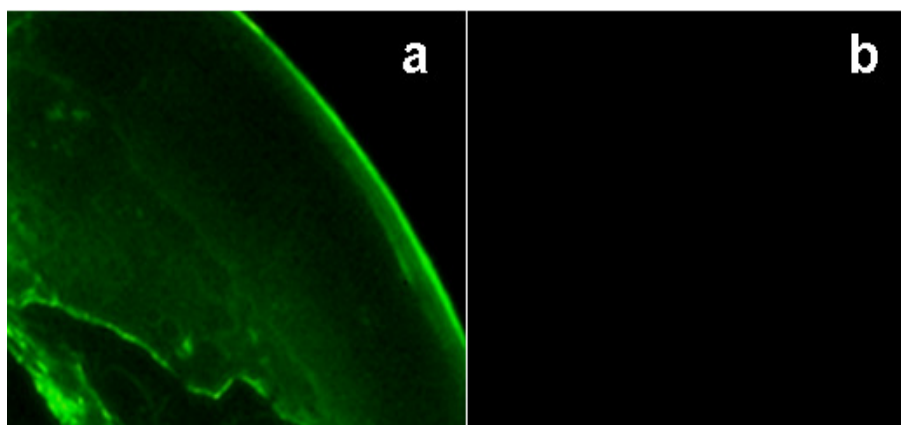


Figure 3.17. Fluorescence microscope images of functionalized hydrogels (*a*) with biotin azide (*b*) control without catalyst

The hydrogel that is reacted with biotin azide in the presence of CuSO_4 – sodium ascorbate catalyst system and immersed into FITC labeled streptavidin shows a fluorescent image under fluorescence microscope. The hydrogel reacted without the catalyst system shows that there is almost no physical absorption of the biotin and streptavidin molecules (Figure 3.17).

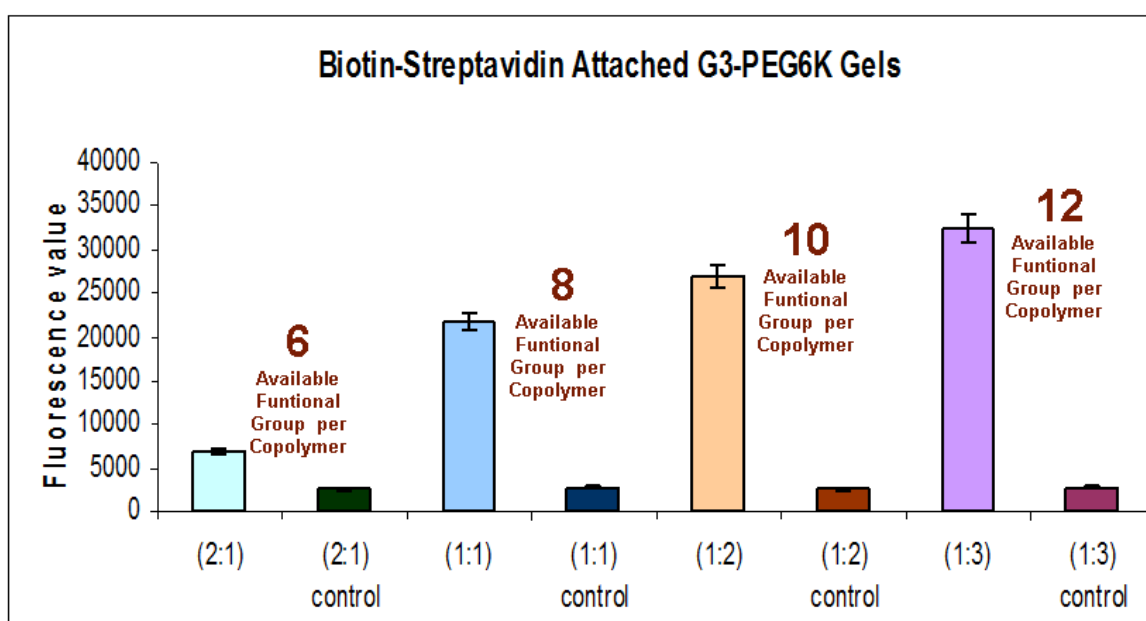


Figure 3.18. Relative fluorescence intensities of functionalized hydrogels with streptavidin and their controls that contain descending amount of functional groups. (Under 50 ms fluorescence light)

The same trend with bodipy attached hydrogels was observed for fluorescence intensities of the biotin functionalized and streptavidin attached hydrogels. As the number of the available alkyne groups in the hydrogel increases, the fluorescence intensity of the hydrogel increases. The most fluorescent one is the hydrogel of G36K_(1:3) which has the largest number of available alkyne groups among the all hydrogels.

3.6. Microcontact Molding of Hydrogels

3.6.1. PDMS Molding

Hydrogels are patterned by using PDMS mold. Onto a silicon wafer that was first functionalized with 3(trimethoxysilyl)propylacrylate, a PDMS mold having channels in micron size was put. The gel precursor which is prepared according to the same procedure with the bulk hydrogels was dropped from the edge of mold and let it move through the channels of mold and cured under UV light for 5 minutes. Finally the mold was removed and the hydrogel modified surface was washed with solvents (Figure 3.19). Optical microscopy image of the hydrogel (Figure 3.21, a), the fluorescent microscopy images of bodipy azide and biotin azide functionalized hydrogels (Figure 3.21, b, c) and the SEM image of the patterned hydrogel show the well shaped patterns (Figure 3.20).

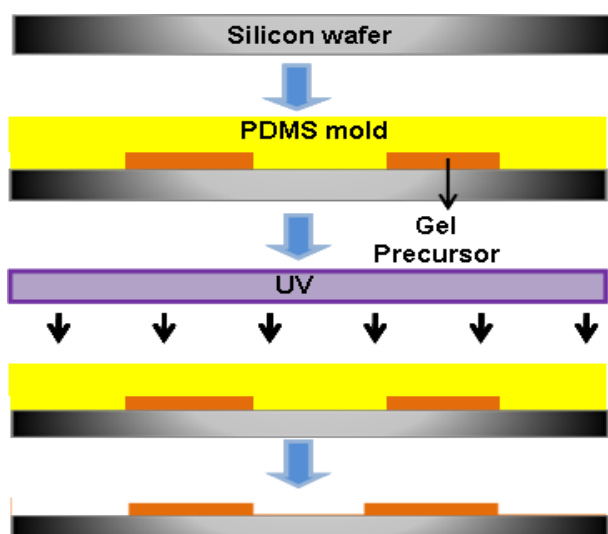


Figure 3.19. Schematic representation of PDMS molding on hydrogels

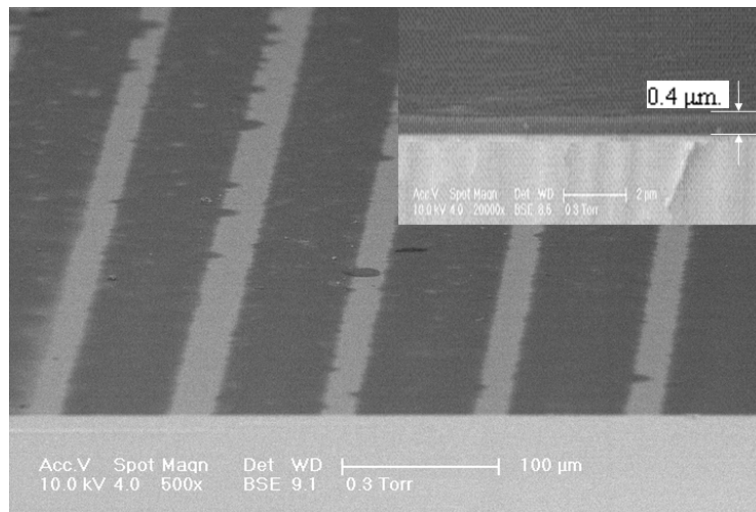


Figure 3.20. SEM images of patterned. hydrogel G36K_(1:1) by PDMS molding

SEM image of surface modified with hydrogel shows well defined patterns having 60 μm width and 0.4 μm thickness.

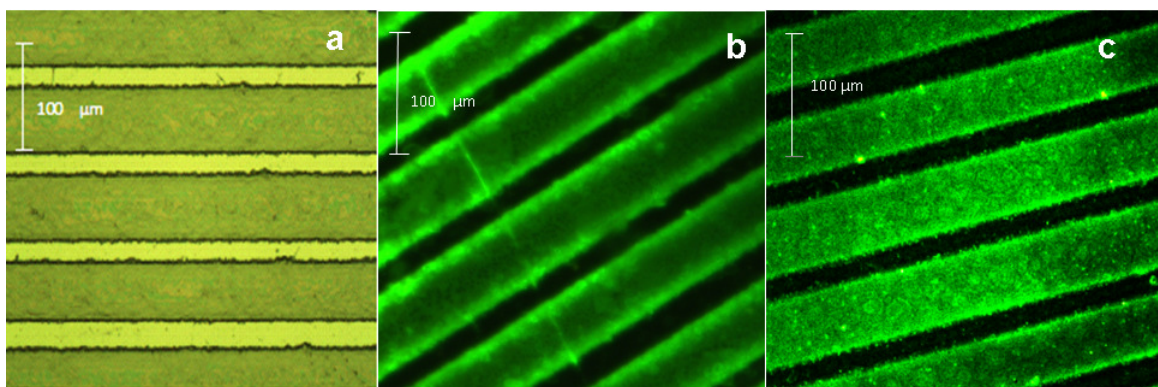


Figure 3.21. The microscope images of hydrogels (a) patterned with PDMS mold (b) patterned and functionalized with bodipy azide; (c) with biotin azide.

In Figure 3.21, the images of patterned hydrogels can be observed. The “a” is the optical microscope image of silicon surface modified with hydrogel from [2:1] [G3]8OR[PEG6K] precursor. The second one, “b” is the fluorescence microscope image of the patterned hydrogel from same precursor that is functionalized with bodipy azide after patterning process, with 1 ms fluorescence light. Finally, “c” is the fluorescence microscope image of the patterned hydrogel from same precursor that is functionalized

with biotin azide and immersed into FITC labeled streptavidine molecule, under 50 ms fluorescence light.

3.6.2. Spin Coating and Patterning via UV Mask

To the silicon wafer that was functionalized with 2% 3(trimethoxysilyl)propylacrylate, the gel precursor that contains the photoinitiator was dropped. The surface was spin coated in 2000 rpm speed for 10 seconds. To avoid the solvent loss before crosslinking, the coated surface was immediately put on a UV mask. The system was cured under UV (475 nm) for 5 minutes. The mask removed and the surface washed with EtOH and THF several times to remove the parts that were not crosslinked.

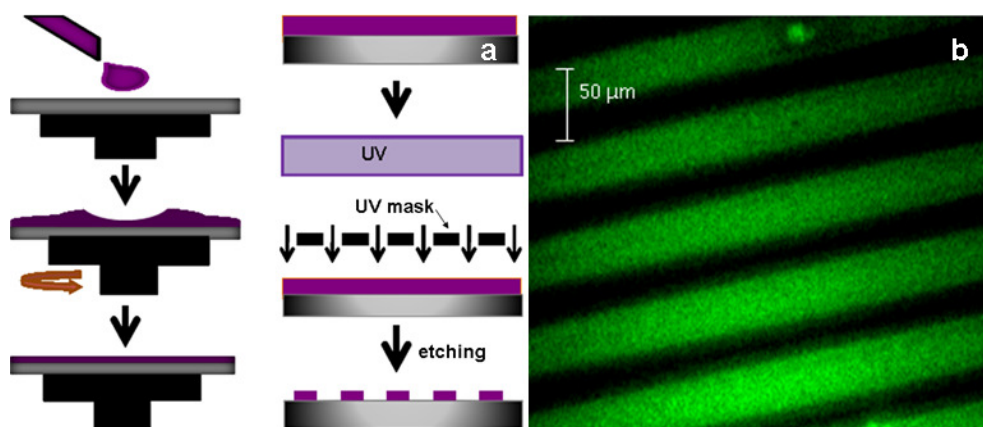


Figure 3.22. (a) Representative scheme of spin coating and UV-mask system, (b) fluorescence microscope images of patterned hydrogels from precursor by this system

Although PDMS molding is a successful method for patterning, the edges of the patterns are not sharp enough, so another method is used to have better shapes. First, onto a silicon wafer previously prepared hydrogel precursor was dropped and let it spin with 2000 rpm speed for ten seconds. Thereafter, a chromium based UV mask was put onto this coated surface and let the precursor crosslinked under UV light for five minutes following the etching process. The fluorescence microscope image of the surface modified with hydrogel from [2:1] [G3]8OR[PEG6K] precursor after functionalization with bodipy azide shows the nice patterns (Figure 3.22). The SEM image of the surface that is modified with

this method shows that the patterns are well defined and the edges are sharper referring better shape control (Figure 3.23).

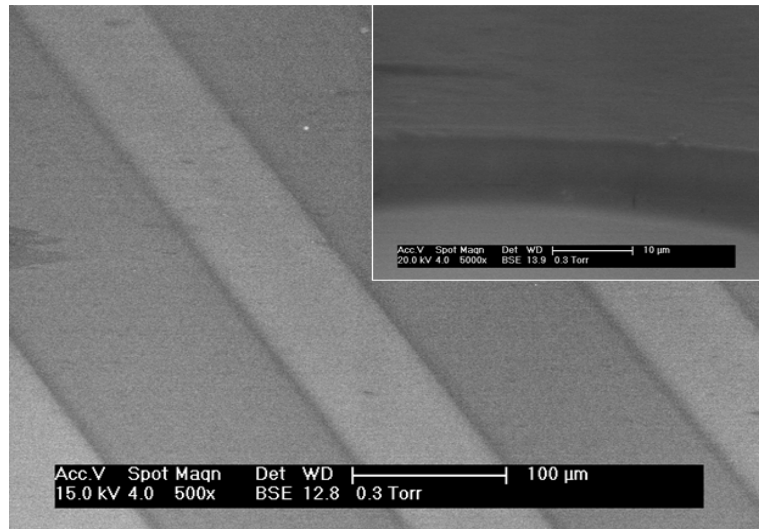


Figure 3.23. SEM images of patterned. hydrogel G36K_(1:1) by “spin coating and UV mask system”

4. EXPERIMENTAL

4.1. General Methods and Materials

2,2-Bis(hydroxymethyl)propionic acid (BMPA), Dowex X50WX2, propargyl alcohol, and 4-pentynoic acid were purchased from Alfa Aesar. All poly(ethylene glycol) were obtained from Fluka. All solvents were purchased from Merck and used as obtained without further purification unless otherwise noted. Azide-functionalized PEGs were synthesized according to literature procedures. [58]

The monomer and copolymer characterizations involved ^1H NMR spectroscopy (Varian 400 MHz) and Fourier transform infrared (ATR-FTIR) spectroscopy (Thermo Fisher Scientific Inc. Nicolet 380). Elemental analyses were obtained from Thermo Electron SpA FlashEA 1112 elemental analyzer (CHNS separation column, PTFE; 2 m; 6 \times 5 mm). The dry and wet surfaces of the hydrogels were observed with an ESEM-FEG/EDAX Philips XL-30 (Philips, Eindhoven, The Netherlands) instrument using an accelerating voltage of 10kV. Functionalized hydrogels were visualized with Zeiss Observer. Z1 inverted fluorescent microscope.

4.2. Preparation of Dendron-Polymer-Dendron ABA Triblock Copolymer Systems

4.2.1. Synthesis of compound [G2]4OH[PEG6K] 2

PEG-6K-diazide (250 mg, 0.040 mmol) and propargyl [G2]4[OH] (50 mg, 0.103 mmol) were dissolved in dry THF (4 mL). In a separate flask were dissolved CuBr (0.6 mg, 0.004 mmol) and N,N,N',N'',N''-Pentamethyldiethylenetriamine (PMDETA, 0.69 μL , 0.004 mmol) in dry THF (1 mL) purging with N_2 . The mixture transferred onto azide-propargyl alcohol solution and stirred at 30 $^\circ\text{C}$ for 24 h. After reaction is completed, the solution is diluted with THF (5 mL) and column with aluminium oxide (Al_2O_3 , 4 cm in small pipette) to remove copper. The solvent was evaporated under *vacuo* and the desired product was precipitated with Et₂O after dissolving in THF (3 mL), filtered and dried under *vacuo* yielding compound (260 mg, 86%) as a yellowish white solid. ^1H NMR (CDCl_3 , δ , ppm) 7.78 (s, 2H), 5.16 (s, 4H), 4.45 (t, 4H, $J = 5.0$ Hz), 4.24 (d, 4H, $J = 11.0$ Hz), 4.17 (d, 4H, $J = 11.0$ Hz), 3.78 (t, 4H, $J = 5.0$ Hz), 3.72-3.36 (m, 180H), 2.57 (s, 8H) 1.19 (s, 6H),

0.96 (s, 12H). FTIR (cm^{-1}): 3408, 2881, 1733. $\text{C}_{126}\text{H}_{236}\text{N}_6\text{O}_{64}$ Calcd: C, 52.97; H, 8.25 N, 2.94. Found: C, 53.01; H, 8.51 N, 3.00.

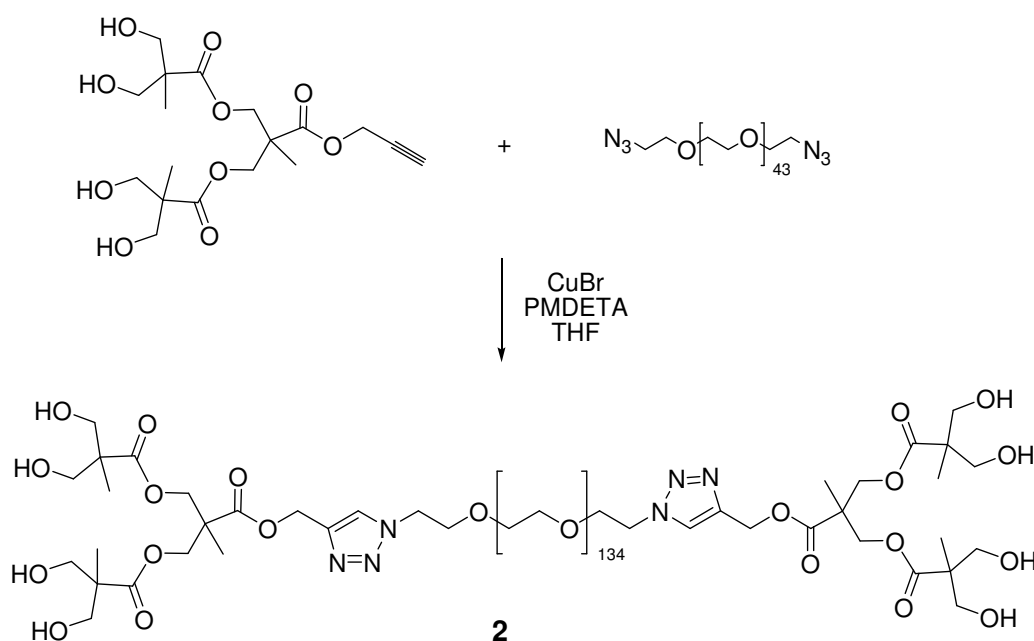


Figure 4.1. Schematic synthesis of compound [G2]4OH[PEG6K] **2**

4.2.2. Synthesis of compound [1:1] [G2]4OR[PEG6K] **3**

[G2]4OH[PEG6K] (60 mg, 0.008 mmol), pyridine (0.2 mL) and DMAP (1.0 mg, 0.008 mmol) dissolved in dry CH_2Cl_2 (5 mL) in a round bottom flask. To the stirring reaction mixture was added methacrylic anhydride (4.78 μL , 0.032 mmol) and continued stirring for 24 h at 40 $^\circ\text{C}$ under N_2 . Then, 4-pentynoic anhydride (6.25 mg, 0.032 mmol) was added to the reaction mixture and continued stirring for another 24h at 30 $^\circ\text{C}$ under N_2 . Crude product was purified by precipitation in diethyl ether to give a yellowish solid (56 mg, 77%). ^1H NMR (CDCl_3 , δ , ppm) 7.79 (s, 2H), 6.04 (s, 4H), 5.56 (s, 4H), 5.22 (s, 4H), 4.53 (s, 6H), 4.21 (s, 16H), 3.86 (t, 10H, $J = 4.7$ Hz), 3.79 (s, 8H), 3.69 (s, 8H), 3.68-3.59 (m, 540H), 2.68 (t, 4H, $J = 6.59$ Hz), 2.47 (t, 4H, $J = 6.2$ Hz), 1.96 (s, 2H), 1.89 (s, 8H), 1.23 (s, 6H), 1.20-1.17 (m, 12H). FTIR (cm^{-1}): 3317, 2882, 1738. $\text{C}_{344}\text{H}_{632}\text{N}_6\text{O}_{163}$ Calcd: C, 54.23; H, 8.79 N, 1.54. Found: C, 54.49; H, 8.98 N, 1.66.

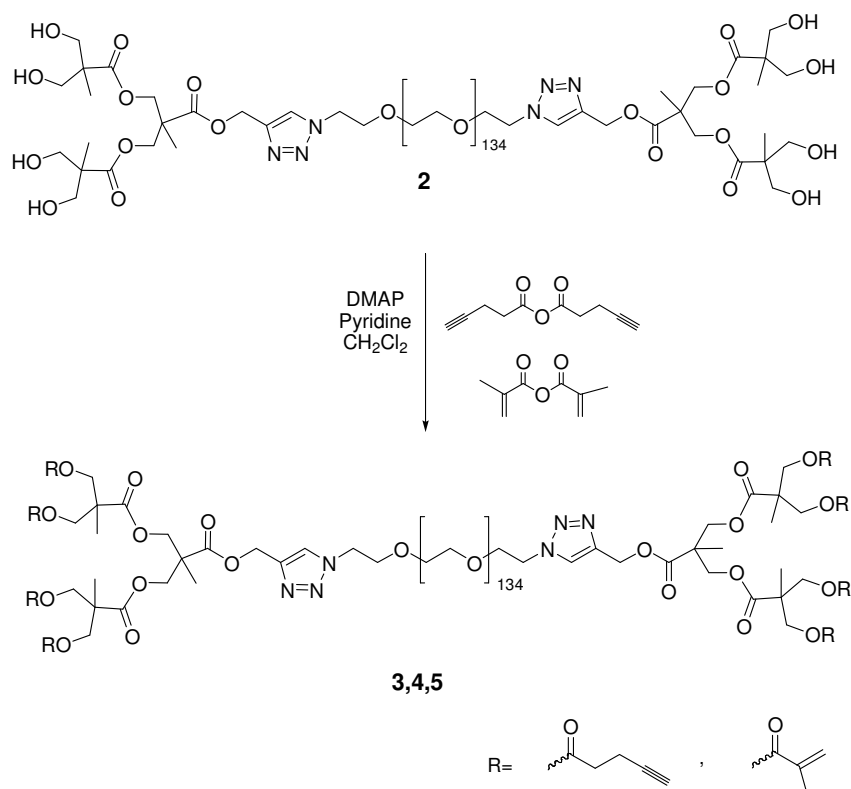


Figure 4.2. Schematic synthesis of compounds [G2]4OR[PEG6K] **3**, **4**, **5**

4.2.3. Synthesis of compound [1:2] [G2]4OR[PEG6K] **4**

Synthesized with the same procedure as compound (**3**) by using [G2]4OH[PEG6K] (60 mg, 0.008 mmol), pyridine (0.2 mL) and DMAP (1.0 mg, 0.008 mmol), dry CH₂Cl₂ (5 mL), methacrylic anhydride (6.53 μ L, 0.024 mmol), 4-pentynoic anhydride (4.68 mg, 0.040 mmol) yielding product as a yellowish viscous liquid (65 mg, 91%). ¹H NMR (CDCl₃, δ , ppm) 7.78 (s, 2H), 6.06 (s, 2H), 5.56 (s, 2H), 5.29 (s, 6H), 4.52 (s, 6H), 4.24 (s, 16H), 3.8 (t, 10H, $J = 4.75$ Hz), 3.77 (s, 8H), 3.69 (s, 8H), 3.66-3.58 (m, 540H), 2.54 (t, 8H, $J = 5.79$ Hz), 2.46 (t, 8H, $J = 4.66$ Hz), 1.99 (s, 2H), 1.86 (s, 8H), 1.2 (s, 6H), 1.19-1.13 (m, 12H). FTIR (cm⁻¹): 3288, 2880, 1738. C₃₄₅H₆₃₂N₆O₁₆₃ Calcd: C, 56.97; H, 9.25 N, 1.64. Found: C, 56.45; H, 9.38 N, 1.35.

4.2.4. Synthesis of compound [2:1] [G2]4OR[PEG6K] **5**

Synthesized with the same procedure as compound (**3**) by using [G2]4OH[PEG6K] (100 mg, 0.015 mmol), pyridine (0.3 mL) and DMAP (1.4 mg, 0.011 mmol), dry CH₂Cl₂ (8 mL), methacrylic anhydride (10.88 μ L, 0.073 mmol), 4-pentynoic anhydride (7.8 mg,

0.044 mmol) yielding product as a yellowish viscous liquid (80 mg, 67%). ^1H NMR (CDCl_3 , δ , ppm) 7.81 (s, 2H), 6.05 (s, 6H), 5.56 (s, 6H), 5.23 (s, 3H), 4.50 (s, 6H), 4.23 (s, 16H), 3.88 (t, 10H, $J = 4.72$ Hz), 3.79 (s, 8H), 3.68 (s, 8H), 3.65-3.58 (m, 540H), 2.54 (t, 3H, $J = 6.42$ Hz), 2.46 (t, 3H, $J = 5.9$ Hz), 1.97 (s, 2H), 1.88 (s, 8H), 1.26 (s, 6H), 1.22-1.16 (m, 12H). FTIR (cm^{-1}): 3288, 2881, 1738. $\text{C}_{343}\text{H}_{632}\text{N}_6\text{O}_{163}$ Calcd: C, 53.97; H, 9.25 N, 1.94. Found: C, 53.88; H, 9.11 N, 1.36.

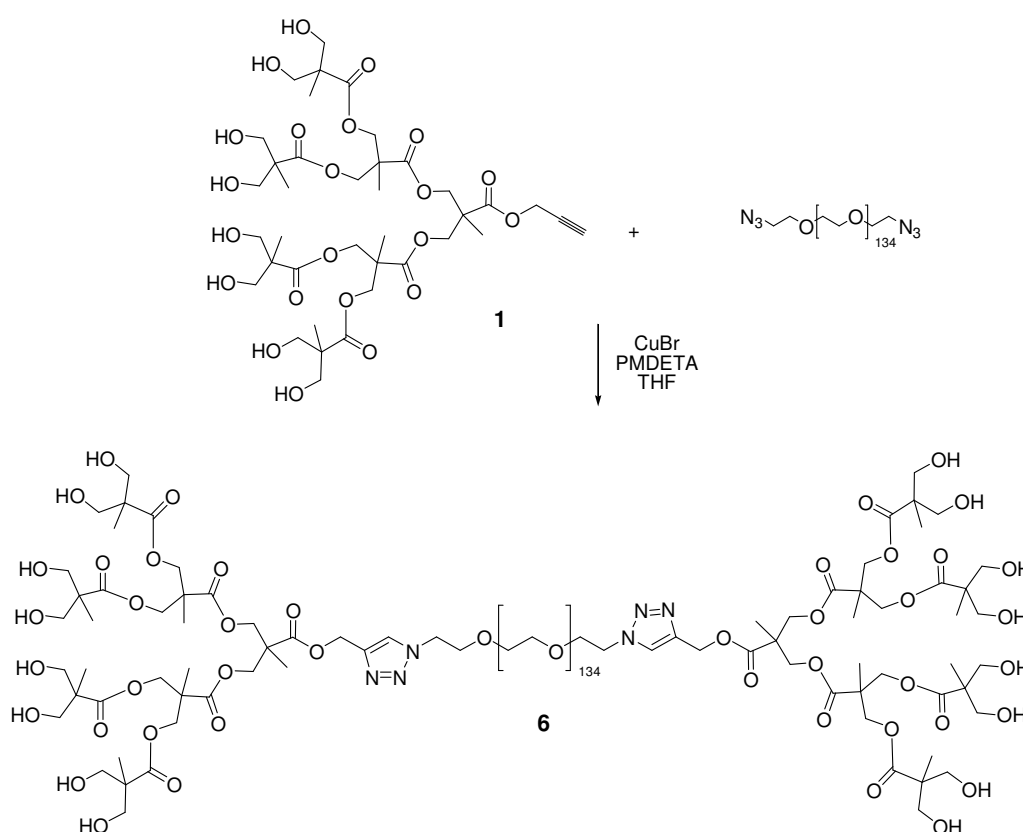


Figure 4.3. Schematic synthesis of compound [G3]8OH[PEG6K] **6**

4.2.5. Synthesis of compound [G3]8OH[PEG6K] **6**

PEG-6K-Diazide (750 mg, 0.12 mmol) and propargyl [G3]8[OH] (250 mg, 0.29 mmol) were dissolved in dry THF (8 mL). In a separate flask were dissolved CuBr (1.8 mg, 0.013 mmol) and $\text{N,N,N',N'',N'''}\text{ Pentamethyldiethylenetriamine (PMDETA, 2.61 } \mu\text{L, 0.013 mmol)}$ in dry THF (2 mL) and purged with N_2 . The mixture was then transferred onto azide-propargyl alcohol solution and stirred at $30\text{ }^\circ\text{C}$ for 24 h. The solution is diluted

with THF (10 ml) and column with aluminium oxide (Al_2O_3 , 4 cm in small pipette) to remove copper. The solvent was evaporated under *vacuo* and the desired product was precipitated with diethyl ether after dissolving in THF (3 mL), filtered and dried under *vacuo* yielding compound (850 mg, 85%) as a white solid. ^1H NMR (CDCl_3 , δ , ppm) 7.91 (s, 2H), 5.27 (s, 4H), 4.54 (t, 4H, $J = 4$ Hz), 4.28-4.19 (m, 24H), 3.85 (t, 4H, $J = 4$ Hz), 3.80-3.42 (m, 540H), 1.25-1.17 (m, 24H), 1.06 (s, 18H). FTIR (cm^{-1}): 3444, 2882, 1732. $\text{C}_{348}\text{H}_{664}\text{N}_6\text{O}_{179}$ Calcd: C, 50.97; H, 8.25 N, 3.04. Found: C, 50.67; H, 8.54 N, 3.29.

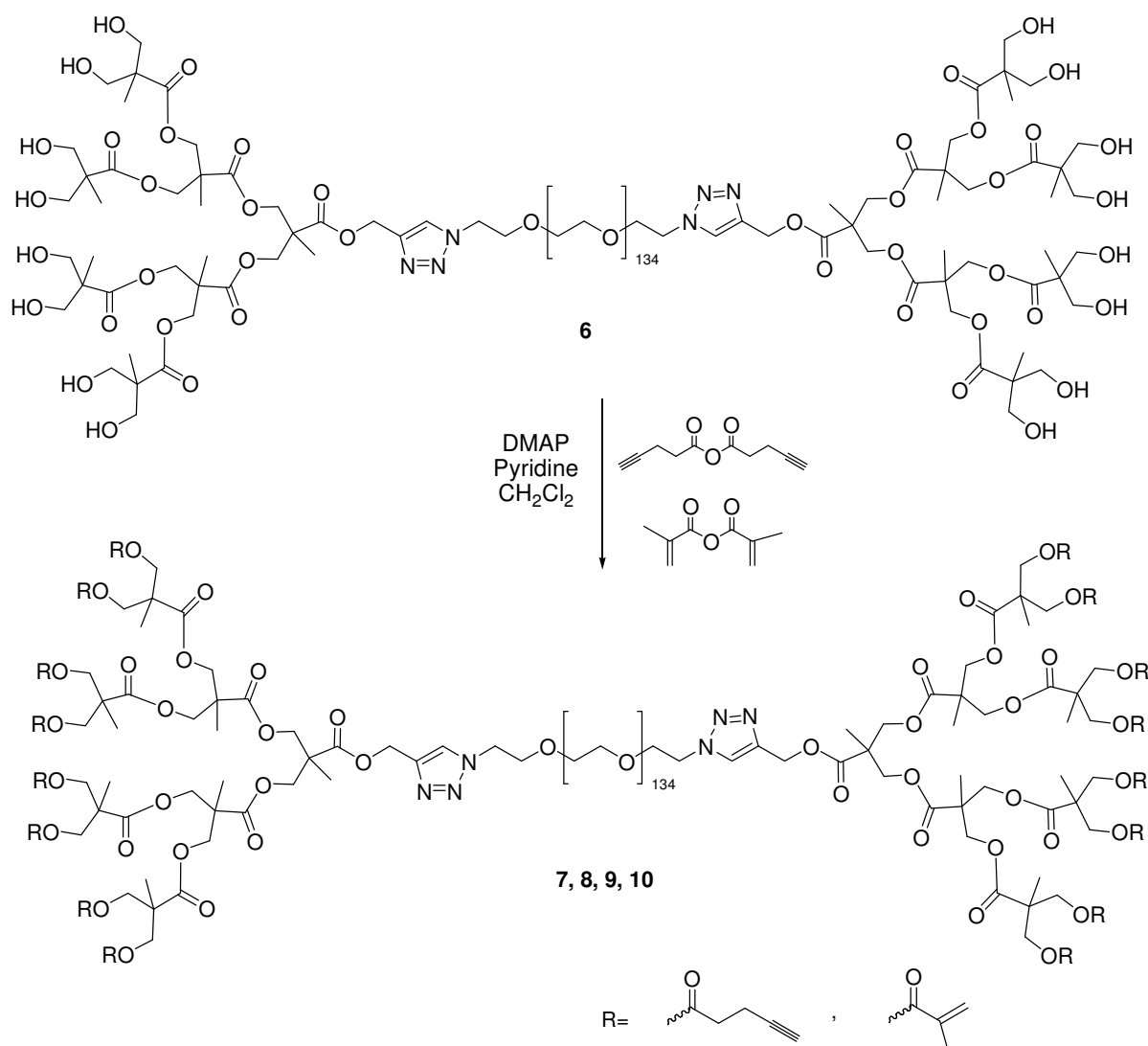


Figure 4.4. Schematic synthesis of compounds [G3]8OR[PEG6K] 7, 8, 9, 10

4.2.6. Synthesis of compound [2:1] [G3]8OR[PEG6K] 7

[G3]8OH[PEG6K] (80 mg, 0.01 mmol), pyridine (0.2 mL) and DMAP (1.2 mg, 0.012 mmol) were dissolved in dry CH₂Cl₂ (5 mL) in a 25 mL round bottom flask. To the stirring reaction mixture was added methacrylic anhydride (15.3 μ L, 0.1 mmol) and continued stirring for 24 h at 40 °C under N₂. Then 4-pentynoic anhydride (11 mg, 0.06 mmol) added to the reaction and continued stirring overnight at room temperature under N₂. Crude was purified by precipitation in diethyl ether to give 80 mg of a yellowish solid. (75 % yield). ¹H NMR (CDCl₃, δ , ppm) 7.80 (s, 2H), 6.04 (s, 10H), 5.58 (s, 10H), 5.22 (s, 5H), 4.51 (t, 4H, *J* = 5.2 Hz), 4.23-4.19 (m, 56H), 3.88 (t, 2H, *J* = 4.9 Hz), 3.80-3.42 (m, 540H), 2.54 (t, 10H, *J*=6.89 Hz), 2.45 (t, 10H, *J*=6.81 Hz), 1.97 (s, 12H), 1.9 (s, 18H), 1.62 (s, 40H), 1.24 (s, 24H), 1.20 (s, 6H). FTIR (cm⁻¹): 3280, 2869, 1735. C₄₁₈H₇₂₈N₆O₁₉₄ Calcd: C, 55.97; H, 8.25 N, 3.04. Found: C, 56.07; H, 8.26 N, 3.29.

4.2.7. Synthesis of compound [1:1] [G3]8OR[PEG6K] 8

Synthesized using the same procedure using [G3]8OH[PEG6K] (100 mg, 0.012 mmol), pyridine (0.2 mL) and DMAP (1.2 mg, 0.012 mmol), dry CH₂Cl₂ (8 mL), methacrylic anhydride (16 μ L, 0.100 mmol), 4-pentynoic anhydride (18.3 mg, 0.092 mmol). Yielding product as a yellowish viscous liquid (93 mg, 81 %). ¹H NMR (CDCl₃, δ , ppm) 7.81 (s, 2H), 6.07 (s, 4H), 5.56 (s, 4H), 5.23 (s, 4H), 4.54 (t, 4H, *J* = 5 Hz), 4.25-4.18 (m, 56H), 3.85 (t, 2H, *J* = 5 Hz), 3.80-3.42 (m, 540H), 2.55 (t, 16H, *J*=6.7 Hz), 2.45 (t, 16H, *J*=6.4 Hz), 1.98 (s, 12H), 1.92 (s, 18H), 1.6 (s, 40H), 1.24 (s, 24H), 1.22 (s, 6H). FTIR (cm⁻¹): 3280, 2879, 1737. C₄₂₀H₇₂₈N₆O₁₉₄ Calcd: C, 53.97; H, 8.25 N, 1.94. Found: C, 53.63; H, 8.28 N, 1.81.

4.2.8. Synthesis of compound [1:2] [G3]8OR[PEG6K] 9

Synthesized using [G3]8OH[PEG6K] (100 mg, 0.012 mmol), pyridine (0.2 mL) and DMAP (1.2 mg, 0.012 mmol), dry CH₂Cl₂ (8 mL), methacrylic anhydride (11.5 μ L, 0.072 mmol), 4-pentynoic anhydride (22.85 mg, 0.116 mmol). Yielding product as a yellowish viscous liquid (95 mg, 82 %). ¹H NMR (CDCl₃, δ , ppm) 7.82 (s, 2H), 6.08 (s, 3H), 5.58 (s, 3H), 5.23 (s, 7H), 4.54 (t, 8H, *J* = 5 Hz), 4.25-4.18 (m, 56H), 3.85 (t, 2H, *J* = 5.12 Hz), 3.80-3.42 (m, 540H), 2.58 (t, 20H, *J*=6.1 Hz), 2.44 (t, 20H, *J*=6.5 Hz), 1.98 (s, 14H), 1.92

(s, 20 H), 1.6 (s, 40H), 1.24 (s, 24H), 1.22 (s, 6H). FTIR (cm^{-1}): 3261, 2877, 1734. $\text{C}_{422}\text{H}_{728}\text{N}_6\text{O}_{194}$ Calcd: C, 52.97; H, 8.25 N, 1.94. Found: C, 52.84; H, 8.26 N, 2.02.

4.2.9. Synthesis of compound [1:3] [G3]8OR[PEG6K] 10

Synthesized using [G3]8OH[PEG6K] (100 mg, 0.012 mmol), pyridine (0.2mL) and DMAP (1,2 mg, 0.012 mmol), dry CH_2Cl_2 (8 mL), methacrylic anhydride (7.68 μL , 0.051 mmol), 4-pentynoic anhydride (27.4 mg, 0.154 mmol). Yielding product as a yellowish viscous liquid (98 mg, 83 %). ^1H NMR (CDCl_3 , δ , ppm) 7.80 (s, 2H), 6.06 (s, 2H), 5.60 (s, 2H), 5.23 (s, 4H), 4.54 (t, 4H, $J = 5$ Hz), 4.25-4.18 (m, 56H), 3.85 (t, 2H, $J = 5.1$ Hz), 3.80-3.42 (m, 540H), 2.59 (t, 24H, $J=6.8$ Hz), 2.43 (t, 24H, $J=6.7$ Hz), 1.98 (s, 18H), 1.92 (s, 14 H), 1.6 (s, 40H), 1.24 (s, 24H), 1.22 (s, 6H). FTIR (cm^{-1}): 3280, 2880, 1736, 1658. $\text{C}_{424}\text{H}_{728}\text{N}_6\text{O}_{194}$ Calcd: C, 56.97; H, 8.85 N, 2.04. Found: C, 56.87; H, 9.06 N, 2.21.

4.2.10. Synthesis of compound [G3]8OH[PEG2K] 11

PEG-2K-Diazide (105 mg, 0.05 mmol) and propargyl [G3]8[OH] (95 mg, 0.11 mmol) were dissolved in dry THF (4 mL). In a separate flask were dissolved CuBr (1.5 mg, 0.0108 mmol) and N,N,N',N'',N''' Pentamethyldiethylenetriamine (PMDETA, 2.5 μL , 0.0125 mmol) in dry THF (1 mL) and purged with N_2 . The mixture was then transferred onto azide-propargyl alcohol solution and stirred at 30 °C for 24 h. The solution is diluted with THF (10 ml) and column with aluminium oxide (Al_2O_3 , 4 cm in small pipette) to remove copper. The solvent was evaporated under *vacuo* and the desired product was precipitated with diethyl ether after dissolving in THF (3 mL) , filtered and dried under *vacuo* yielding a brownish viscous compound (145 mg, 73 %) ^1H NMR (CDCl_3 , δ , ppm) 7.87 (s, 2H), 5.22 (s, 4H), 4.5 (t, 4H, $J=3.97$), 4.21-4.18 (m, 28H), 3.74 (d, 14 H), 3.67 (d, 18H), 3.63 (s, 16H), 3.6-3.55 (m, 140H), 3.42 (s, 10H), 2.1 (s, 8H), 1.97 (s, 4H), 1.2-1.18 (m, 18H), 1.01 (s, 20H). FTIR (cm^{-1}): 3390, 2878, 1731. $\text{C}_{170}\text{H}_{308}\text{N}_6\text{O}_{90}$ Calcd: C, 49.67; H, 8.16 N, 3.98. Found: C, 49.81; H, 7.90 N, 4.02.

4.2.11. Synthesis of compound [1:1] [G3]8OR[PEG2K] 12

[G3]8OH[PEG2K] (85 mg, 0.029 mmol), pyridine (0.2 mL) and DMAP (1.0 mg, 0.008 mmol) dissolved in dry CH_2Cl_2 (5 mL) in a round bottom flask. To the stirring reaction

mixture was added methacrylic anhydride (26.9 μL , 0.183 mmol) and continued stirring for 24 h at 40 °C under N_2 . Then, 4-pentynoic anhydride (32.1 mg, 0.183 mmol) was added to the reaction mixture and continued stirring for another 24h at 30 °C under N_2 . Crude product was purified by precipitation in diethyl ether to give a yellowish solid (95 mg, 94 %). ^1H NMR (CDCl_3 , δ , ppm) 7.85 (s, 2H), 6.05 (s, 4H), 5.56 (s, 4H), 5.23 (s, 4H), 4.53 (s, 4H), 4.28-4.20 (m, 36H), 3.86 (t, 4H, $J=4.67$ Hz), 3.81-3.78 (m, 150H), 3.44 (t, 4H, $J=4.82$ Hz), 3.37 (t, 4H, $J=5.03$), 3.22 (s, 4H), 2.54 (t, 4H, $J=6.42$ Hz), 2.47 (t, 4H, $J=5.95$ Hz), 1.96 (s, 8H), 1.9 (s, 20H), 1.27 (s, 10H), 1.24 (s, 24H), 1.19 (s, 18H). FTIR (cm^{-1}): 3264, 2877, 1737, 1673. $\text{C}_{242}\text{H}_{372}\text{N}_6\text{O}_{105}$ Calcd: C, 53.08; H, 8.16 N, 2.44. Found: C, 53.43; H, 7.84 N, 2.12.

4.2.12. Synthesis of compound [G3]8OH[PEG4K] 13

PEG-4K-Diazide (200 mg, 0.049 mmol) and propargyl [G3]8[OH] (100 mg, 0.115 mmol) were dissolved in dry THF (6 mL). In a separate flask were dissolved CuBr (1.4 mg, 0.009 mmol) and N,N,N',N'',N''' Pentamethyldiethylenetriamine (PMDETA, 1.31 μL , 0.009 mmol) in dry THF (1 mL) and purged with N_2 . The mixture was then transferred onto azide-propargyl alcohol solution and stirred at 30 °C for 24 h. The solution is diluted with THF (10 ml) and column with aluminium oxide (Al_2O_3 , 4 cm in small pipette) to remove copper. The solvent was evaporated under *vacuo* and the desired product was precipitated with diethyl ether after dissolving in THF (3 mL), filtered and dried under *vacuo* yielding a brownish viscous compound (268 mg, 89%) ^1H NMR (CDCl_3 , δ , ppm) 7.9 (s, 2H), 5.26 (s, 4H), 4.54 (t, 8H, $J=4.13$ Hz), 4.29-4.20 (m, 42H), 3.85 (t, 8H, $J=5$ Hz), 3.79-3.76 (m, 34H), 3.7 (s, 22H), 3.64-3.6 (m, 360H), 3.5 (s, 12H), 3.44 (t, 18H, $J=5.07$ Hz), 3.38 (t, 18H, $J=5.18$ Hz), 2.38 (s, 10H), 2.3 (s, 10H), 2.15 (s, 6H), 1.23 (s, 68H), 1.06 (s, 46H). FTIR (cm^{-1}): 3408, 2883, 1735. $\text{C}_{258}\text{H}_{484}\text{N}_6\text{O}_{134}$ Calcd: C, 52.97; H, 8.25 N, 1.34. Found: C, 53.02; H, 8.54 N, 1.09.

4.2.13. Synthesis of compound [1:1] [G3]8OR[PEG4K] 14

Synthesized by the same procedure as compound (11) via using [G3]8OH[PEG4K] (225 mg, 0.038 mmol), pyridine (0.3mL) and DMAP (5.0 mg, 0.04 mmol), dry CH_2Cl_2 (7 mL), methacrylic anhydride (46,1 μL , 0.311 mmol), 4-pentanoic anhydride (48.3 mg, 0.311

mmol) yielding product as a white solid (215 mg, 86 %). ^1H NMR (CDCl_3 , δ , ppm) 7.8 (s, 2H), 6.04 (s, 8H), 5.56 (s, 8H), 5.23 (s, 4H), 4.53 (t, 4H, $J=5$ Hz), 4.28-4.19 (m, 60H), 3.86 (s, 4H), 3.79 (s, 3H), 3.74-4.54 (m, 360H), 3.44 (s, 4H), 3.22 (d, 8H), 2.54 (t, 12H, $J=6.65$ Hz), 2.46 (t, 12H, $J=6.3$ Hz), 1.96 (s, 10H), 1.89 (s, 24H), 1.27-1.17 (m, 48H). FTIR (cm^{-1}): 3276, 2883, 1764, 1644. $\text{C}_{330}\text{H}_{548}\text{N}_6\text{O}_{149}$ Calcd: C, 54.97; H, 8.25 N, 1.94. Found: C, 55.32; H, 8.34 N, 1.69.

4.3. General Synthesis of Hydrogels via Photocrosslinking Chemistry

Formation of hydrogel photocrosslinking was achieved according to literature. Poly(ethyleneglycol)-bis-oktaacetylene **7** (20 mg, 2.52 μmol), was dissolved in 1:1 EtOH:H₂O mixture (0.05 mL). To another vial was added 2-2-Dimethoxy-2-phenylacetophenone (99 %) (3 mg, 0.012 mmol) and was dissolved in N-vinyl pyrrolidone (20 μL). This solution was mixed with gel precursor under ultrasound to give a clear solution. The final mixture was cured under UV light (475 nm) for 5 minutes. The crosslinked material was washed with MeOH and the vial was broken to let the hydrogel out. To remove the solvents and unreacted chemicals, hydrogels were washed with MeOH for 2 hours and finally was with deionized water. The hydrogel sample was quickly frozen and further freeze-dried under *vacuo* until the solvent removed, yielding **6KG3(1:1)** (14.2 mg, 84% gel content).

4.4. Functionalisation of Hydrogels

4.4.1 Functionalization with BODIPY azide

Two identical cylindrically shaped hydrogels were synthesized (each about 20 mg) and placed into two different vials. Bodipy azide (0.25 mg, 0.00058 mmol), (Figure 4.5) in THF (2.5 mL) was added to each of the vials. PMDETA (1.20 μL , 0.0058 mmol) and CuBr (1.00 mg, 0.007 mmol) were added to vial #1 for copper catalyzed cycloaddition. Vial#2 was left without catalyst addition to control the nonspecific adsorptions of the hydrogels. The reactions were stirred at room temperature for 12 h. After the reaction was completed hydrogels were washed with EtOH to remove any trapped dye molecules and then washed with an aqueous EDTA solution (5%, pH ~7-8) to extract the trapped Cu(I)Br and finally washed with deionized water.

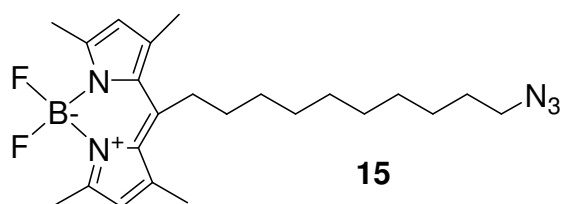


Figure 4.5. Chemical structure of BODIPY azide

4.4.2 Functionalization with Biotin azide

Similarly, two identical cylindrically shaped hydrogels were synthesized (20 mg) and placed into two different vials and reacted with biotin azide (1 mg, 3.3 μmol), (Figure 4.6) in the presence of CuSO_4 (1 mg, 0.0063 mmole) and sodium ascorbate (1 mg, 0.005 mmole) for 12h. As a control the same hydrogel is treated with biotin azide in the absence of CuSO_4 and sodium ascorbate. After the reaction completed at 30 $^\circ\text{C}$, the gel was first transferred to a pH \sim 7-8 EDTA water solution (5%) to extract the trapped CuSO_4 and finally washed with pure deionized water. Thereafter, hydrogels are incubated with FITC labeled streptavidin (0.1 mg/ml of PBS buffer, pH 7.4) for 15 minutes. After incubation, hydrogels are kept in water for another 15 minutes, washed with water several times.

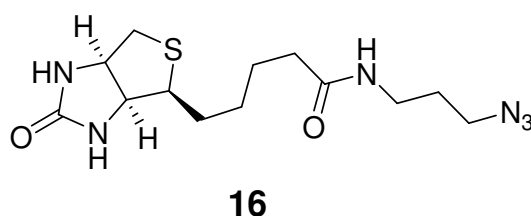


Figure 4.6. Chemical structure of Biotin azide

4.5. Microcontact Molding of Hydrogels

4.5.1. PDMS Molding

Poly(ethyleneglycol)-bis-oktaacetylene **7** (20 mg, 2.52 μmol), was dissolved in 1:1 EtOH:H₂O mixture (0.05 mL). To another vial was added 2,2-Dimethoxy-2-phenylacetophenone (99 %) (3 mg, 0.012 mmol) and was dissolved in N-vinyl pyrrolidone (20 μL). This solution was mixed with gel precursor to give a clear solution. A silicon wafer functionalized by immersing the surface into 2% 3(trimethoxysilyl)propylacrylate

solution in ethanol/water (95/5) for 2 hours then by heating at 110 °C for 1 hour. Onto this silicon wafer a PDMS mold which has 60 to 30 micron size -polymer to channel- was put. The gel precursor was dropped from the edge of mold and let it move through the channels of mold. This system cured under UV (475 nm) for 5 minutes and waited for 12h. Finally the mold was removed and the hydrogel modified surface was washed with EtOH and THF several times.

4.5.2. Spin Coating and Patterning via UV mask

A silicon wafer was functionalized with 2% 3(trimethoxysilyl)propylacrylate as in the PDMS molding method and the gel precursor that contains the photoinitiator was dropped. The surface was spin coated in 2000 rpm speed for 10 seconds. To avoid the solvent loss before crosslinking, the coated surface was immediately put on a UV mask. The system was cured under UV (475 nm) for 5 minutes. The mask removed and the surface washed with EtOH and THF several times to remove the polymer that was not crosslinked on the silicon wafer surface.

4.6. Measurements

4.6.1. Scanning Electron Microscopy (SEM) Analysis

The hydrogel samples first swelled with distilled water and were frozen to be ready for lyophilization. The ones that are patterned on a silicon wafer were dried with N₂ gas. The dry hydrogels studied by a scanning microscope.

4.6.2. Physical Property Analysis

The weight of the hydrogel dried under *vacuum* is recorded and water uptake test is performed by recording the new weight of the gel in water in every 5 minutes. Measurements done until the equilibrium hydration degree was reached. Swelling ratio (W) was calculated by the Equation (1) in which M_f is the weight in equilibrium and M_i is the initial weight of the sample.

$$W = (M_f - M_i) / M_i \times 100$$

Equation (1)

5. CONCLUSIONS

Synthesis of functionalizable hydrogels by click chemistry is done by combining G2 and G3 polyester dendrons with PEG. Attachment of active groups like alkene and alkyne to the surface of these copolymers gives the property of multifunctionality. Photo initiated polymerization gives the hydrogels that are further functionalizable by click chemistry.

Characterizations of the molecules are reported and the claimed properties of hydrogels are proved by different methodologies.

Synthesized hydrogels are great candidates for biomedical applications, electronics and material science due to their physical and chemical properties.

APPENDIX A: SPECTROSCOPY DATA

¹H NMR and FTIR spectra of the synthesized compounds are given below. Needed regions of NMR data were extended.

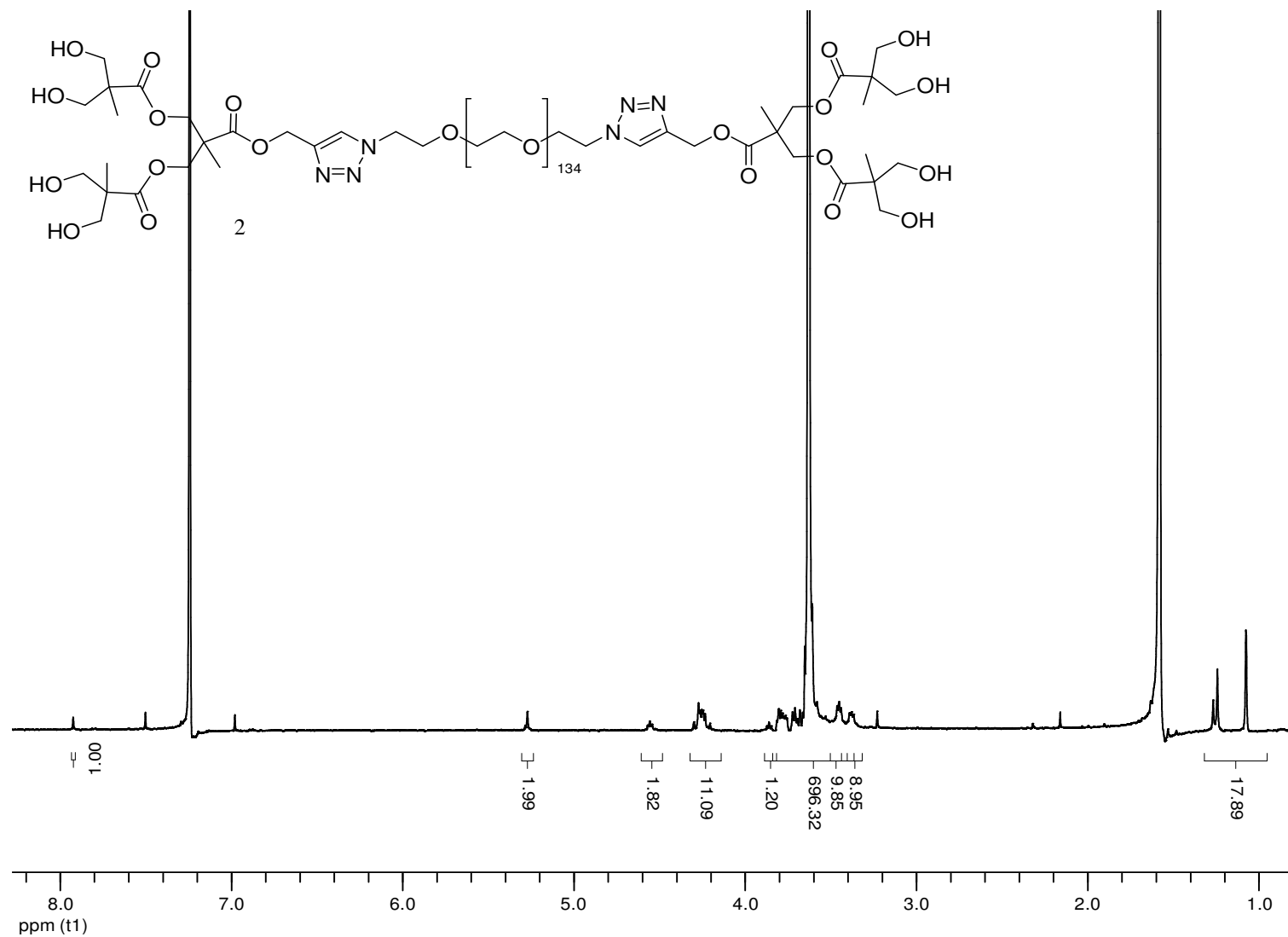


Figure A.1. ^1H NMR spectrum of $[G_2]4\text{OH}[PEG6K] \mathbf{2}$

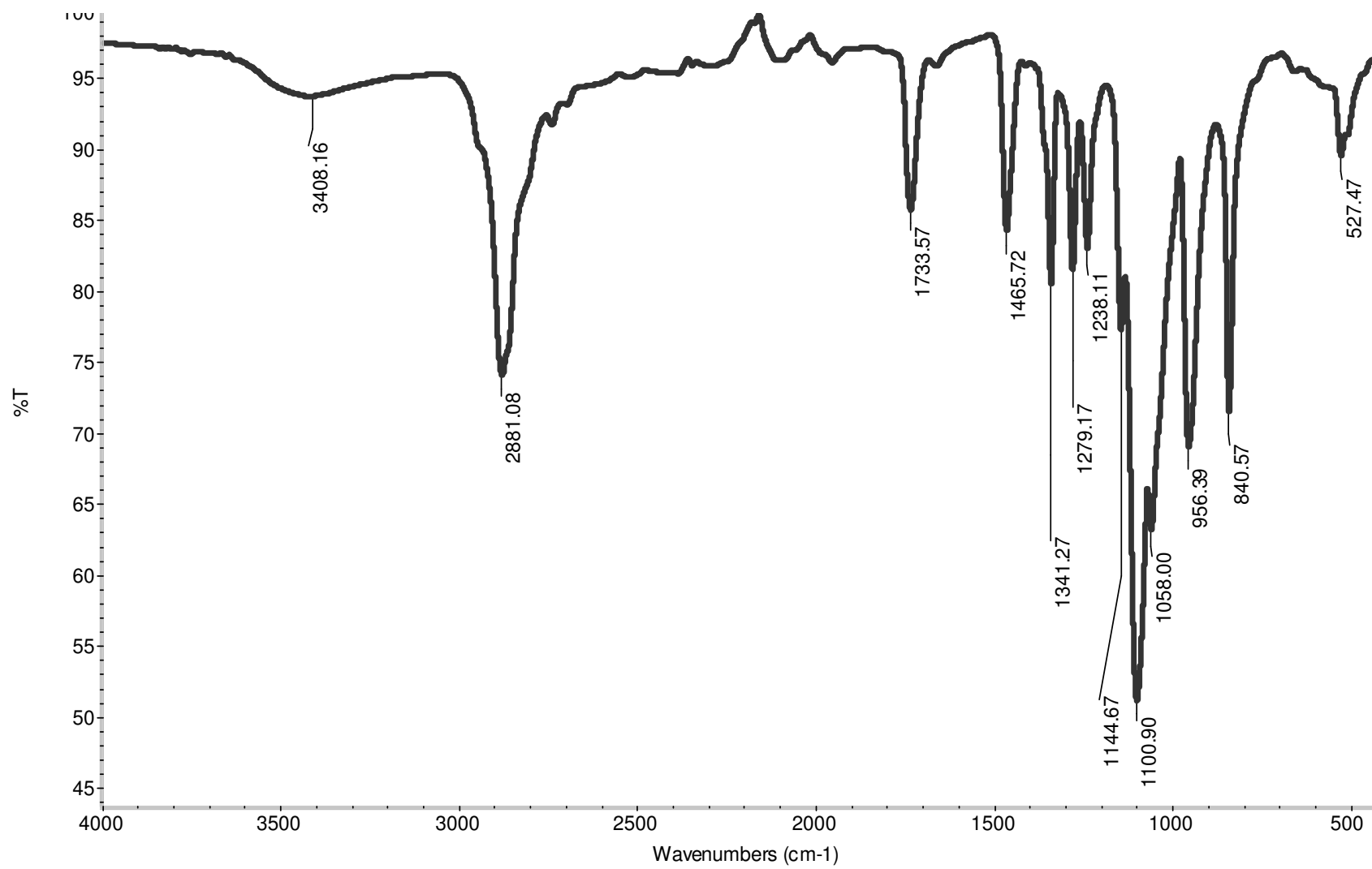


Figure A.2. IR spectrum of [G2]4OH[PEG6K] 2

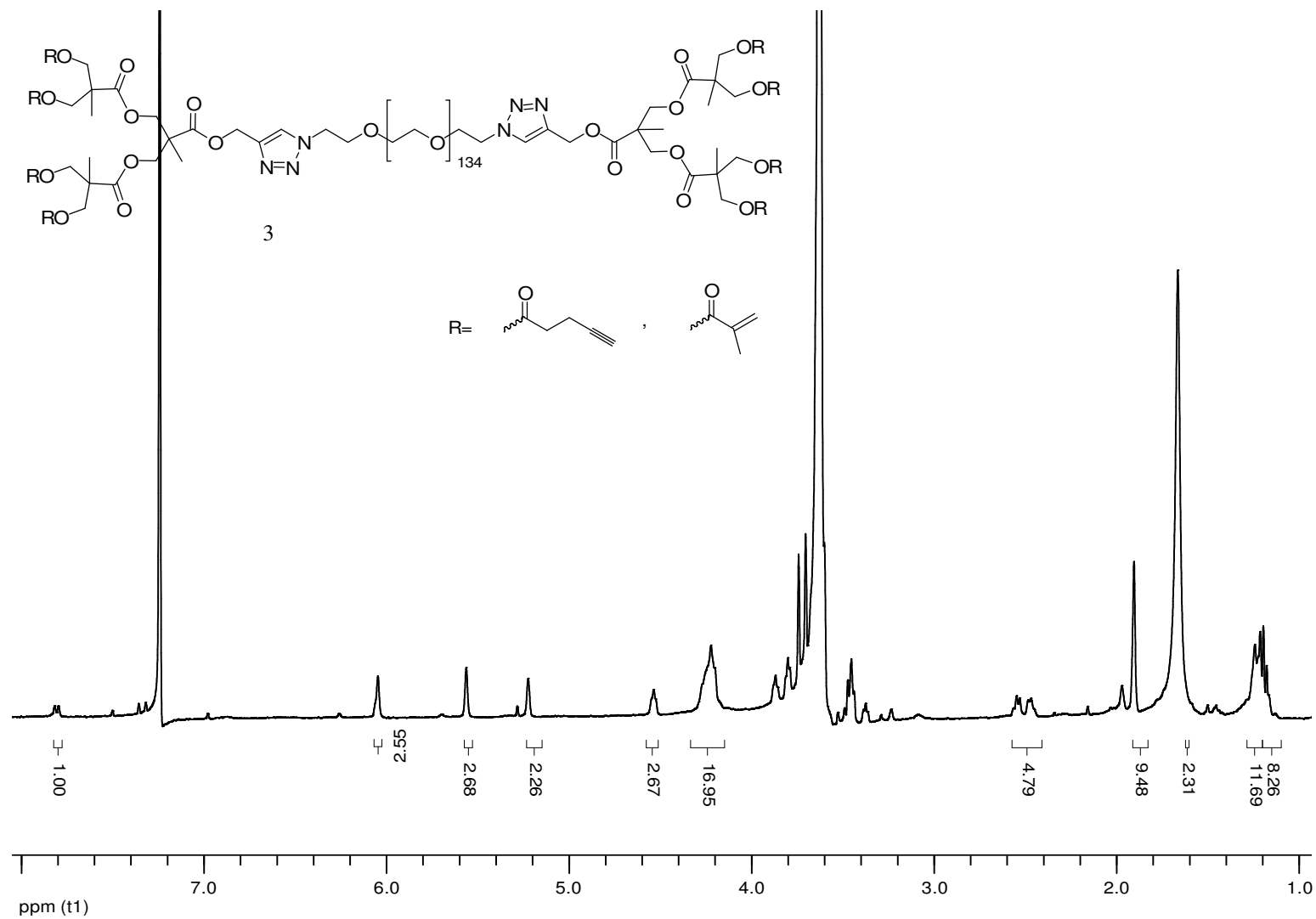


Figure A.3. ^1H NMR spectrum of $[1:1]$ $[G2]4OR[PEG6K]$ **3**

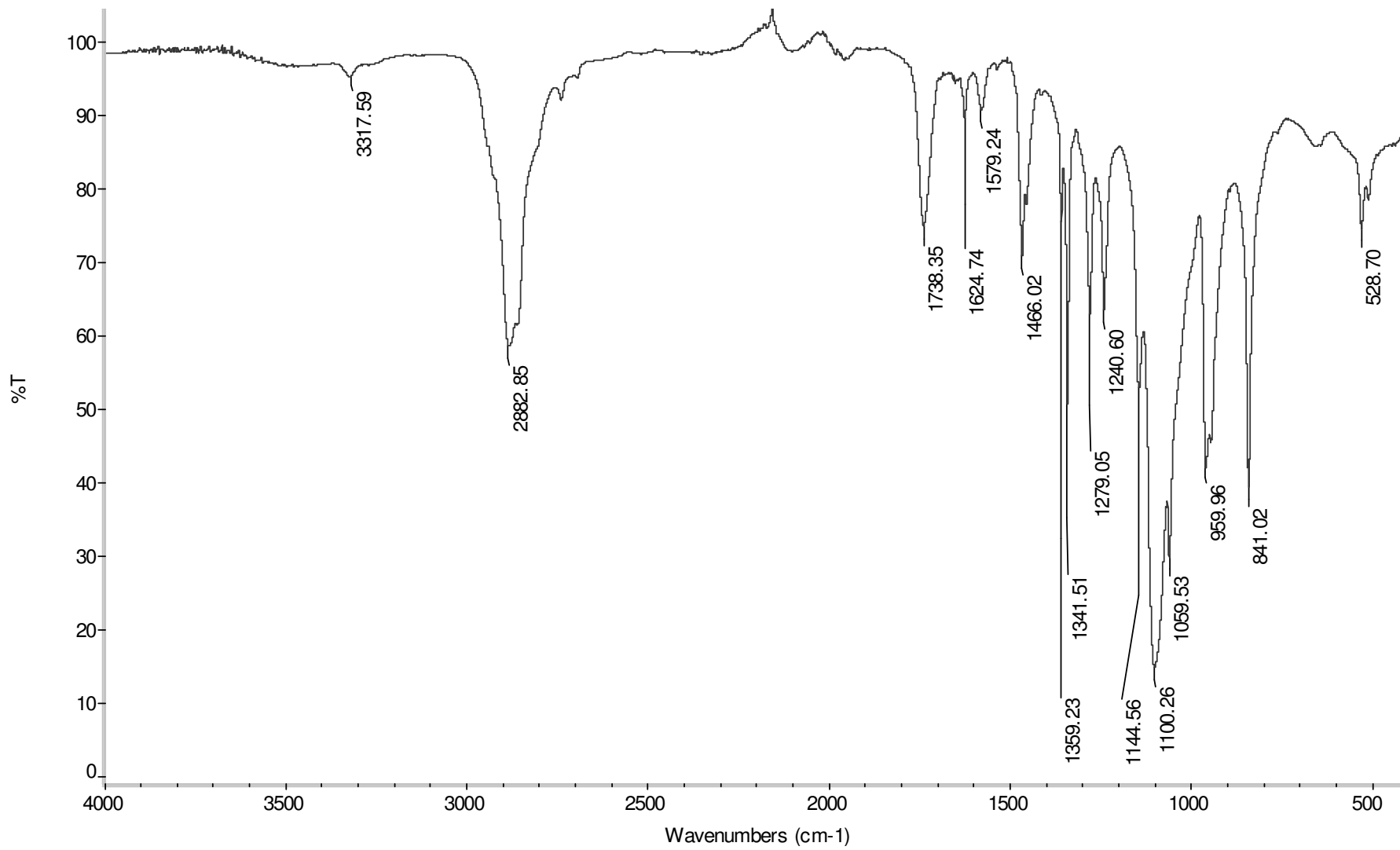


Figure A.4. IR spectrum of [1:1] [G2]4OR[PEG6K] 3

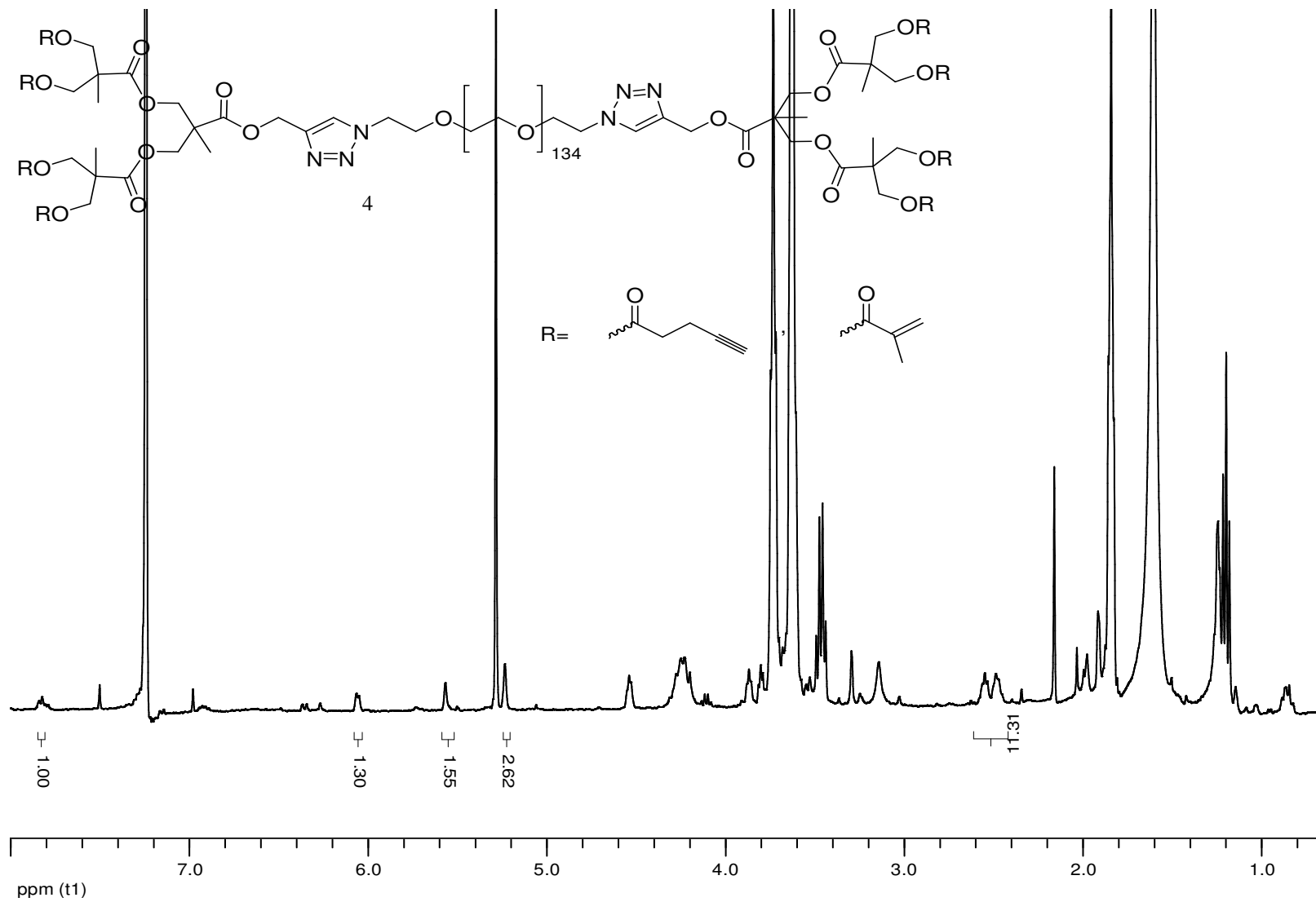


Figure A.5. ^1H NMR spectrum of $[1:2] [G_2]_4\text{OR}[PEG_6K] \mathbf{4}$

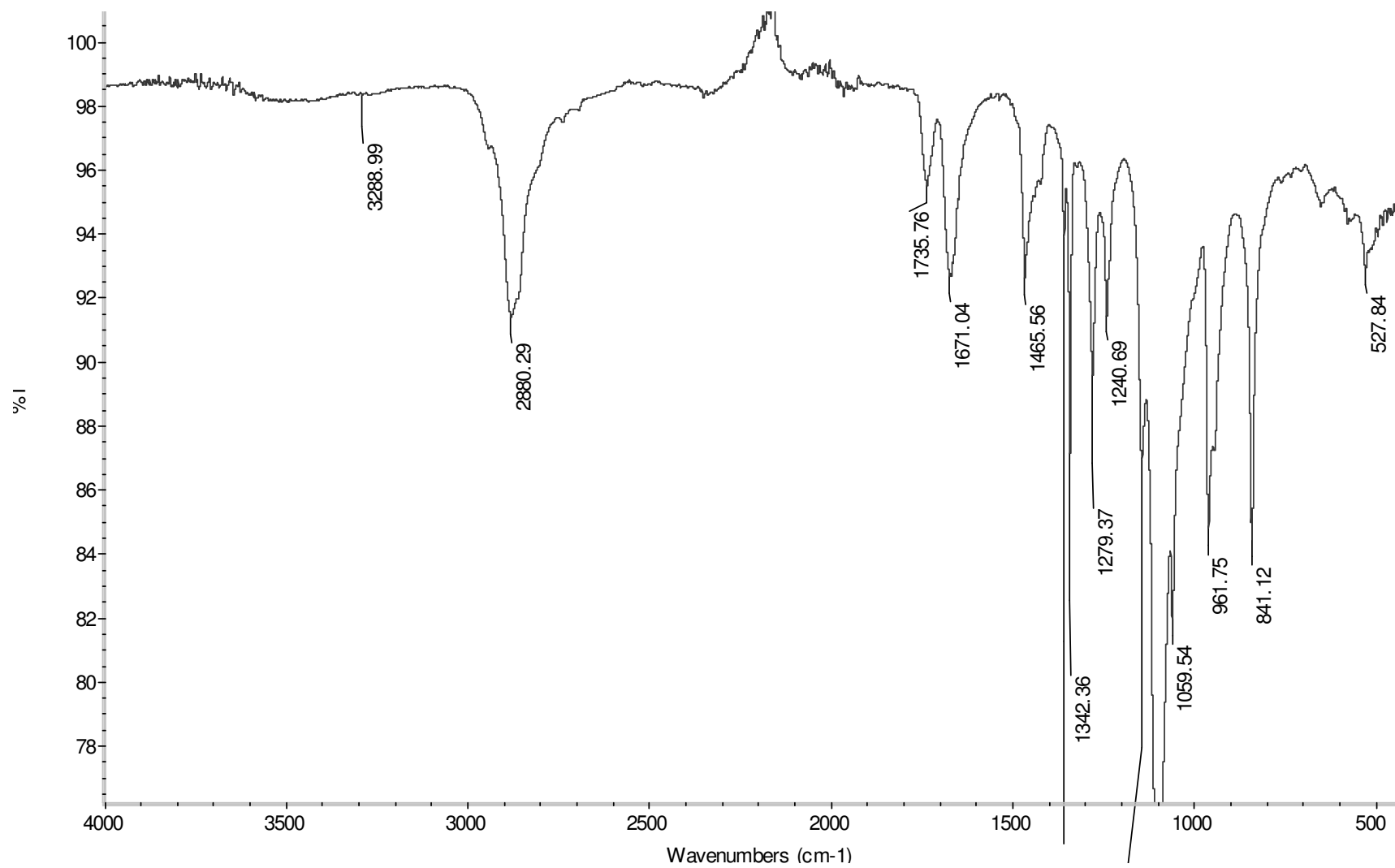


Figure A.6. IR spectrum of [1:2] [G2]4OR[PEG6K] 4

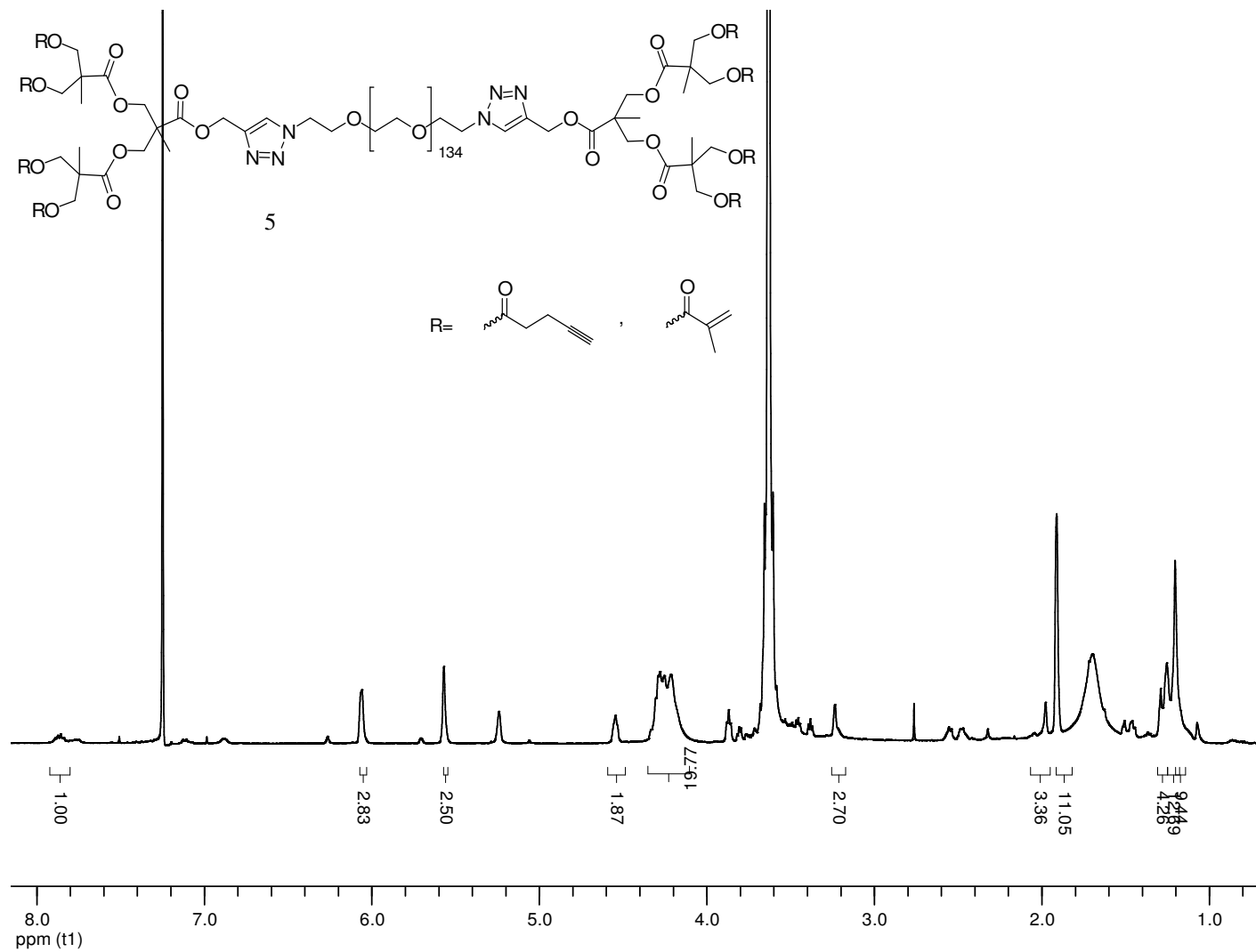


Figure A.7. ^1H NMR spectrum of $[2:1] [G_2]_4\text{OR}[\text{PEG}6\text{K}] \mathbf{5}$

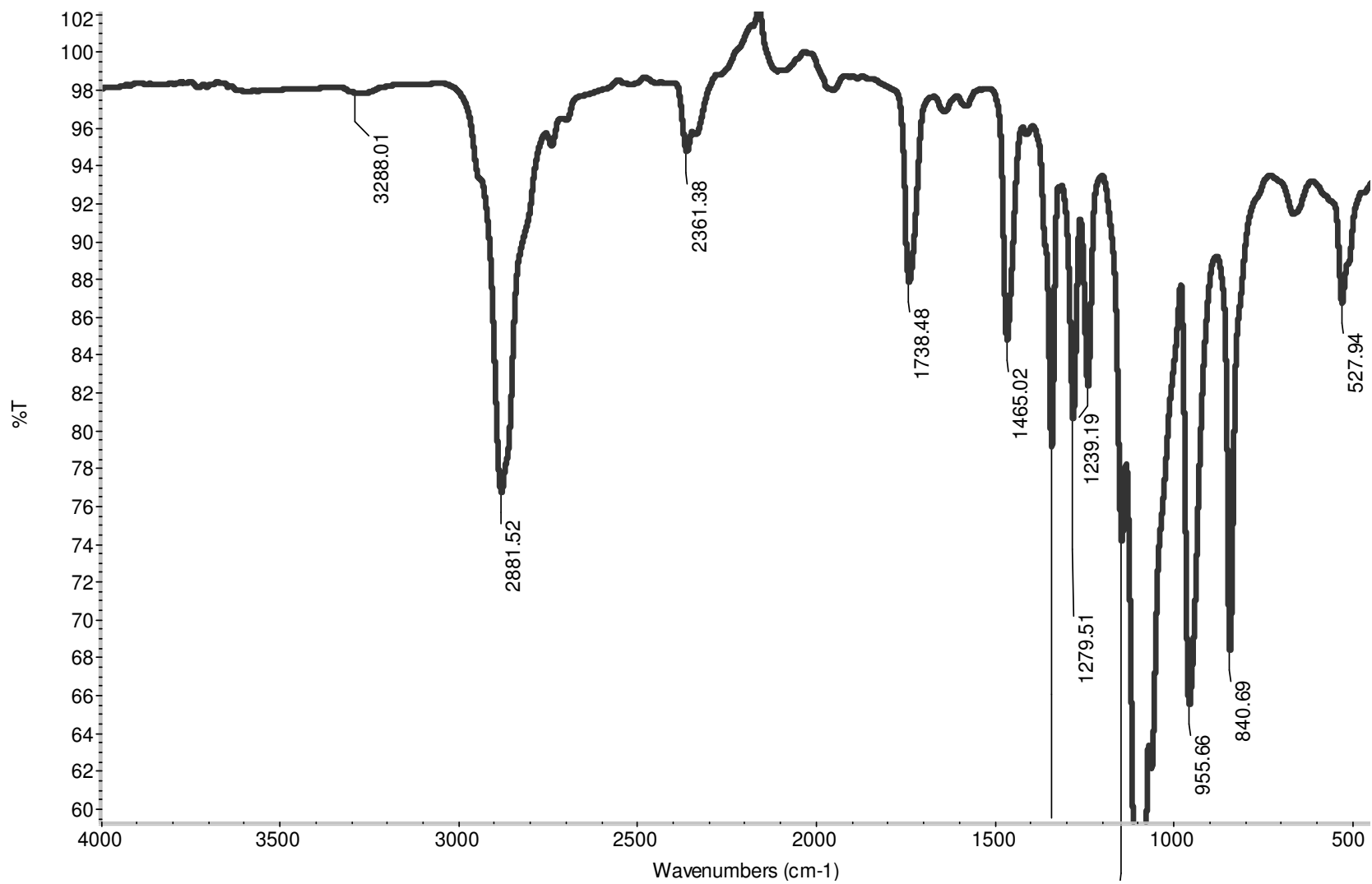


Figure A.8. IR spectrum of [2:1] [G2]4OR[PEG6K] 5

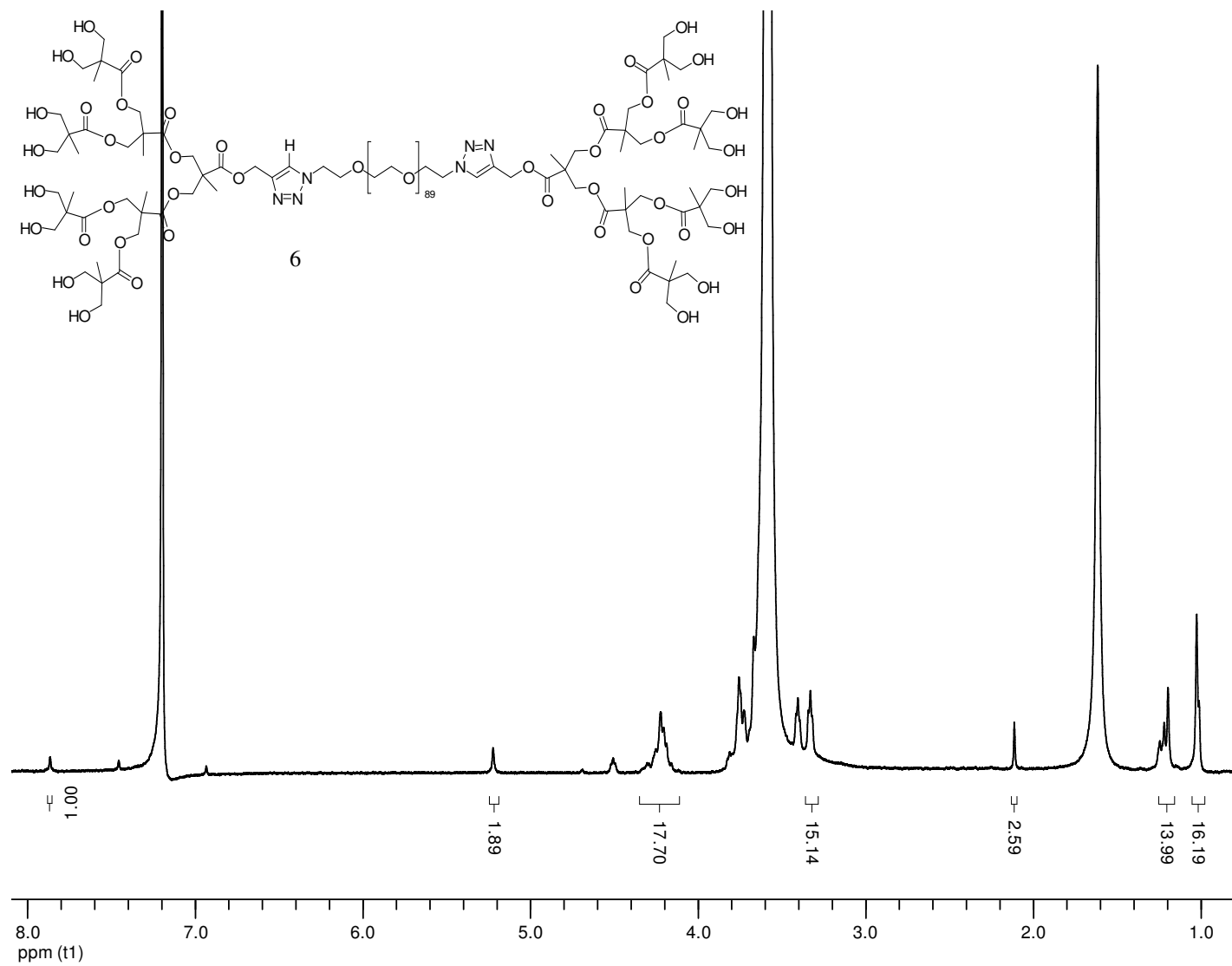


Figure A.9. ^1H NMR spectrum of $[G3]8\text{OH}[PEG6K] \mathbf{6}$

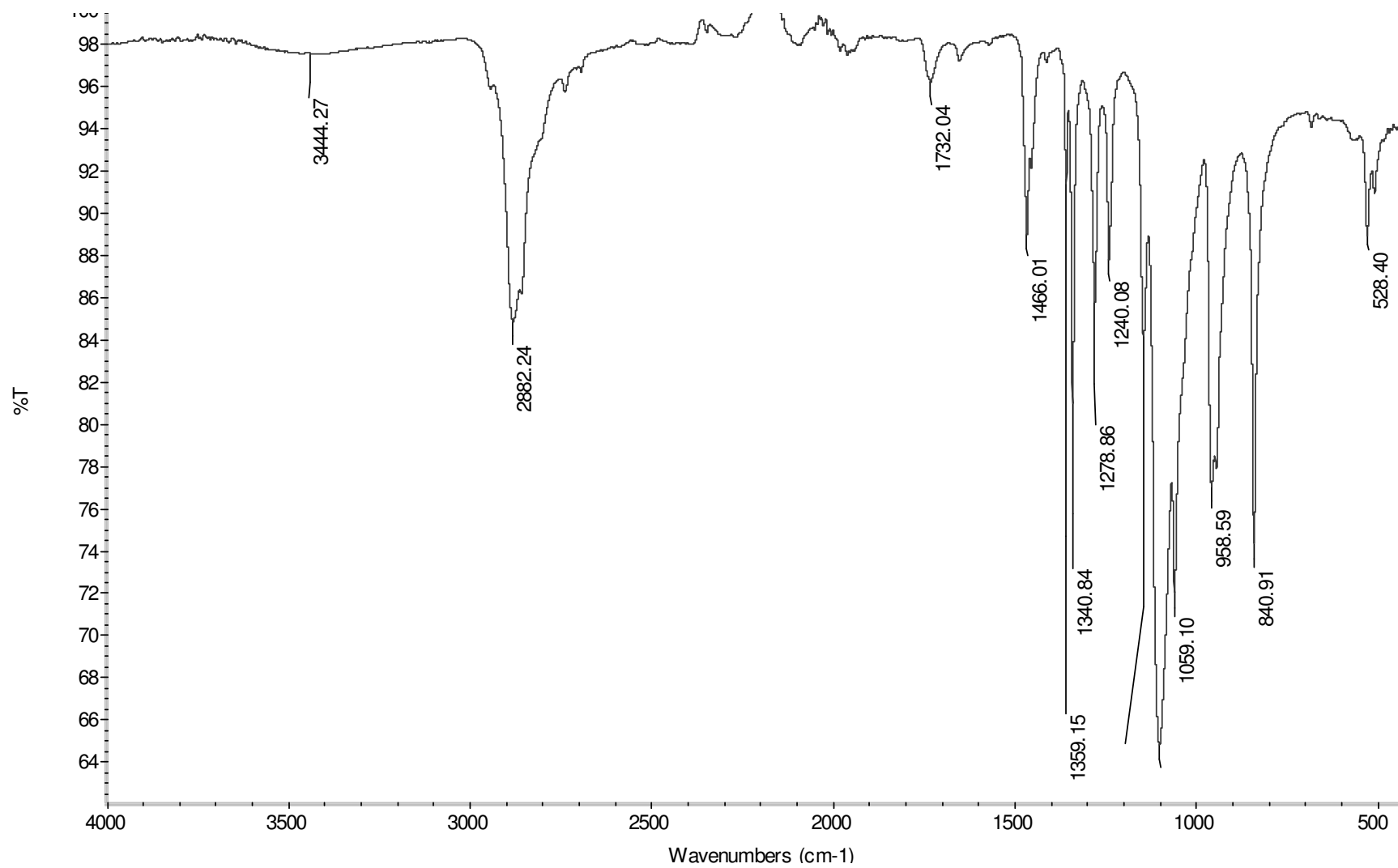


Figure A.10. IR spectrum of *[G3]8OH[PEG6K] 6*

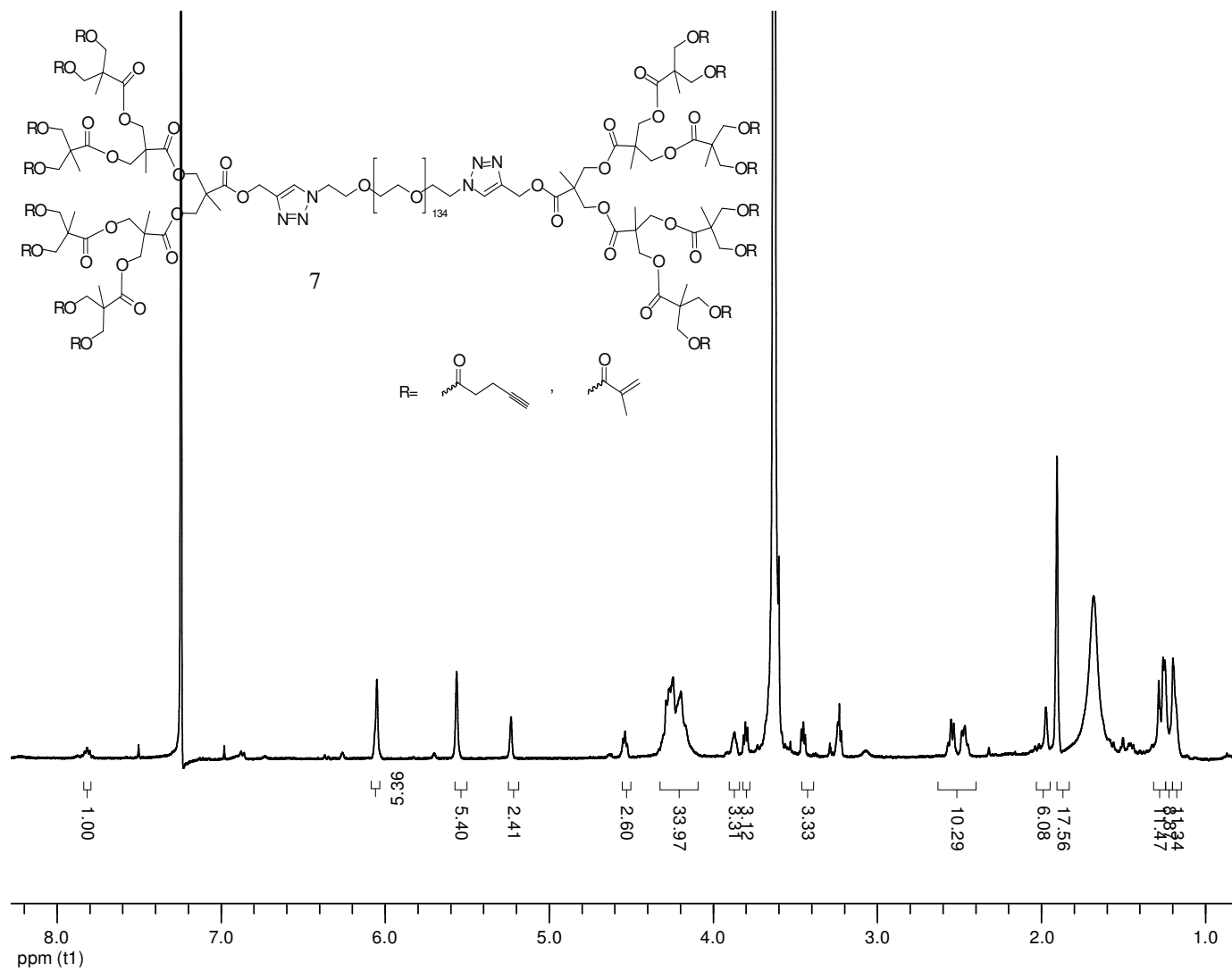


Figure A.11. ¹H NMR spectrum of [2:1] [G3]8OR[PEG6K] **7**

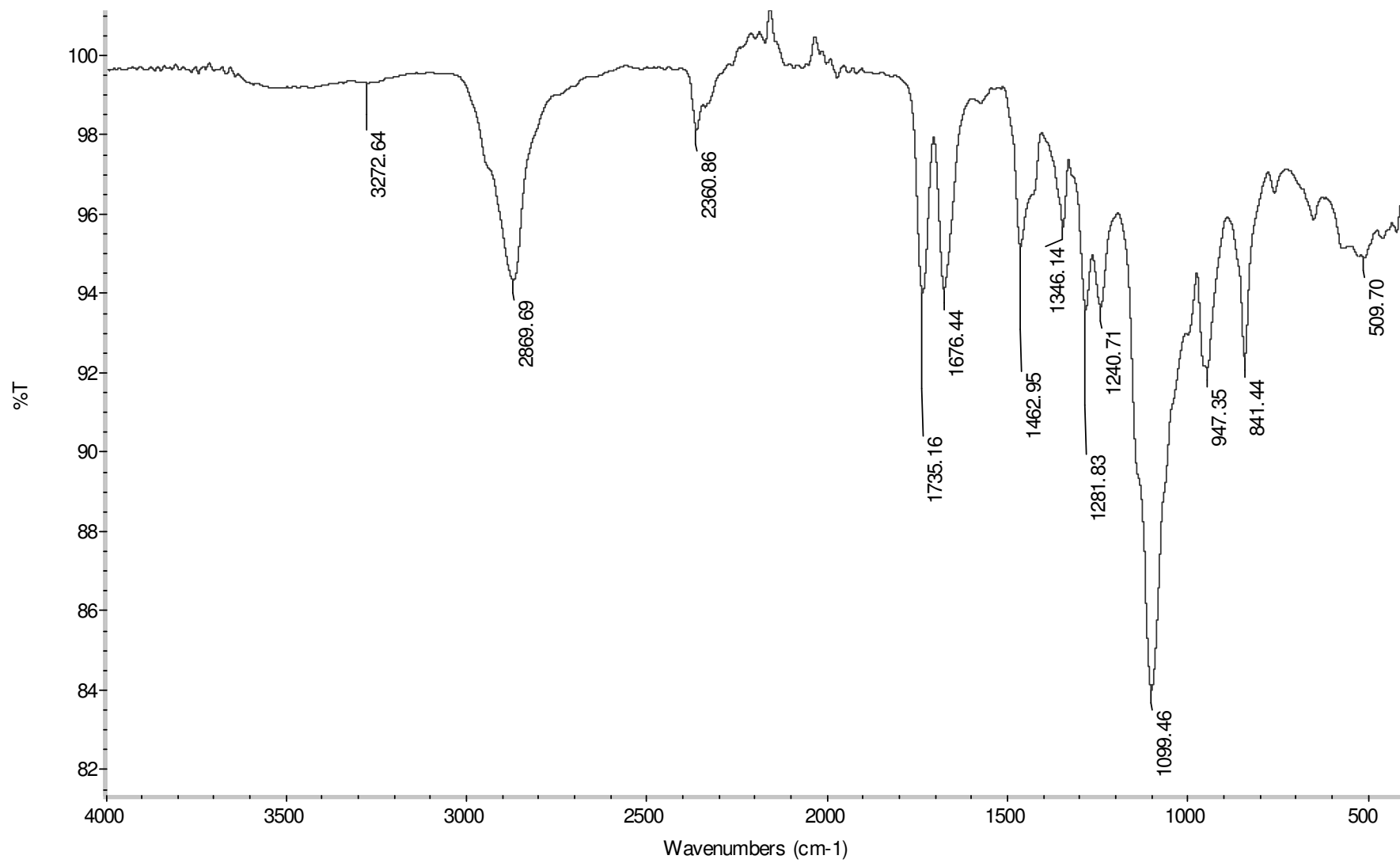


Figure A.12. IR spectrum of [2:1] [G3]8OR[PEG6K] 7

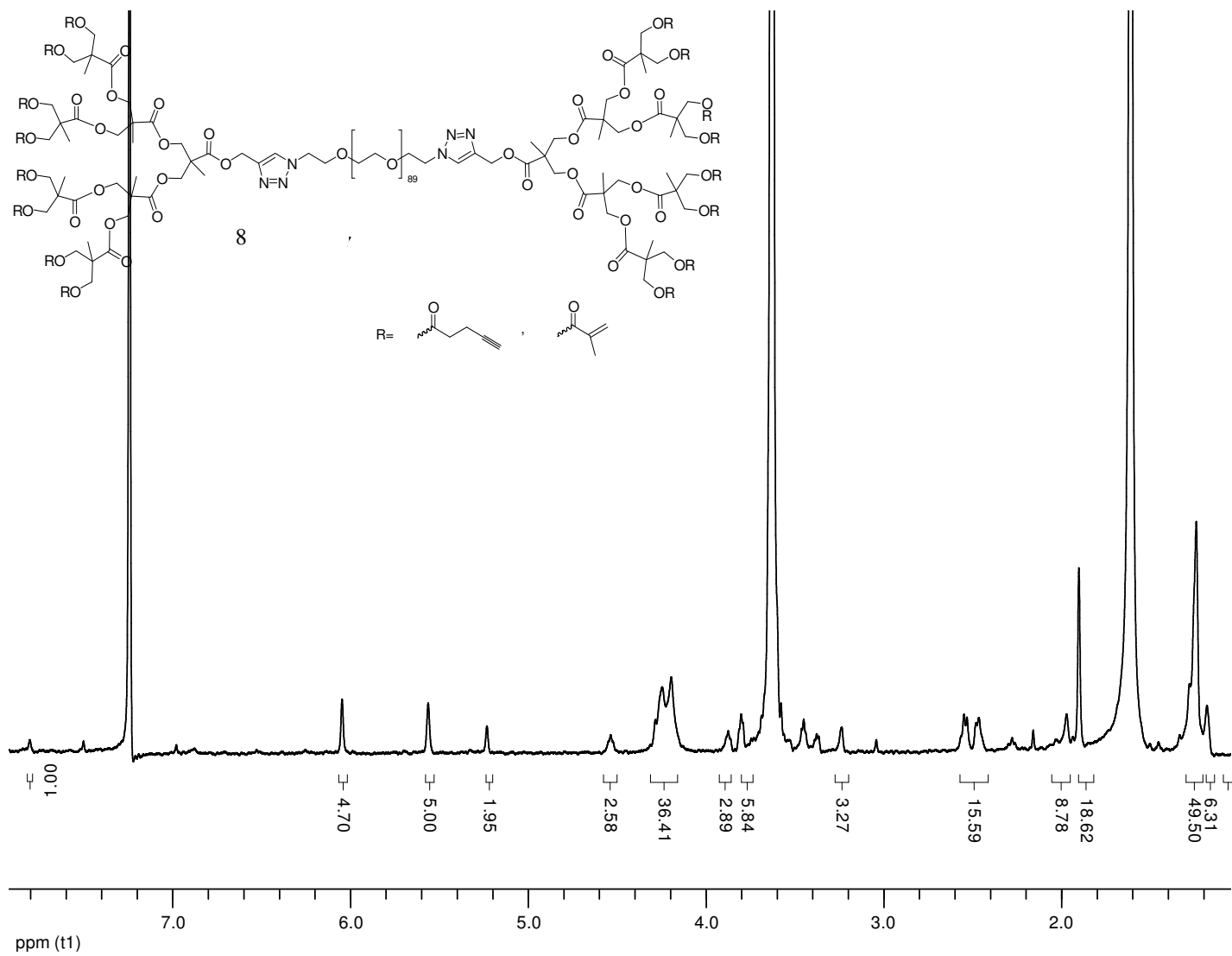


Figure A.13. ^1H NMR spectrum of $[1:1]$ $[G3]8OR[PEG6K]$ **8**

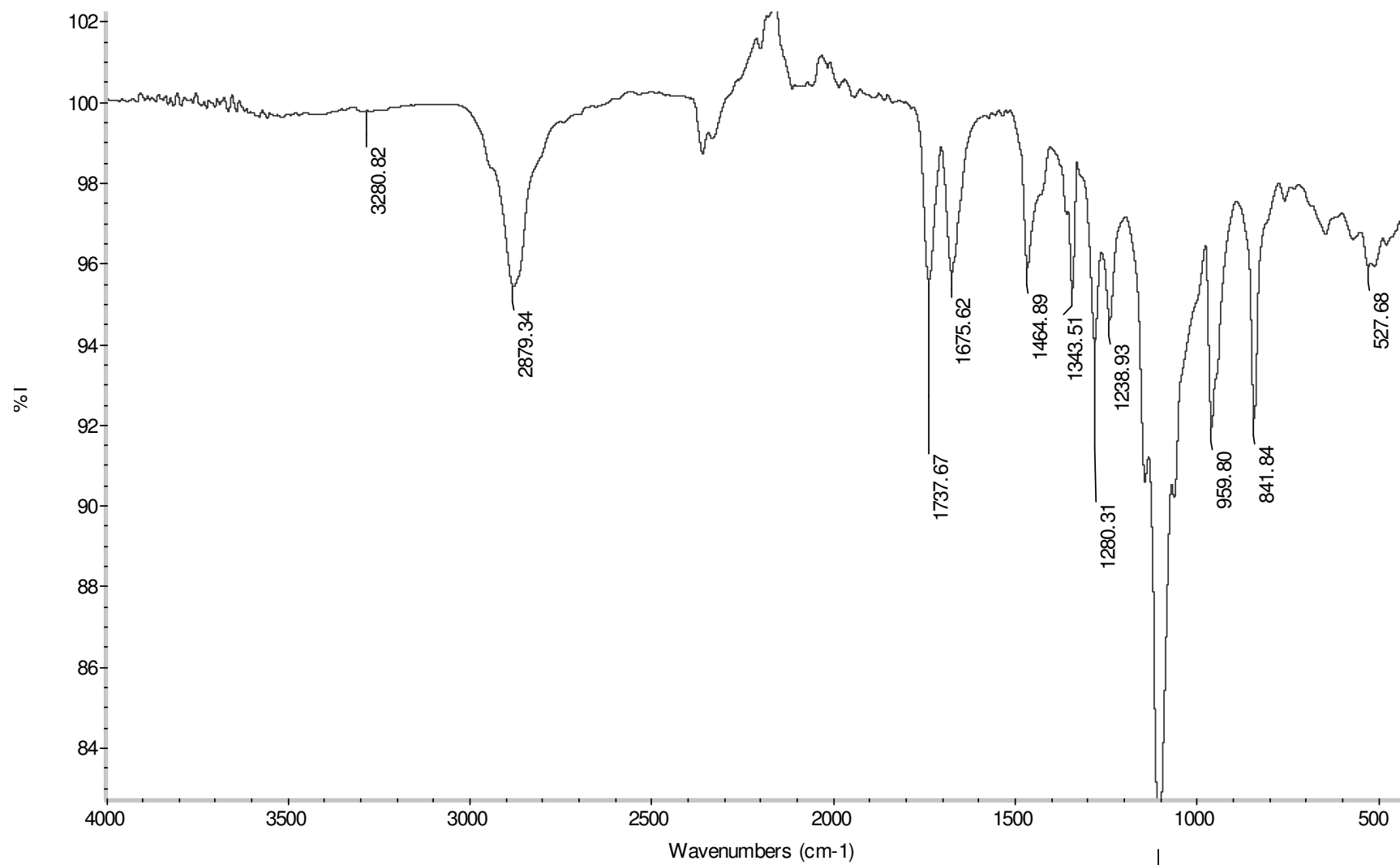


Figure A.14. IR spectrum of [1:1] [G3]8OR[PEG6K] 8

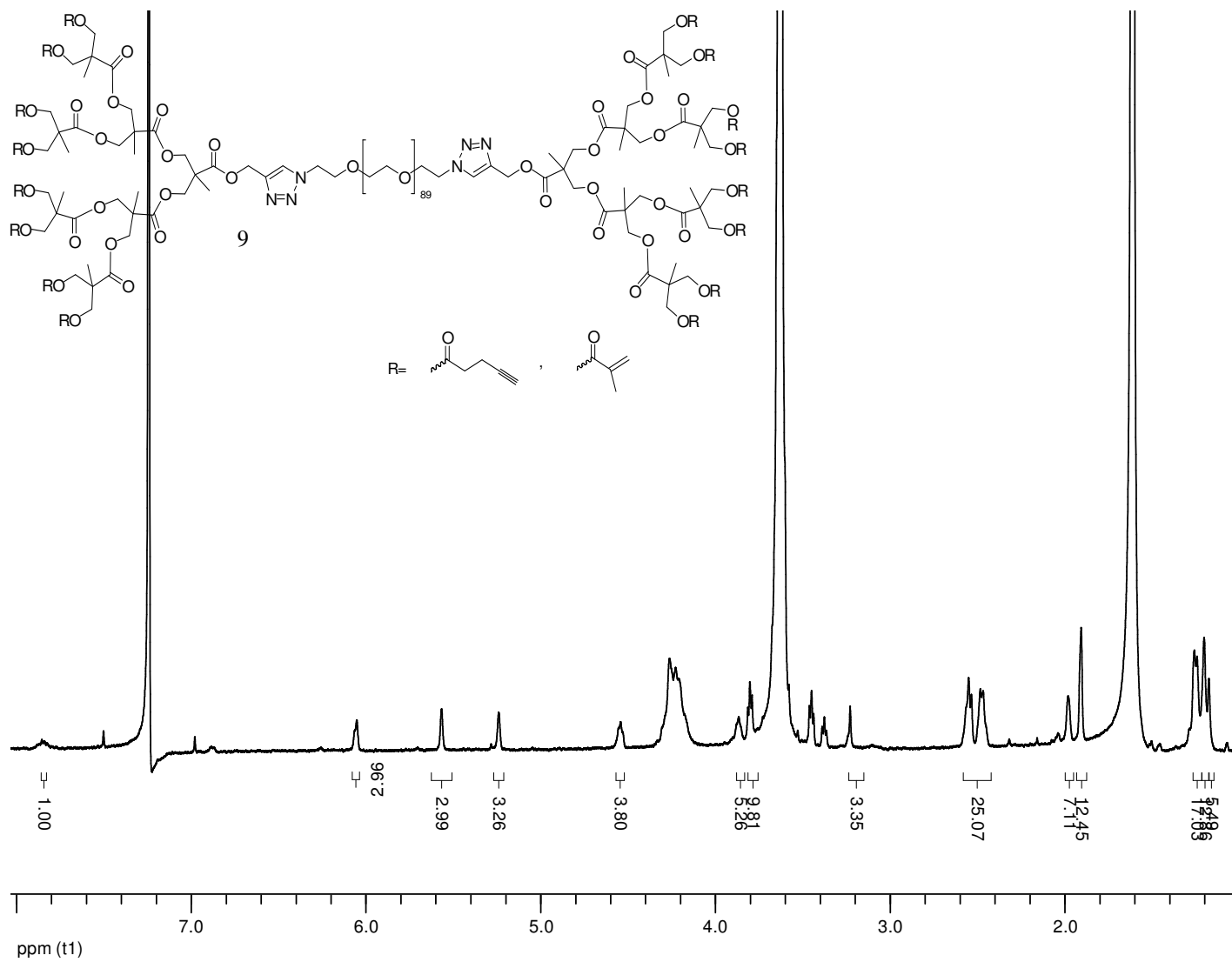


Figure A.15. ^1H NMR spectrum of $[1:2]$ $[G3]4OR[PEG6K]$ **9**

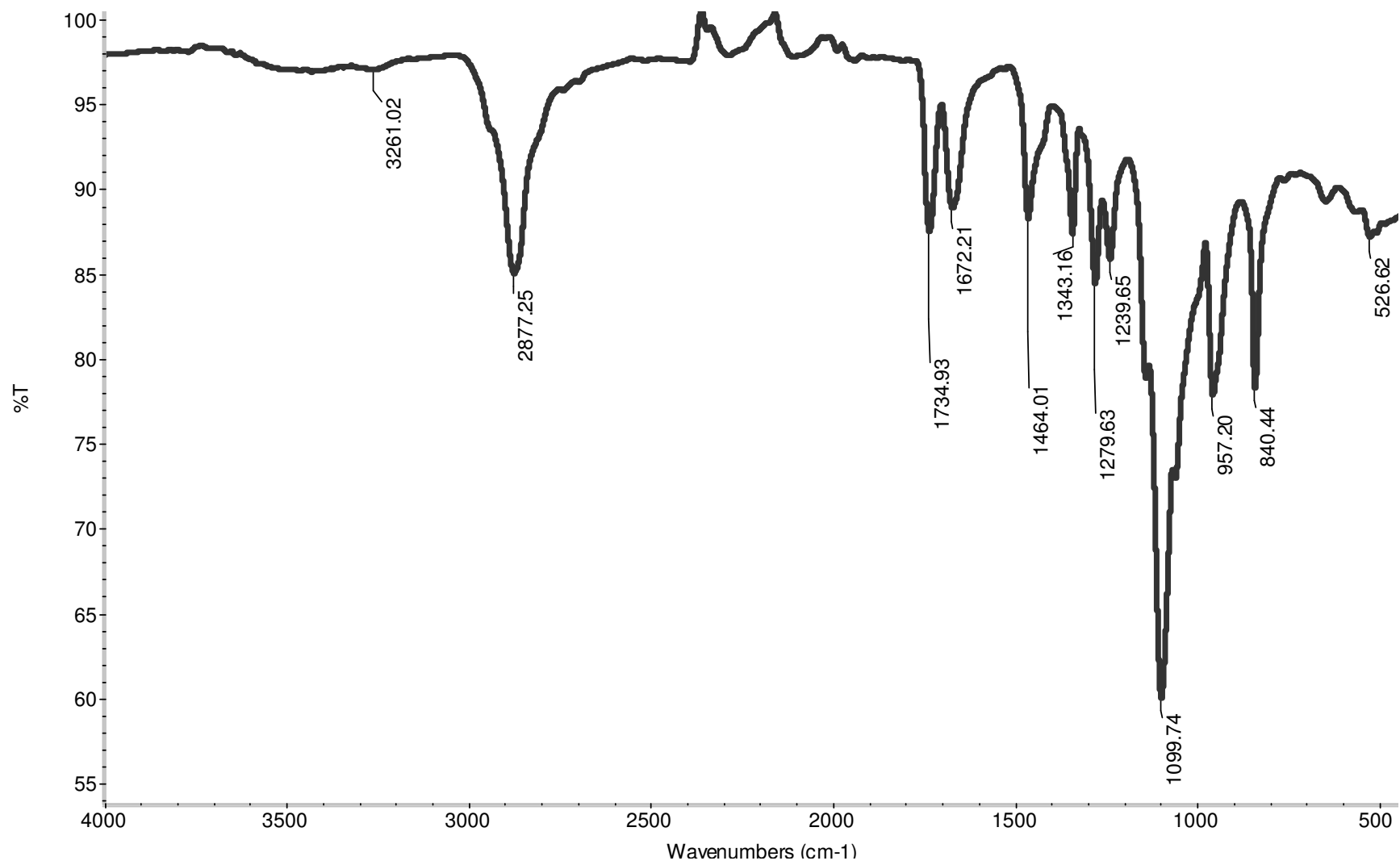


Figure A.16. IR spectrum of [1:2] [G3]4OR[PEG6K] 9

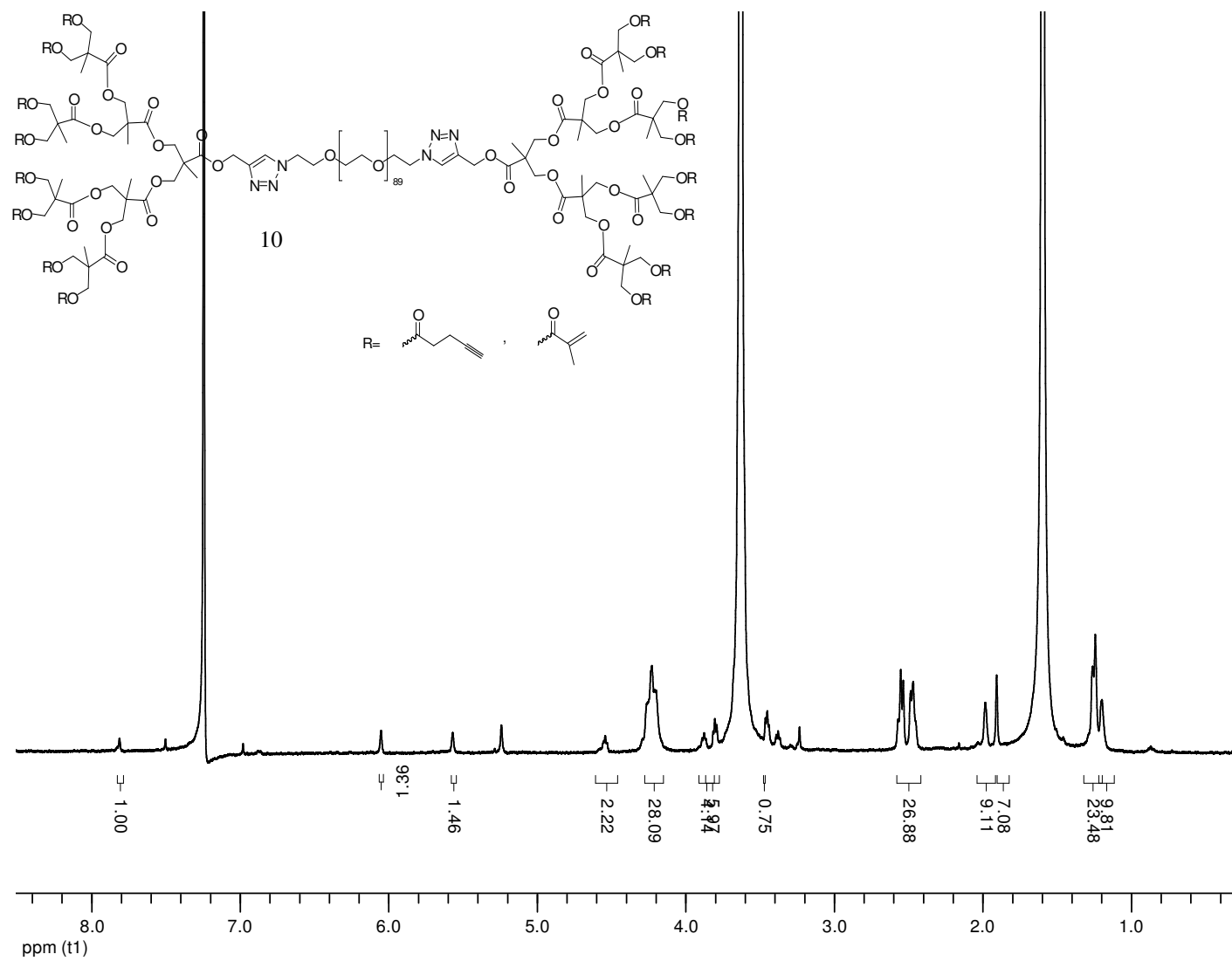


Figure A.17. ¹H NMR spectrum of [1:3] [G3]8OR[PEG6K] **10**

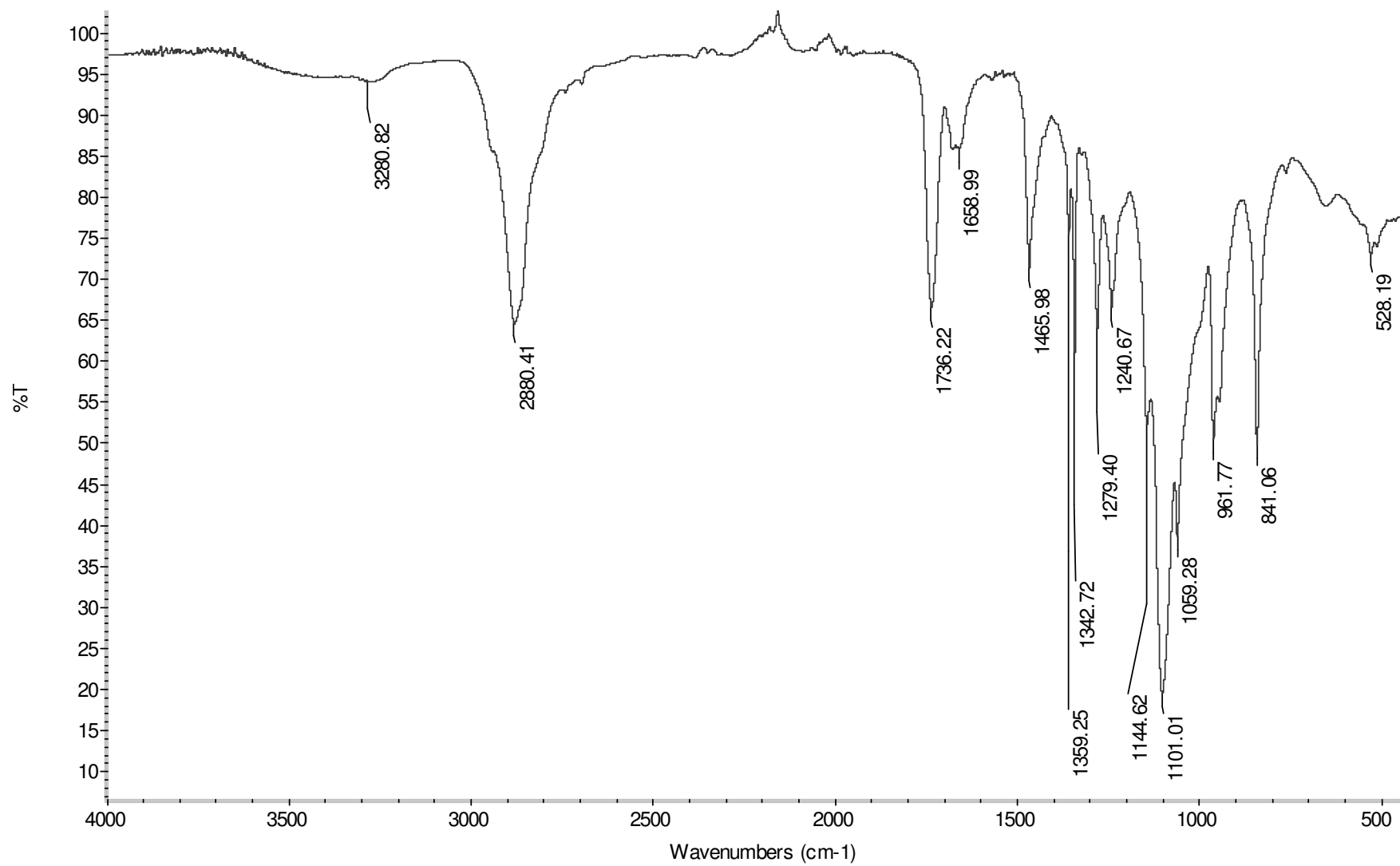


Figure A.18. IR spectrum of [1:3] [G3]8OR[PEG6K] 10

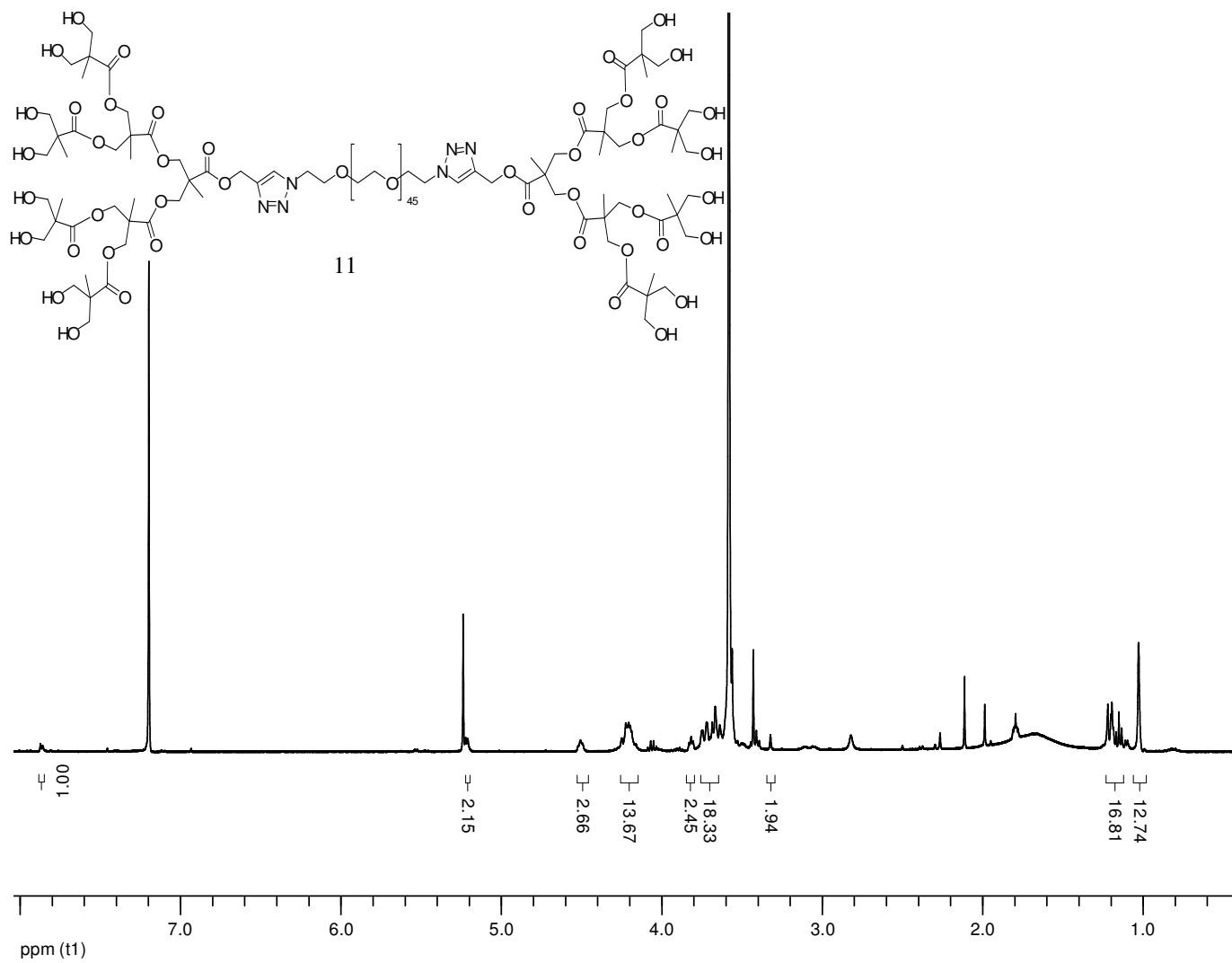


Figure A.19. ¹H NMR spectrum of [G₃]8OH[PEG_{2K}] **11**

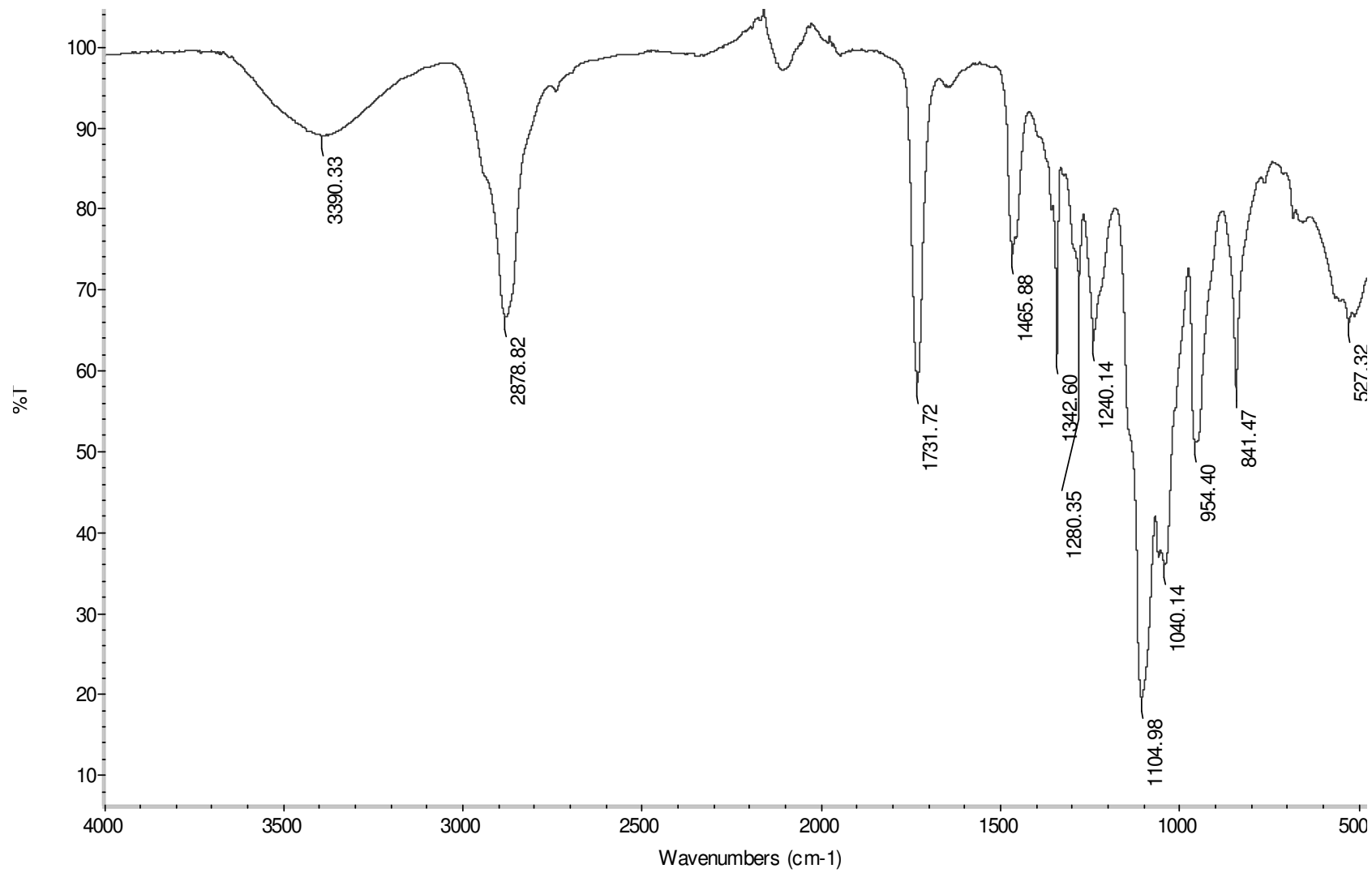


Figure A.20. IR spectrum of [G3]8OH[PEG2K] 11

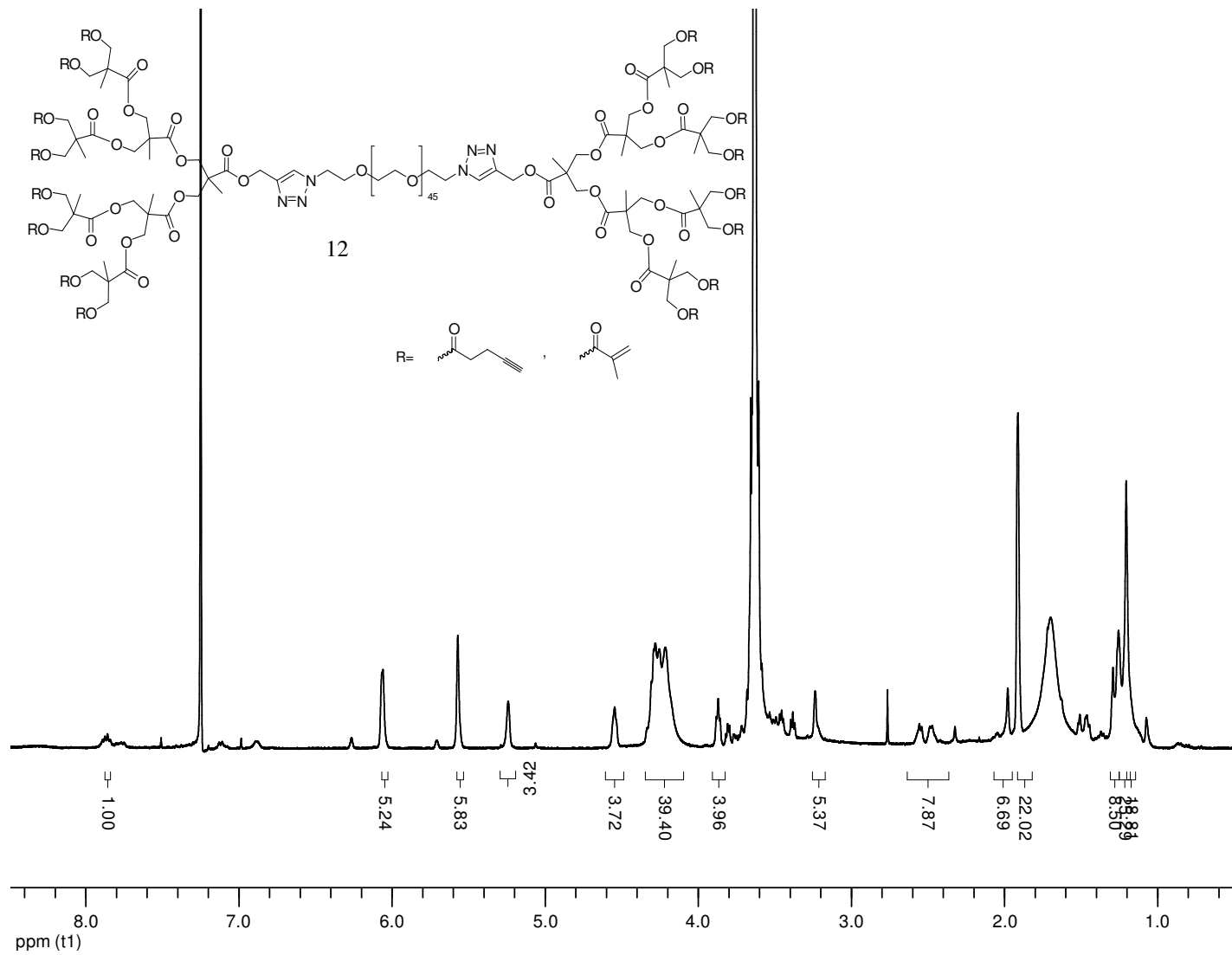


Figure A.21. 1H NMR spectrum of $[1:1] [G_3]_8OR[PEG_2K] \mathbf{12}$

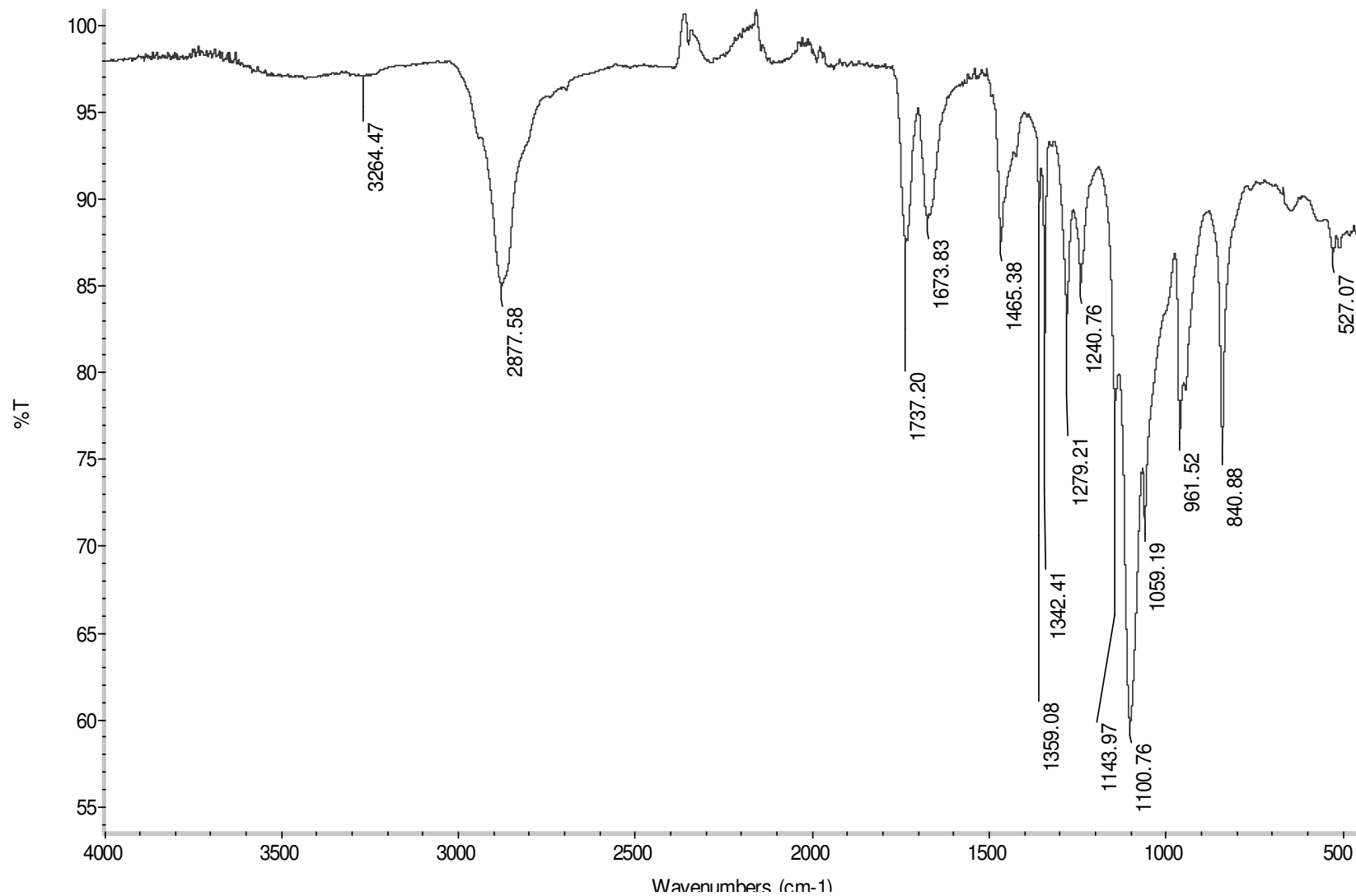


Figure A.22. IR spectrum of [1:1] [G3]8OR[PEG2K] 12

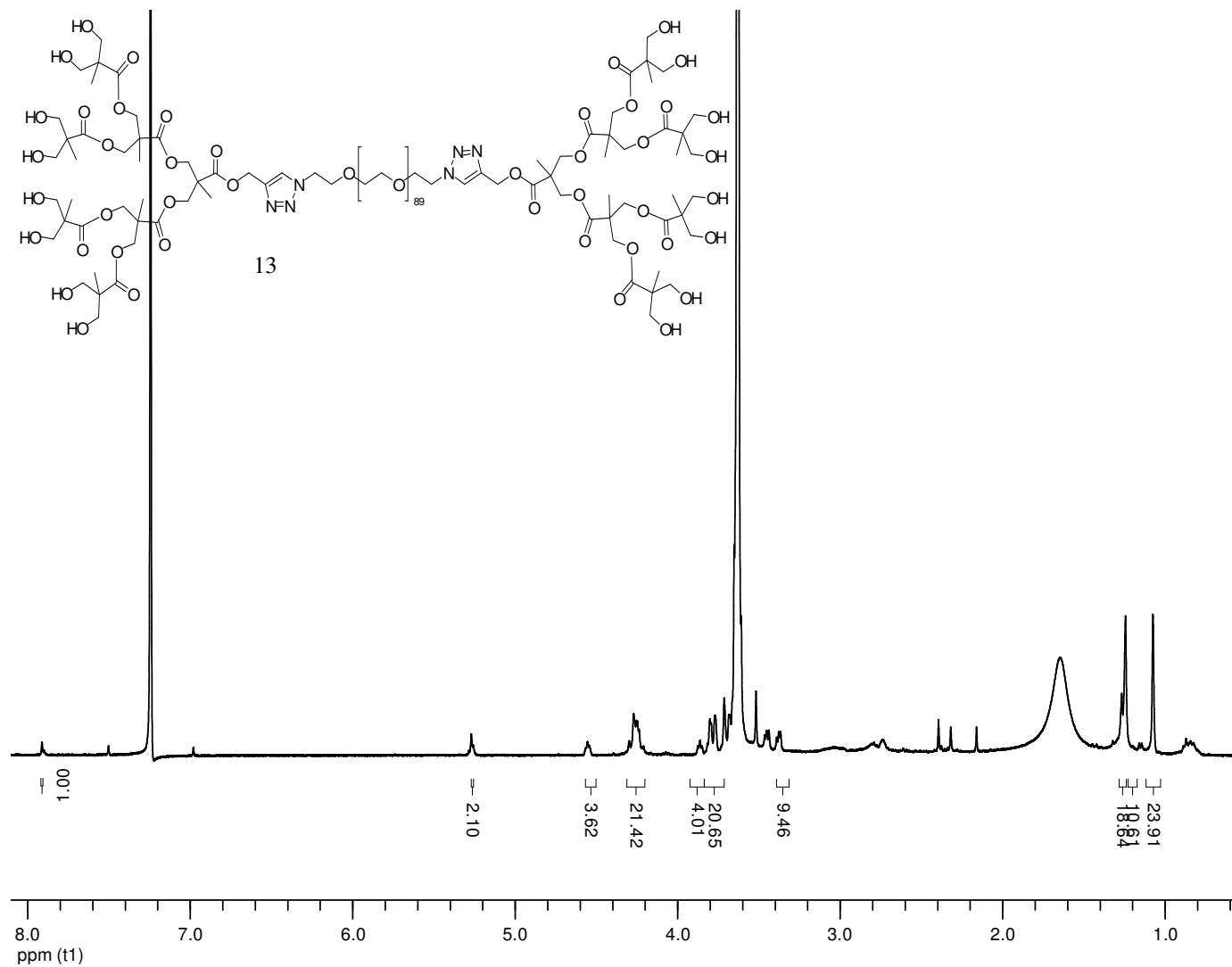


Figure A.23. ^1H NMR spectrum of $[G3]8\text{OH}[PEG4K] \mathbf{13}$

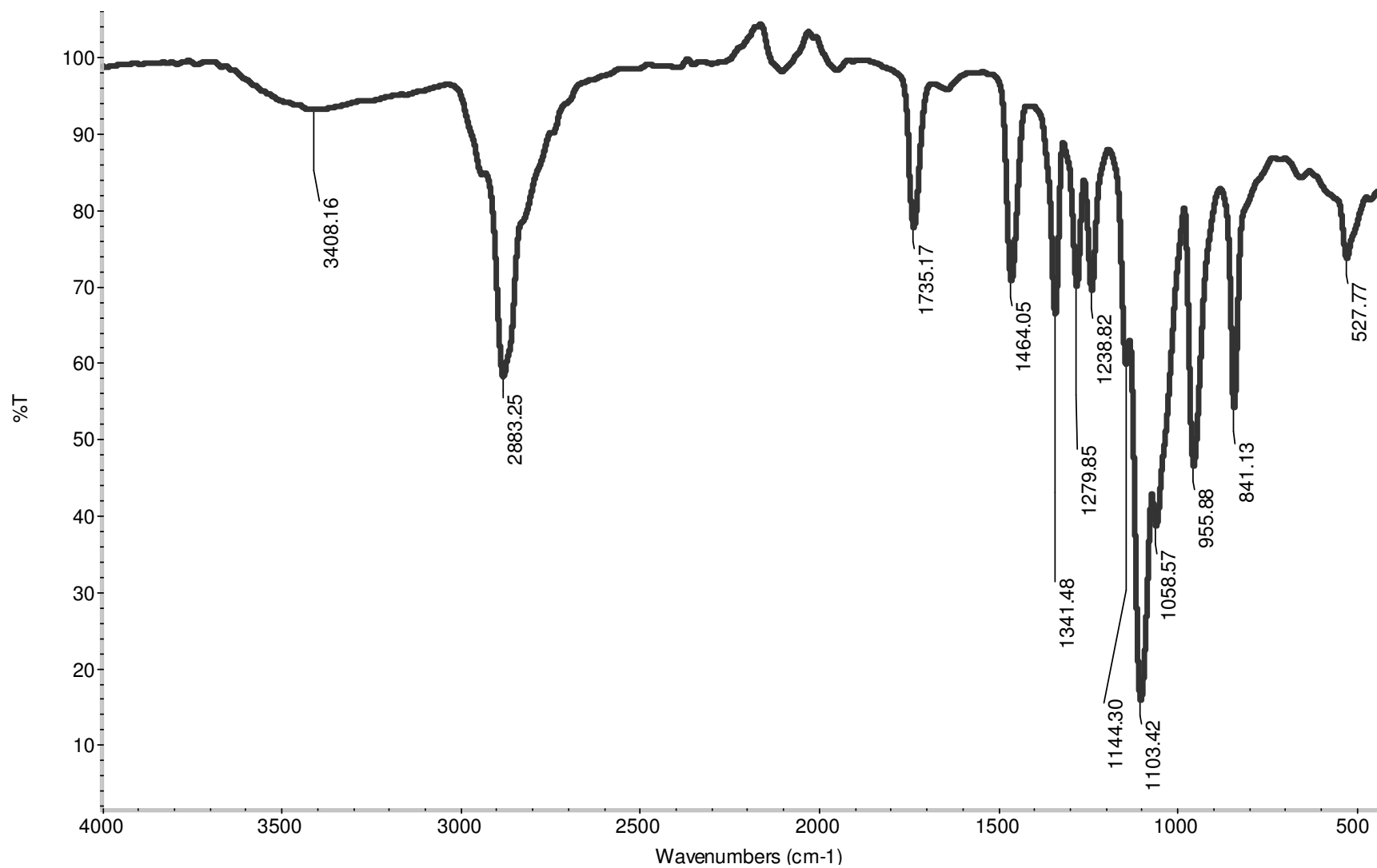


Figure A.24. IR spectrum of *[G3]8OH[PEG4K] 13*

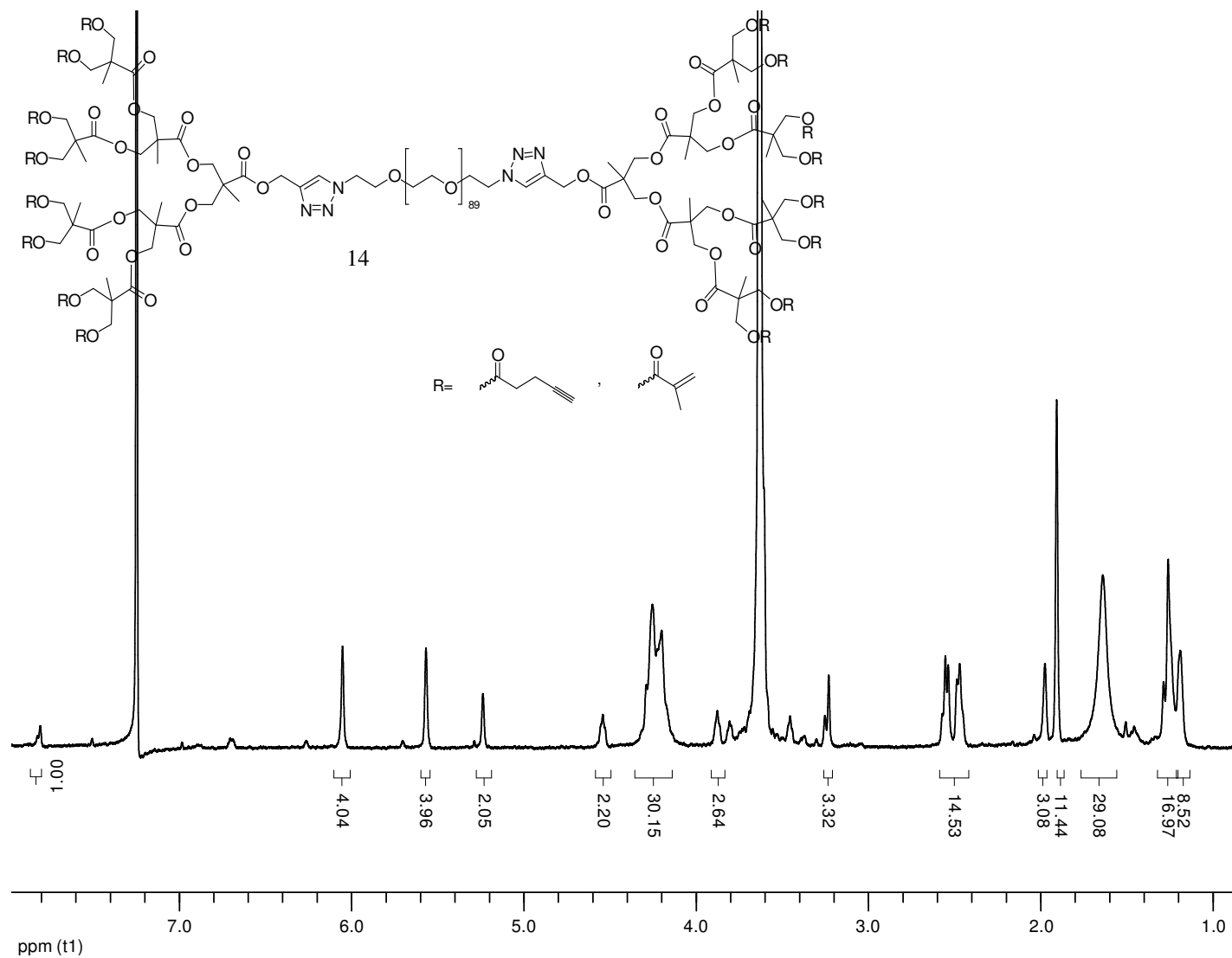


Figure A.25. ^1H NMR spectrum of $[1:1]$ $[G3]8OR[PEG4K]$ **14**

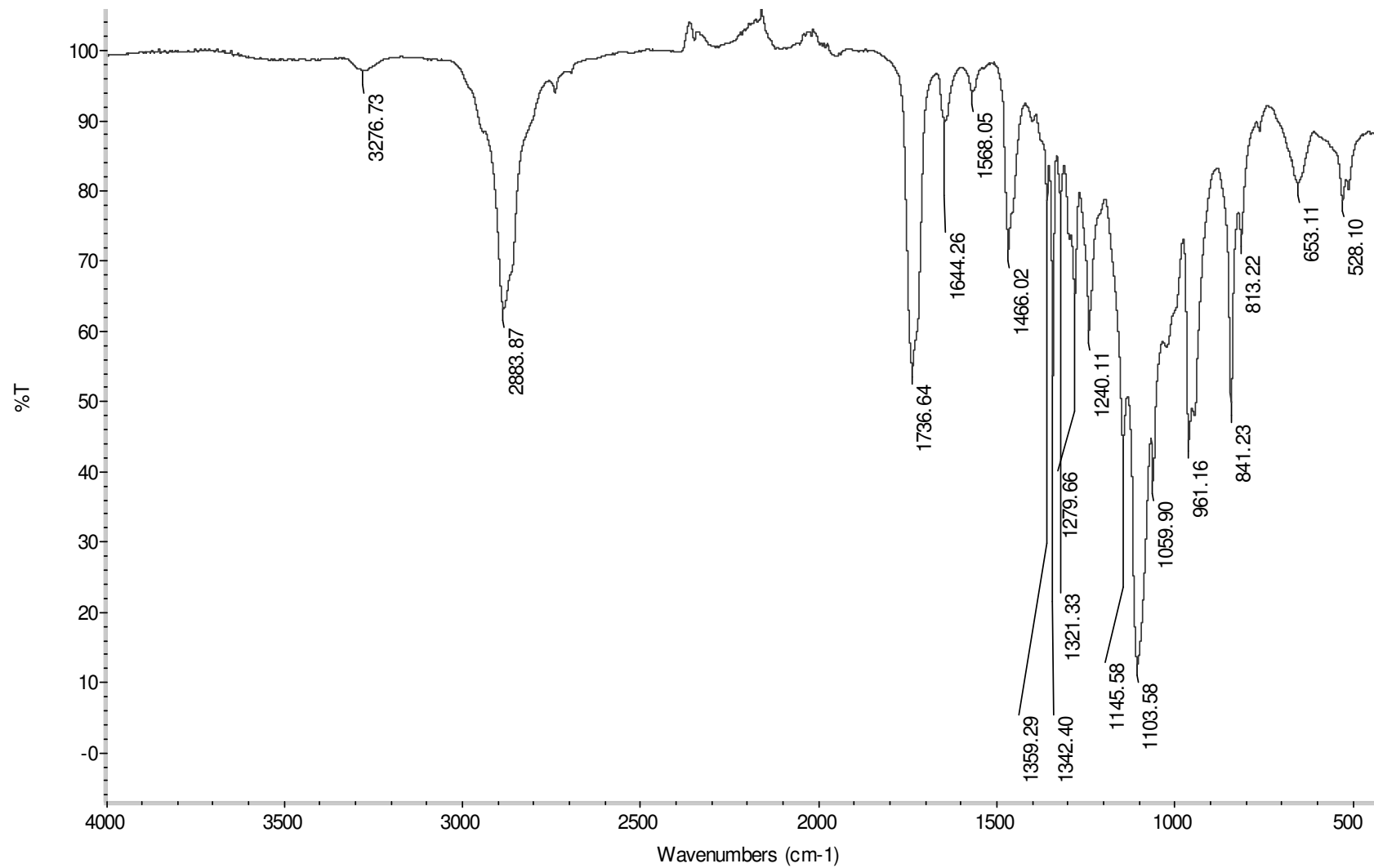


Figure A.26. IR spectrum of [1:1] [G3]8OR[PEG4K] 14

6. REFERENCES

1. Wang, B., Zhu, W., Zhang, Y., “Synthesis of a chemically-crosslinked thermo-sensitive hydrogel film and in situ encapsulation of model protein drugs”, *Reactive & Functional Polymers*, Vol. 66, pp. 509–518, 2006.
2. Park, K. “Biodegradable Hydrogels for Drug Delivery”, Lanchester: Technomic Publishing Co., 1993.
3. Liu, V., Bhatia, S., “Three Dimensional Photopatterning of Hydrogels Containing Living Cells”, *Biomedical Microdevices*, Vol. 4:4, pp. 257-266, 2002.
4. Albrecht, R., Tsang, V., “Photo- and electropatterning of hydrogel-encapsulated living cell arrays”, *TECHNICAL NOTE*, DOI: 10.1039/b406953f, 24th November 2004.
5. Lin, C., Gitsov, I., “Synthesis and Physical Properties of Reactive Amphiphilic Hydrogels Based on Poly(p-chloromethylstyrene) and Poly(ethylene glycol): Effects of Composition and Molecular Architecture”, *Macromolecules*, Vol. 43, pp. 3256–3267, 2010.
6. Burnham, M., Turner, J., “Biological functionalization and surface micropatterning of polyacrylamide hydrogels”, *Biomaterials*, Vol. 27, pp. 5883–5891, 2006.
7. Kızılel, S., Pe´rez-Luna, V., “Photopolymerization of Poly(Ethylene Glycol) Diacrylate on Eosin-Functionalized Surfaces”, *Langmuir*, Vol. 20, pp. 8652-8658, 2004,.
8. Revzin, A., Pishko, M., “Fabrication of Poly(ethylene glycol) Hydrogel Microstructures Using Photolithography”, *Langmuir*, Vol. 17, pp. 5440-5447, 2001.
9. Kuckling, D., “Responsive hydrogel layers—from synthesis to applications”, *Colloid Polym Sci*, 287:881–891, 2009.

10. Hosseinkhani, H., Hosseinkhani, M., “Emerging Applications of Hydrogels and Microscale Technologies in Drug Discovery”, *Disease and Targets, DRUGDISCOVERY*, 2006.
11. Jen, A., Mikos, A., "Review: Hydrogels for Cell Immobilization" *Biotechnology and Bioengineering*, Vol. 50, Pp. 357-364, 1996.
12. Athawale, V., Lele, V., “Recent Trends in Hydrogels Based on Starch-graft-Acrylic Acid: A Review”, *Starch/Stärke* Vol. 53, pp. 7–13, 2001.
13. Ruel-Gariepy, E., Leroux, J., “In situ-forming hydrogels-review of temperature -sensitive systems”, *European Journal of Pharmaceutics and Biopharmaceutics*, Vol. 58, pp. 409–426, 2004.
14. Ratner, B., Hoffman, A., “Synthetic Hydrogels for Biomedical Applications”, ACS Symposium Series; American Chemical Society: Washington, DC, 1976.
15. Suh, K., Lahann, J., “A Novel Photodefinable Reactive Polymer Coating and its Use for Microfabrication of Hydrogel Elements”, *Adv. Mater.*, 16, No. 16, pp. 1401-1405, 2004.
16. Li, R., Altreuter, D., “Transport Characterization of Hydrogel Matrices for Cell Encapsulation”, *Biotechnology and Bioengineering*, Vol. 50, pp. 365-373, 1996.
17. Williams, C., Elisseff, J., “Variable cytocompatibility of six cell lines with photoinitiators used for polymerizing hydrogels and cell encapsulation”, *Biomaterials*, Vol. 26, pp. 1211–1218, 2005.
18. Sudhir Khetan, Jason Burdick, “Cellular Encapsulation in 3D Hydrogels for Tissue Engineering”, *Journal of Visualized Experiments*, DOI: 10.3791/1590, pp. 1-4, 2009.

19. Benoit, D., “Hydrogel culture environments for regenerative medicine applications”, Benoit Lab Therapeutic Biomaterials, University of Rochester, 2010.
20. Benoit, D., “Hydrogels for local delivery of therapeutics”, Benoit Lab Therapeutic Biomaterials, University of Rochester, 2010.
21. Berger, J., Gurny, R., “Structure and interactions in covalently and ionically crosslinked chitosan hydrogels for biomedical applications”, *European Journal of Pharmaceutics and Biopharmaceutics*, Vol. 57, pp. 19–34, 2004.
22. Schacht, E., “Polymer chemistry and hydrogel systems”, *Journal of Physics: Conference Series* 3, pp. 22–28, 2004.
23. Liu, S., Tay, R., “Synthetic Hydrogels for Controlled Stem Cell Differentiation”, *Soft Matter*, Vol. 6, pp. 67 - 81, 2010.
24. Mazzola, L., “Commercializing nanotechnology”, *Nature Biotechnology*, Vol. 21, pp. 1137 – 1143, 2003.
25. Wang, Q., Mynar, J.L., Yoshida, M., Lee, E. Lee, M., Okuro, K. Kinbara, K. & Aida, T., “High-water-content mouldable hydrogels by mixing clay and a dendritic molecular binder”, *Nature*, Vol. 463, pp. 339-343, 2010.
26. Tomalia, D. A.; Durst, H. D., *Top. Curr. Chem.*, Vol. 165, pp. 193-313, 1993.
27. Hawker, C. J., Fréchet, J. M. J., *J. Am. Chem. Soc.*, Vol., 112, pp. 7638-47, 1990.
28. Fréchet, J. M. J. *Science* 1994, 263, 1710-1715.
29. Newkome, G. R., Moorefield, C. N., Vögtle, F., “Dendrimers and Dendrons: Concepts, Syntheses, Applications”, Wiley-VCH: Weinheim, Germany, 2001.

30. Frechet, J. M. J., Tomalia, D. A., Eds., "Dendrimers and other Dendritic Polymers", J. Wiley and Sons, Chichester and New York, 2001.
31. Gillies, E., Frechet, J. M. J., "Designing Macromolecules for Therapeutic Applications: Polyester DendrimersPoly(ethylene oxide) "Bow-Tie" Hybrids with Tunable Molecular Weight and Architecture", J. AM. CHEM. SOC., Vol. 124, pp. 14137-14146, 2002.
32. Huisgen, R., "Cenetary Lecture – 1,3-Dipolar Cycloadditions", Proceedings of the Chemical Society of London, pp. 357, 1961.
33. Kolb, H. C., Finn, M. G., Sharpless, K. B., "Click Chemistry: Diverse Chemical Function from a Few Good Reactions", Angew. Chem. Int. Ed., Vol. 40, pp. 2004-21, 2001.
34. Ihre, H., Padilla De Jesus, O. L., Szoka, F. C., Frechet, J. M. J., Bioconjugate Chem., Vol. 13, pp. 433-452, 2002.
35. Padilla De Jesu's, O. L., Ihre, H. R., Gagne, L., Frechet, J. M. J., Szoka, F. C., Bioconjugate Chem., Vol. 13, 453-461, 2002.
36. Wu, P., Malkoch, M., Hunt, J.N., Vestberg, R., Kaltgrad, E., Finn, M. G., Fokin, V.V., Sharpless, K. B., Hawker, C. J., "Multivalent, bifunctional dendrimers prepared by click chemistry", Chem. Commun., pp. 5775–5777, 2005.
37. Diaz, D. D., Punna, S., Holzer, P., McPherson, A. K., Sharpless, K. B., Fokin, V. V., Finn, M. G., J. Polym. Sci., Sect A: Polym. Chem., Vol. 42, pp. 4392–4403, 2004.
38. Newkome, G. R.; Moorefield, C. N.; Vögtle, F., "Dendrimers and Dendrons, Concepts, Syntheses, Applications", Wiley-VCH: Weinheim, Germany, 2001.
39. Frechet, J. M. J., Tomalia, D. A., Eds, "Dendrimers and Other Dendritic Polymers" Wiley: New York, 2002.

40. Gitsov, I., Zhu, C., “Amphiphilic Hydrogels Constructed by Poly(ethylene glycol) and Shape-Persistent Dendritic Fragments”, *Macromolecules*, Vol. 35, pp. 8418-8427, 2002.
41. Bryant, S. J., Nuttelmen, C. R., Anseth, K. S., “Cytocompatibility of ultraviolet and visible light photoinitiating systems on cultured NIH/3T3 broblasts *in vitro*”, *J. Biomater. Sci. Polym. Ed.*, Vol. 11, pp. 439-57, 2000.
42. Sawhney, A. S., Pathak, C. P., Hubbell, J. A., “Modification of islet of langerhans surfaces with immunoprotective poly(ethylene glycol) coatings via interfacial photopolymerization”, *Biotechnol. Bioengng.*, Vol. 44, pp. 383-6, 1994.
43. Cruise, G. M., Hegre, O. D., Scharp, D. S., Hubbell, J. A., “A sensitivity study of the key parameters in the interfacial photopolymerization of poly(ethylene glycol) diacrylate upon porcine islets”, *Biotechnol. Bio Engng.*, Vol. 57, pp. 655-65, 1998.
44. Anseth, K. S., Kline, L. M., Walker, T. A., Anderson, K. J., Bowman, C. N., “Reaction-kinetics and volume relaxation during polymerizations of multiethylene glycol dimethacrylates”, *Macromolecules*, Vol. 28, pp. 2491-9, 1995.
45. Bryant, S. J., Anseth, K. S., “The effects of scaffold thickness on tissue engineered cartilage in photocrosslinked poly(ethylene oxide) hydrogels”, *Biomaterials*, Vol. 22, pp. 619-626, 2001.
46. Altin, H., Kosif, I., Sanyal, R., “Fabrication of “Clickable” Hydrogels via Dendron–Polymer Conjugates”, *Macromolecules*, Vol. 43 (8), pp. 3801-3808, 2010.
47. Kosif, I., Park E., Sanyal, R., Sanyal, A., “Fabrication of Maleimide Containing Thiol Reactive Hydrogels via Diels-Alder/Retro-Diels-Alder Strategy”, *Macromolecules*, Vol. 43, pp. 4140–4148, 2010.
48. Cheung, C. Y., Anseth, K. S., “Synthesis of Immunoisolation Barriers That Provide Localized Immunosuppression for Encapsulated Pancreatic Islets”, *Bioconjugate*

- Chem., Vol. 17, pp. 1036-1042, 2006.
49. Luo, Y., Shoichet, M. S., "A photolabile hydrogel for guided three-dimensional cell growth and migration", *Nature Materials*, Vol. 3, pp. 249-253, 2004.
 50. Musoke, P., Shoichet, M. S., "Development of biomaterial scaffold for nerve tissue engineering: Biomaterial mediated neural regeneration", *Biomed. Mater.*, Vol. 1, pp. 162-169, 2006.
 51. Wosnick, J. H., Shoichet, M. S., "Three-dimensional Chemical Patterning of Transparent Hydrogels", *Chem. Mater.*, Vol. 20, pp. 55-60, 2008.
 52. Chou, L., Firth, J. D., Uitto, V. J., Brunette, D. M., "Substratum surface topography alters cell shape and regulates fibronectin mRNA level, mRNA stability, secretion and assembly in human fibroblasts", *J. Cell Sci.* Vol. 108 (Pt 4), pp. 1563-73, 1995.
 53. Dubey, N., Letourneau, P. C., Tranquillo, R. T., "Guided neurite elongation and schwann cell invasion into magnetically aligned collagen in simulated peripheral nerve regeneration" *Exp. Neurol.* Vol. 158 (2), 338-50, 1999.
 54. Kim, B. S., Nikolovski, J., Bonadio, J., Money, D. J., "Cyclic mechanical strain regulates the development of engineered smooth muscle tissue", *Nature Biotechnology*, Vol. 17 (10), pp. 979-83, 1999.
 55. Seguraa, T., Andersona, B. C., Chungb, P. H., Webberc, R. E., Shullc, K.R., Shea, L. D., "Crosslinked hyaluronic acid hydrogels: a strategy to functionalize and pattern", *Biomaterials*, Vol. 26, pp. 359-371, 2005,
 56. Nandivada, H.; Chen, H. Y.; Bondarenko, L.; Lahann, J., "Reactive polymer coatings that "click."", *Angew. Chem., Int. Ed.* 2006, 45, 3360-3363.

57. Lahann, J., Klee, D., Hocker, H., “Surface Modification of Confined Microgeometries via Vapor-Deposited Polymer Coatings”, *Macromol. Rapid Commun.* Vol. 19, pp. 441–444, 1998.
58. Tsarevsky, N. V., Sumerlin, B. S., Matyjaszewski, N., “Step Growth “Click” Coupling of Telechelic Polymers Prepared by Atom Transfer Radical Polymerization”, *Macromolecules*, vol. 35, pp. 6142, 2002.